A Study of Partitiviruses Infecting *Saccharomyces cerevisiae* and Their Interactions with Host Antiviral Systems

A thesis

Presented in Partial Fulfillment of the Requirements for the

Degree of Master of Science

with a

Major in Biology

in the

College of Graduate Studies

University of Idaho

by

Nathan Taggart

Approved by:

Major Professor: Paul A. Rowley, Ph.D.

Committee members: Jill Johnson, Ph.D., Marc Meneghini, Ph.D., Tanya Miura, Ph.D.

Department Administrator: Tanya Miura, Ph.D.

December 2023

ABSTRACT

Fungi are key components of the biosphere and serve key functions, such as aiding plant nutrient absorption and decomposing organic matter, yet these contributions coexist with significant threats, as fungal pathogens can cause extensive crop losses and endanger biodiversity. Mycoviruses are prevalent in fungal taxa and often coexist without apparent symptoms but can influence host physiology, impacting symbioses with other organisms, toxin production, and pathogenicity. Understanding these interactions holds promise for disease control and enhancing plant resilience.

Partitiviruses (PVs) are double-stranded RNA (dsRNA) viruses from the family *Partitiviridae* that infect plants, fungi, insects, and protozoa. They replicate within the cytoplasm of their host and are transmitted by cell fusion and cell division. While many PVs are cryptic and have no apparent effects on their host, some cause altered morphology, reduced growth rate, and disrupted sexual reproduction in their fungal hosts. Some PVs infecting pathogenic fungi can reduce their virulence, such as in the Chestnut blight fungus *Cryphonectria parasitica*, while others cause hypervirulence, such as in the human pathogen *Talaromyces marneffei*. There have been a few studies investigating how partitiviruses alter host physiology, but the family *Partitiviridae* is, by and large, understudied, and there is little to no understanding of how these viruses protect their genomes and transcripts from host surveillance mechanisms. A large factor in this knowledge gap is the lack of a robust model system.

A large-scale screen aimed at revealing the dsRNA “virome” of the baker’s yeast *Saccharomyces cerevisiae* identified three novel species of partitivirus and were named Saccharomyces cerevisiae partitivirus 1, -2, and -3. Notably, nearly all ScPV-infected yeast strains were isolated from coffee and cacao fermentations and carried ScPV1 and/or ScPV2. ScPV3 is found winemaking strains. ScPV infection was confirmed by sequencing the viral dsRNAs and subsequent purification and visualization of non-enveloped, isometric viral particles. The particles lacked any obvious protrusions that are characteristic of other PVs. The full genome sequences of ScPV1-3 were obtained

by short-read sequencing and 5’ rapid amplification of cDNA ends. ScPVs have significant predicted secondary structure, which is hypothesized to play roles in packaging and replication. Phylogenetic analysis revealed that ScPVs are most closely related to Cryptosporidium parvum virus 1 (CSpV1), which infects the mammal-pathogenic protozoan *Cryptosporidium parvum*. Models of the ScPV capsid protein (CP) and RNA-dependent RNA polymerase (RdRP) were generated and found to be structurally homologous to those of other PVs.

ScPVs demonstrate stability during laboratory cultivation and successful transmission to haploid progeny after sporulation. ScPVs were also horizontally transmitted by strain hybridization. These characteristics allowed preliminary study of interactions between ScPVs and host antiviral genes, such as the 5’-3’ exoribonuclease *XRN1*, *NUC1*, and the SKI complex/exosome. ScPVs are resistant to Xrn1 overexpression, and *SKI2* deletion is associated with increased copy number, suggesting viral transcripts lack poly(A) tails. Sporulation of a *SKI3/ski3Δ* strain was associated with loss of ScPVs from all meiotic progenies. There is no obvious relationship between ScPV copy number and deletion of either *NUC1* or *SKI7*.

This work details the discovery of the first novel dsRNA viruses discovered in *S. cerevisiae* in nearly half a century. *S. cerevisiae*, a widely employed model organism for exploring diverse cellular mechanisms, including host-virus interactions, offers a unique opportunity to develop a novel model system to fill a knowledge gap in the understanding of partitivirus biology.

ACKNOWLEDGEMENTS

I am profoundly grateful to Dr. Paul A. Rowley for his invaluable guidance and unwavering support throughout the entirety of this research endeavor. His profound insights and steadfast mentorship have not only shaped the trajectory of this project but have also been instrumental in shaping my career path. I extend my heartfelt appreciation to Dr. Marc Meneghini, Dr. Jill Johnson, and Dr. Tanya Miura for their exceptional advice and profound insights, which have significantly enriched the depth and quality of this work. Their collective wisdom and dedicated engagement have been a source of inspiration and motivation. I would also like to express my sincere appreciation to Dr. Maitreya Dunham, her lab manager, Emily Mitchell, and other members of her lab. Their collaborative spirit, shared knowledge, and willingness to share their expertise have greatly enhanced my learning journey. I am especially grateful for help that the former lab manager of the Rowley lab, Angela Crabtree, has given me over the last four years and for her patience with my many, many questions. I want to thank members and alumni of the Rowley lab as well for helping me with experiments and teaching me various techniques.

DEDICATION

Thank you for your immense support these past few months and for your patience during my many late-night writing sessions.

To the wonderful people of r/labrats, thank you all for the wealth of advice and tips.

TABLE OF CONTENTS

LIST OF FIGURES

LIST OF TABLES

STATEMENT OF CONTRIBUTION

The metagenomic study of dsRNAs pooled from 520 *S. cerevisiae* strains was performed by Angela M. Crabtree (Fig 2.1A). Josephine M. Boyer, Camden D. Doering, Mason A. Shipley, Nic Hoffman, and Darby Fox contributed to the dsRNAs survey (Fig 2.1B and 2.1G, Table 2.1, and Appendix C). The RNase III digestion of PV dsRNAs was performed by Mason A. Shipley (Fig 2.1C). Cycloheximide curing of M2 in strain CYC1172 was performed by Josephine M. Boyer (Fig 2.1E). The *Partitiviridae* phylogenetic tree was generated by Dr. Paul A. Rowley (Fig 2.2C). 5' rapid amplification of cDNA ends was performed, in large part, by Angela M. Crabtree (Fig 2.6A). Dr. Paul A. Rowley used mFold to make secondary structure predictions of ScPV dsRNAs (Fig 2.6A-B and Fig B.2). Dr. Shunji Li aided with partitivirus particle purification, and Dr. Ignacio de la Higuera (Center for Life in Extreme Environments, Department of Biology, Portland State University) performed the electron microscopy to image the particles (Fig 2.7A). Protein structure models were produced by Jack W. Creagh (Fig 2.7B-E, Fig B.3, Fig B.4, Fig B.5, and Appendix I). Dr. Jill Johnson dissected one strain (Fig 3.1C).

CHAPTER 1: LITERATURE REVIEW

1.1 Significance of fungi and their viruses

Fungi are key members of the biosphere. Mycorrhizal fungi form mutually beneficial symbioses with most plants, aiding the plant in absorbing nutrients and in resisting stress[1]. Saprophytic fungi are decomposers and break down plant matter. Fungi are also the source of the discovery of several medicines, including antibiotics and anti-cancer and cholesterol-reducing drugs[2]. However, fungi can also pose major threats. For instance, fungal pathogens destroy up to 65% of crops in the United States each year, amounting to $23.5 billion when factoring in costs of controlling pathogens[3].

Fungi can be vectored by humans and domesticated species, as well as infected hosts[4]. For instance, the Great Famine in Ireland was caused by introduction of *Phytophthora infestans*-infected potatoes from South America[5–7]. Chytridiomycosis is a disease caused by the highly pathogenic fungus *Batrachochytrium dendrobatidis*, which can infect hundreds of amphibian species, causing up to 100% mortality in susceptible species. Trade of disease-resistant African bullfrogs and African clawed frogs can introduce the fungus into naïve populations.[5–7] Some areas have experienced local extinctions of 40% of amphibian species, and over half of amphibian species worldwide are in decline, which threatens biodiversity and ecosystem health[2,4,8,9].

New pathogens can emerge and spread quickly. For instance, *Pseudogymnoascus destructans*, the causative agent of white nose syndrome in bats, was discovered in New York in 2007, and, by 2010, it could be found in over 115 roosts across Canada and the United States. Bat populations have decreased by 70% since[4]. Because of their high infectivity, fungal pathogens can infect an entire population, possibly leading to regional extinction of that species. Or it can reduce the population and leave it vulnerable to another catastrophe. According to Fisher et al., plant and animal biodiversity is at greater risk from fungal pathogens than from pathogens in other taxa, including protists, viruses, bacteria, and helminths, combined. And their analyses show that the threat is growing rapidly[4].

An important feature of many fungal pathogens is that they are facultative parasites; they can persist in the environment as resilient spores, sclerotia, or conidia or as saprophytes, growing on decaying organic matter[4]. This allows them to become ubiquitous in the environment. Another important feature is the ability of some fungi to undergo genetic recombination, hybridization, and horizontal gene transfer. This allows for non-pathogenic fungi to become pathogenic and for current pathogens to acquire new host species[10].

One high-profile fungal pathogen that has had huge economic and ecological impacts is *Cryphonectria parasitica*, the causative agent of chestnut blight. *C. parasitica* is native to east Asia and spread to other continents on infected chestnut plants[11,12]. It was discovered in North America in New York City in 1904, and, within 50 years, it had largely ousted the American chestnut from its status as the dominant overstory tree species[13]. Chestnut trees were an integral part of the forest ecosystem in southern New England. The fruit was a staple food, valued for its versatility and long shelf-life, and the wood was valued for toolmaking, building construction, and for producing charcoal[14]. Related chestnut species fill similar niches across the globe[15]. Thus, the obliteration of the American chestnut population has been deemed “a plant tragedy second to none.”[16]

C. parasitica infects the stems and branches of chestnut trees and enters its host through injuries in the bark. These can be caused by many things such as drought, fire, cutting, natural competition, and even the galls of the chestnut gall wasp[17,18]. There are several symptoms of *C. parasitica* infection. An early symptom in adult trees is formation of a flag, which is a branch whose leaves have wilted, which typically remain on the branch after autumn. The fungus also produces cankers, which are necrotic lesions with a reddish-brown color and sunken appearance (Fig 1.1A). When the fungus sporulates, orange structures called stromata that contain sexual and asexual fruiting bodies protrude from the cankers (Fig 1.1B).

Figure 1.1: Symptoms of *C. parasitica* infection in American chestnuts.
(**A**) Virulent strains produce reddish brown cankers that sink in when the internal cambium tissue dies. (**B**) Stromata, containing the sexual and asexual fruiting bodies, protrude from cankers when the fungus sporulates. (**C**) Hypovirulent strains do not completely kill the cambium. New layers form beneath the infected tissue, causing the outer bark layer to expand and crack.

The tree reacts to infection by lignifying cells within the cambium and forming a wound periderm. However, the fungus forms structures called mycelial fans that secrete oxalic acid and cell wall degrading enzymes that penetrate the lignified barrier and inhibit periderm formation by killing host cells[19]. Mycelial fans also build up physical pressure that can burst host cells, allowing the fungus to advance into the cambium tissue. If the cambium dies, the surrounding barks sinks inward, giving cankers their characteristic appearance. Mycelial fans may rapidly encircle a stem or branch, causing the entire stem or branch to die. *C. parasitica* may be infected with a virus called Cryphonectria hypovirus 1 (CHV1), which reduces the virulence of its host, allowing the tree to resist *C. parasitica* infection. In this case, new layers of bark form beneath the infected layers, causing the outer bark layer to crack and giving cankers a swollen, calloused appearance (Fig 1.1C)[20].

These virus-infected, hypovirulent *C. parasitica* strains were successfully applied in Europe as biocontrol agents to protect chestnut trees from noninfected, virulent *C. parasitica* strains. However, this approach was not successful in the United States[21]. This is due to the complex vegetative compatibility (vc) system of *C. parasitica*. Six loci with

two alleles each form at least 64 vc groups[22–24]. If two *C. parasitica* isolates carry the same alleles at all loci, they are said to be vegetatively compatible. If vc cultures are grown on the same agar plate, their hyphae will fuse, a process called hyphal anastomosis, and the cultures will merge into a single culture (Fig 1.2). But when non-vc cultures attempt to anastomose, programmed cell death is triggered, and a visible divide called a barrage zone forms between the cultures[25]. Vegetative compatibility systems are very common in fungi and are thought to prevent cytoplasmically transmitted diseases, such as viruses, and such was the case of CHV-1 application in the United States[26].

It is now apparent that mycoviruses are nearly ubiquitous across all fungal groups[27]. Most have double-stranded RNA (dsRNA) genomes and persist in their host without any apparent symptoms, such as changes in colony morphology, microscopic features,

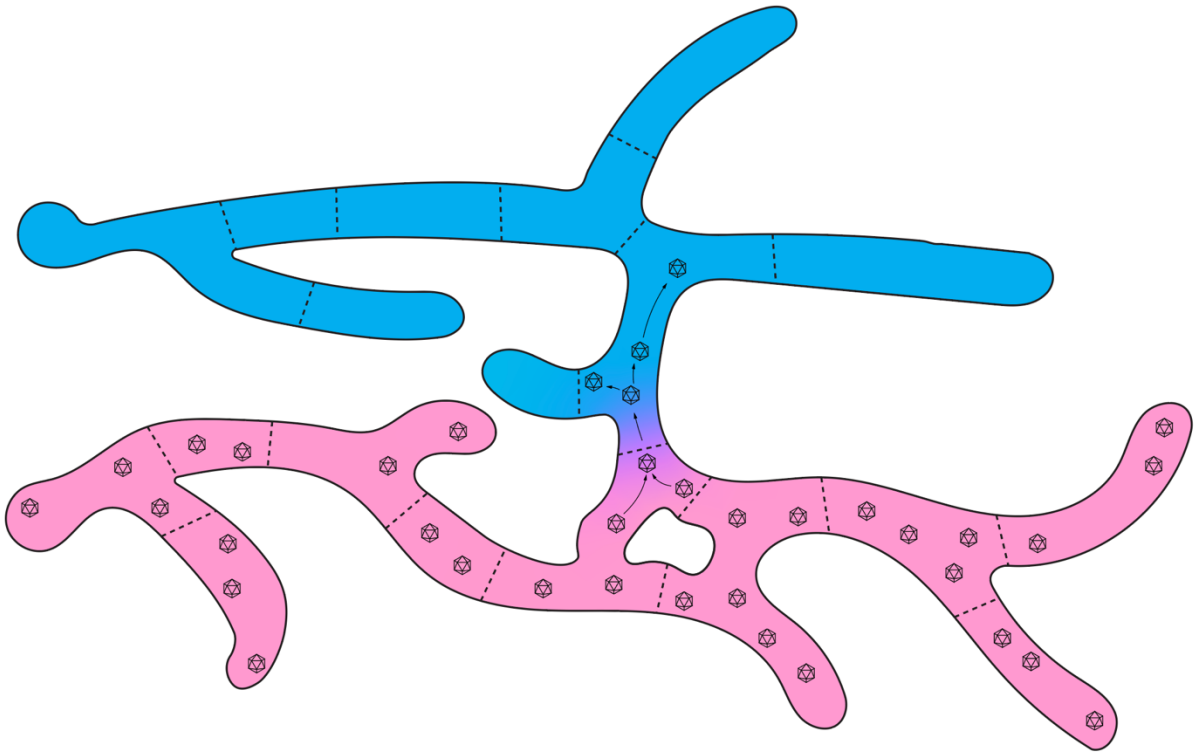

Figure 1.2: Hyphal anastomosis allows transmission of viruses.
The blue and pink cultures are in the same vc group, which allows hyphal anastomosis, or fusion of the hyphae (pink to purple to blue gradient). This allows the transmission of viruses (depicted by icosahedrons) and other cytoplasmic entities (not shown). Dotted lines indicate septa separating neighboring cells.

and growth rates[21,28]. However, some can influence the physiology of their host, including those pathogenic to plants, insects, or humans, making them the subject of intense study[29–35].

Another example of hypovirulence is SsHADV-1, which downregulates virulence factors in its host *Sclerotinia sclerotiorum*, which, in turn, regulates the expression of hormone signaling, circadian rhythm, and defense genes in rapeseed[33]. Experiments were conducted in which SsHADV-1-infected *S. sclerotiorum* was sprayed onto rapeseed, and stem rot decreased by 67.7% and yield improved by 14.9%. On the other hand, mycoviruses can also cause hypervirulence in their hosts, which is undesirable in plant pathogenic fungi but desirable in insect pathogenic fungi, especially if the insect is a pest or is a vector for another pathogen[21]. Some mycoviruses induce or repress the production of mycotoxins. A virus of the wheat pathogen *Fusarium graminearum* causes hypovirulence and reduces its toxin production 60-fold, and a virus of *Aspergillus ochraceus* greatly enhances the production of ochratoxin A, a carcinogenic mycotoxin that can contaminate food and livestock feed[21,36–38].

Some mycoviruses are mutualistic. For instance, *Curvularia protuberata* is an endophytic fungus that lives within the tissues of *Dichanthelium lanuginosum*, a panic grass that grows in Yellowstone National Park. Only when the fungus is infected with a certain mycovirus can the plant and fungus grow in the hot soil, which can reach 65°C[32]. The mycovirus also allows for increased growth rate of the plant and higher drought tolerance. While the molecular mechanism for heat tolerance is unknown, the researchers were able to reproduce the thermotolerant phenotype in tomato plants, which are eudicots, while panic grass is a monocot, suggesting that the mechanism is conserved between the two groups.

For most mycovirus-fungus pairs, the molecular mechanisms behind the modulation of host physiology are unknown. However, for most mycoviruses studied, it involves regulation of gene expression. Regarding hypovirulence, it is possible that the virus is

simply sequestering the resources that the host would have otherwise used to infect its host[21].

Some fungi employ RNA silencing (aka RNA interference (RNAi)) against mycoviruses. In this approach, dsRNAs are recognized by a protein called Dicer and cleaved into small interfering RNAs (siRNAs). siRNAs associate with a protein called Argonaute, among others, and form the RNA-induced silencing complex (RISC). This leads to the degradation, and/or transcriptional or translational repression of homologous sequences (Fig 1.3)[21,39]. Some mycoviruses have evolved mechanisms to repress RNA silencing. For instance, CHV-1 in *C. parasitica* accomplishes this by downregulating the expression of Dicer and Argonaute[40,41]. Some fungi, such as *S. cerevisiae*, lack RNA silencing pathways entirely and instead rely on other antiviral pathways (reviewed in section 1.4), which was perhaps driven by the advantages of having dsRNA virus-dependent killer toxin production (see section 1.3)[42,43].

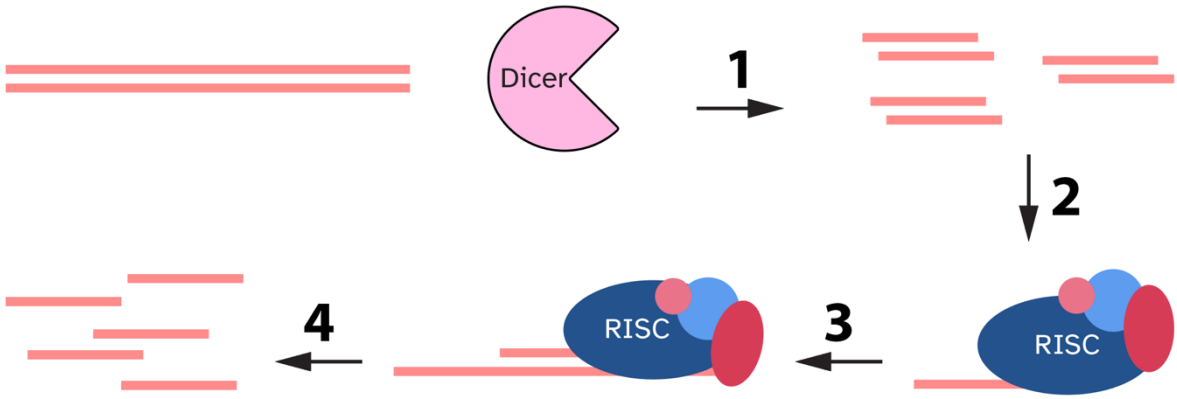

Figure 1.3: A schematic of the basic RNA silencing pathway.
(**1**) Dicer cleaves dsRNA molecules into short (≈20-25 nt) dsRNA molecules called small interfering RNAs (siRNAs). (**2**) One siRNA strand forms a complex with Argonaute and other proteins to form the RNA-induced silencing complex (RISC). (**3**) RISC is targeted to RNA molecules with homologous sequences to the siRNA. (**4**) The homologous RNAs are degraded.

Mycoviruses lack an environmental phase in their replication cycles. However, they are frequently transmitted to new hosts by hyphal anastomosis or transfection to fulfill

Koch's postulates and establish them as the cause of hypo- or hypervirulence or other phenotypic changes[44–54].

1.2 Diversity of mycoviruses, with a focus on partitiviruses

Mycoviruses are identified by two approaches: electrophoresing dsRNAs purified by cellulose chromatography or analyzing transcriptomic data for RNA dependent RNA polymerase (RdRP) sequences[27,55,56]. As of 2023, mycoviruses include 189 species recognized by the International Committee on Taxonomy of Viruses (ICTV), which are classified into 23 families and one unclassified genus[57,58]. Mycoviruses with all genome types have been identified, including (+) ssRNA, (-) ssRNA, reverse transcribing, dsRNA, ssRNA, and dsRNA, and are found in all branches of the Riboviria (RNA virus) phylogenetic tree[27,59]. Mycoviruses infect 81 fungal species from all phyla, including Ascomycota, Basidiomycota, Blastocladiomycota, Chytridiomycota, Cryptomycota, Mucoromycota, Neocallimastigomycota, and Zoopagomycota[60,61]. A 2020 study surveying early diverging fungi lineages analyzed 333 fungal species from all phyla by cellulose chromatography and/or RNA-Seq and found that 21.6% carried at least one virus[27]. Up to 40% of fungal species within a phylum and 88.9% of fungal species within a subphylum were infected. Additionally, coinfection was frequently observed, with a mean number of viruses per host of 2.4, and one fungal species harbored at least 11 distinct viruses. Notably, the phyla were not sampled equally, so rates of viral infection between fungal phyla and subphyla cannot be accurately compared, and the picture of mycoviral prevalence and diversity remains incomplete. While the ecological implications of most mycoviruses are unknown, their hosts fill many niches, including commensals, mutualists, and pathogens.

Partitiviruses (PVs) are unenveloped icosahedral viruses comprising two linear, double-stranded RNA (dsRNA) genome segments that are 1.4-2.4 kbp and are packaged into separate viral particles[62] (Fig 1.4B). The longer segment, dsRNA1, encodes an RdRP, and the shorter segment, dsRNA2, encodes the capsid protein (CP). PV particles measure 25-40 nm and have T = 1 symmetry, composed of 60 homodimeric subunits and contain one to two copies of the RdRP[63]. The 3D structures of five PVs have been

solved, and each has protrusions (P-domains) projecting from the shell (S-domain) of the particle and forms intermolecular interactions between CP monomers[64–70] (Fig 1.4A). Viral transcripts are synthesized in a semiconservative manner and are thought to be extruded through pores at the 5-fold axes into the cytoplasm[71] (Fig 1.4C).

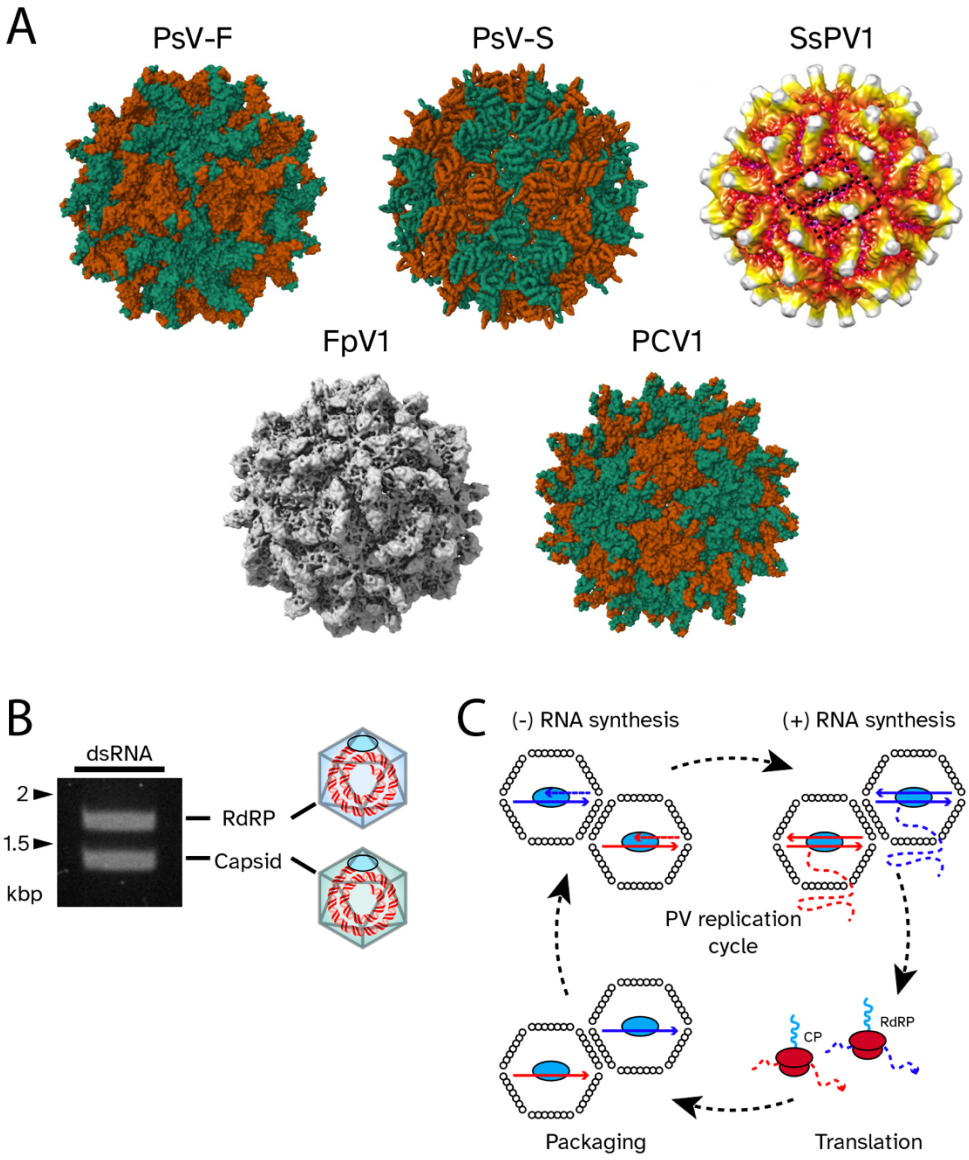

Figure 1.4: Partitivirus capsid structures and replication cycles.
(**A**) Solved partitivirus capsid structures. PsV-F, Penecillium stoloniferum virus F (PDB:3ES5). PsV-S, Penecillium stoloniferum virus S (PsV-S) (PDB: 3IYM). SsPV1, Sclerotinia sclerotiorum partitivirus 1. PCV1, Pepper cryptic virus 1 (PDB:7NCR). FpV1, Fusarium poae virus 1 (EMD: 5161). (**B**) Partitivirus genomes comprise two linear dsRNA molecules that are separately encapsidated. Units are in kilobases. (**C**) Viral (+) ssRNA transcripts are synthesized within the capsid and extruded into the cytoplasm. They are either translated or packaged into new capsids, whereupon the (-) strand is synthesized.

Transcripts are then translated or packaged, whereupon (-) strand synthesis occurs. The PV host range is very broad, including plants, filamentous fungi, and protozoa, and possibly insects[72–75]. PVs have no known extracellular phase to their replication cycle or vector and are transmitted vertically from mother to daughter cell and horizontally by mating[76,77].

There are five genera of *Partitiviridae* officially recognized by ICTV, including *Alphapartitivirus*, *Betapartitivirus*, *Gammapartitivirus*, *Deltapartitivirus*, and *Cryspovirus*, which are demarcated by genome length, host species, and relatedness of the RdRP and CP genes[63,75]. Two more genera of *Partitiviridae* have been proposed, following the discovery of more viruses: *Epsilonpartitivirus* and *Zetapartitivirus*[78,79]. Fungi-infecting PVs are found in all genera, except *Deltapartitivirus* and *Cryspovirus*, which infect plants and protozoa, respectively. Plant-infecting PVs are also found in *Alphapartitivirus* and *Betapartitivirus*. More than a dozen fungus- and plant-infecting PVs are unassigned to a genus due to lack of sequence information.

Many PVs are cryptic and have no apparent effects on their host, and infection is benign. However, some PVs cause altered morphology, a reduced growth rate, reduced conidial formation, and disrupted sexual reproduction in their fungal hosts[51,80–83]. Some PVs may cause hypovirulence in fungal pathogens[70,79,81,84,85], while others cause hypervirulence, such as in the human pathogen *Talaromyces marneffei*[86]. *T. marneffei* is endemic to Southeast Asia and causes penicilliosis in immunocompromised individuals, which is lethal when left untreated[87]. More severe inflammation and higher fungal loads were observed in tissues of mice inoculated with *T. marneffei* infected with a virus called Talaromyces marneffei partitivirus-1 (TmPV1) vs mice inoculated with virus-free *T. marneffei*[28]. In a survival experiment, 10/10 mice inoculated with TmPV1-infected *T. marneffei* died within 20 days, while 2/10 or 3/10 mice inoculated with TmPV1-free *T. marneffei* were still alive at day 90, depending on the isolate of *T. marneffei*.

PVs have also been linked to an increase in the fecundity of another human pathogen, the protozoan *Cryptosporidium parvum*[88]. There have been a few studies investigating how partitiviruses alter host physiology, but the family *Partitiviridae* is, by and large, understudied, and there is little to no understanding of how these viruses evade host antiviral systems. A large factor in this knowledge gap is the lack of a robust model system.

The recent discovery of partitiviruses in *Saccharomyces cerevisiae*, a model organism used to study many cellular processes, including host-virus interactions, presents a unique opportunity to develop a novel model system to fill a knowledge gap in the understanding of partitivirus biology (see chapter 2).

1.3 Viruses and other parasitic genetic elements infecting *Saccharomyces cerevisiae*.

1.3.1 Totiviruses

Totiviruses, members of the virus family *Totiviridae*, are a family of viruses with a broad and diverse host range; they include vertebrate and invertebrate animals, plants, filamentous fungi and yeasts, and protozoa[60,76,89–93]. Species that infect *S. cerevisiae* include ScV-L-A (L-A), the best understood totivirus, and ScV-L-BC (L-BC), both of which have genetically distinct variants[94–97]. They are unenveloped icosahedral viruses comprising one linear, double-stranded RNA genome segment that is ≈4.6 kbp. They both encode a capsid protein, Gag, and a fusion protein of the capsid protein and the polymerase, Gag-Pol, which results from a -1 ribosomal frame shift[98–100]. This controls the ratio of Gag to Gag-Pol and ensures that every capsid incorporates at least one copy of Gag-Pol[101]. The N-terminus of L-A Gag is acetylated by a host protein complex and is essential for virion assembly and viral propagation[102–109]. The L-A and L-BC particles have T = 1 symmetry, with an asymmetric Gag dimer as the unit[110–112]. Replication occurs entirely within the capsid. (+) transcripts are synthesized in a conservative manner and extruded into the cytoplasm and either translated or encapsidated in new viral particles, whereupon (-) strand synthesis occurs (Fig 1.5)[113,114]. While L-A and L-BC do

not cause any obvious pathology, their presence in only 46% of *S. cerevisiae* strains has led to the hypothesis that they have a net detrimental effect on their host[115,116].

1.3.2 Satellite dsRNAs

Killer yeasts produce proteinaceous fungicides called killer toxins (KTs) that inhibit the growth of susceptible yeast cells. While most killer yeast strains have genome encoded KTs, many are encoded by satellite dsRNAs that infect *S. cerevisiae*[116]. Upon synthesis of the preprotoxins in the cytoplasm, they are translocated into the endoplasmic reticulum and transported to the Golgi apparatus, where they are modified by cleavage of the peptide backbone and disulfide bridge formation to form the mature KT, which are then secreted into the extracellular environment[77,117–120].

Satellite dsRNAs are linear molecules that replicate non-autonomously in the yeast cytoplasm[77,121]. They encode neither an RdRP nor a capsid protein but contain packaging and replication signals recognized by Gag and Gag-pol of L-A (Fig 1.5)[29,122,123]. Satellite dsRNAs are less than half the size of L-A, so the L-A capsid can accommodate

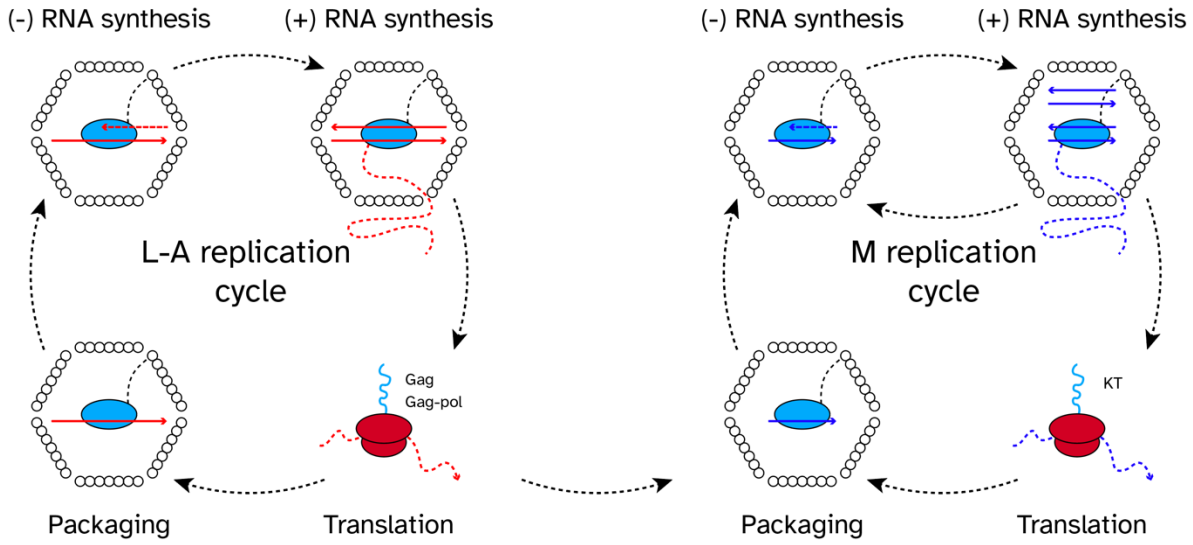

Figure 1.5: A schematic of the replication cycles of L-A and M.
Viral (+) ssRNA transcripts are synthesized within the capsid and extruded into the cytoplasm. They are either translated or packaged into new capsids, whereupon the (-) strand is synthesized. M sequesters Gag and Gag-Pol from L-A for its replication. The L-A capsid can accommodate two M dsRNAs and two rounds of (-) strand synthesis occur before (+) transcripts are extruded into the cytoplasm.

two satellite dsRNA molecules. Generally, a single (+) ssRNA is encapsidated and is the template for (-) strand synthesis. Because the capsid is so spaceous, the (+) transcript is not extruded into the cytoplasm; instead, it templates the synthesis of a second (-) strand. Only then are new (+) strands are extruded into the cytoplasm. This is referred to as head-full replication[77,111,124,125]. It is important to emphasize that M is a satellite dsRNA and is not to be mistaken for a virus nor a satellite virus, an error that many authors make. As defined by ICTV, satellite viruses encode structural proteins, such as capsid proteins and depend on helper viruses for replication only; whereas satellite nucleic acids encode neither structural proteins nor polymerases and depend on helper viruses for both encapsidation and replication.

The best studied satellites are M1 and M28, which encode the K1 and K28 preprotoxins, respectively. After binding to beta-1,6-glucan in the cell wall and Kre1 in the plasma membrane, K1 forms cation-selective pores in the plasma membrane[126,127]. K1 can also trigger apoptosis[128,129]. K28 enters the cell by receptor-mediated endocytosis, travels to the nucleus via retrograde transport, and arrests the cell cycle by inhibiting DNA synthesis[77,130–132]. Immunity to a KT is provided by the preprotoxin[29]. KTs are optimally functional at pH 4.0-5.0 and 20-25°C[133–136].

1.3.3 Narnaviruses

Until recently, *S. cerevisiae* was known to host two narnavirus (naked RNA) species, 20S and 23S[137–139]. They are (+) single stranded RNA (ssRNA) viruses that do not encode a capsid and exist as ribonucleoprotein complexes with their respective RdRP and no additional proteins[138,140–143]. They can coexist in a cell and do not replicate each other's genomes[139,141]. 20S and 23S are associated with dsRNA replication intermediates called W and T elements, respectively, but neither have any known function[142,143]. Due to their low abundance, 5-20 copies per vegetatively growing cell, 20S and 23S are not known to affect host fitness. However, copy number increases to ≈20,000 under sporulation conditions (1% potassium acetate)[77].

Their ability to be expressed, or launched, from a plasmid vector allows their biology to be easily studied[144,145]. For instance, vector studies discovered that narnaviruses possess a terminal repair system[145–147]. When the last two Cs at the viral 3' end in the vector were either eliminated or replaced with other nucleotides, there was no apparent impact on virus generation. However, the terminal Cs were observed in generated viruses, suggesting that they play a crucial role in replication but that the existence of a repair system allows them to be non-essential for the initial launch of the virus. RNA secondary structures have also been discovered: 20S and 23S possess inverted repeats at their 5’ and 3’ termini that form strong stem-loops[146,147].

After finding significant variation in the nuclear, mitochondrial, and 2-micron genomes of the yeast strains of the 100-genomes collection, Vijayraghavan et al. screened the collection for novel viruses and discovered a narnavirus called N1199 (from YJM1199)[148–151]. It was found because it had a very high abundance, enough to be visually observed by electrophoresing total RNAs, which is not possible with 20S and 23S. An RT-PCR screen of the rest of the 100-genomes collection revealed that 98 strains contained N1199 in low copy number, and only one lacked it entirely. Thus, the strains are denoted N1199^{hi}, N11199^{lo}, and N1199^{0}. Experiments showed that N1199^{hi} cells sporulate poorly and have significant growth defects compared to isogenic N1199^{0} cells[150].

1.4 *S. cerevisiae* antiviral systems

1.4.1 RNA turnover and quality control

Turnover and quality control of messenger RNA (mRNA) is important for eliminating aberrant RNAs and regulating gene expression and is an essential process for cell viability. These processes are conserved in eukaryotes. There are several pathways by which an mRNA can be degraded. Generally, a “normal” mRNA will have its poly(A) tail shortened (deadenylation) and then either channeled into the exosome by the Ski complex and degraded 3’-5’ or have its 5’ cap removed (decapping) and be degraded 5’-

3’ by Xrn1 (exoribonuclease 1), if in the cytoplasm, or Rat1 (ribonucleic acid trafficking 1), if in the nucleus (Fig 1.6)[152–163].

There are other degradation pathways that are specialized for different translational aberrancies[164]. The nonsense-mediated decay route is triggered when the cell senses an aberrant translation termination, such as when a frameshift mutation causes a premature stop codon[165–169]. A ribosome that stalls on an mRNA will trigger the no-go decay pathway, resulting in endonucleolytic cleavage[170]. The 5’ fragment is degraded by the exosome, and the 3’ fragment is degraded by Xrn1. mRNAs lacking stop codons will trigger the non-stop decay pathway[171,172].

RNA degradation is highly regulated by many different mechanisms, which are mediated by mRNA-specific features or global cellular conditions. For instance, some sequence-specific mRNA binding proteins promote decapping by recruiting decapping machinery[173,174]. If a cell is under stress, such as during viral replication, mRNAs will accumulate in foci called stress granules, along with associated decapping or deadenylation enzymes. This has the effect of inhibiting initiation of translation[175].

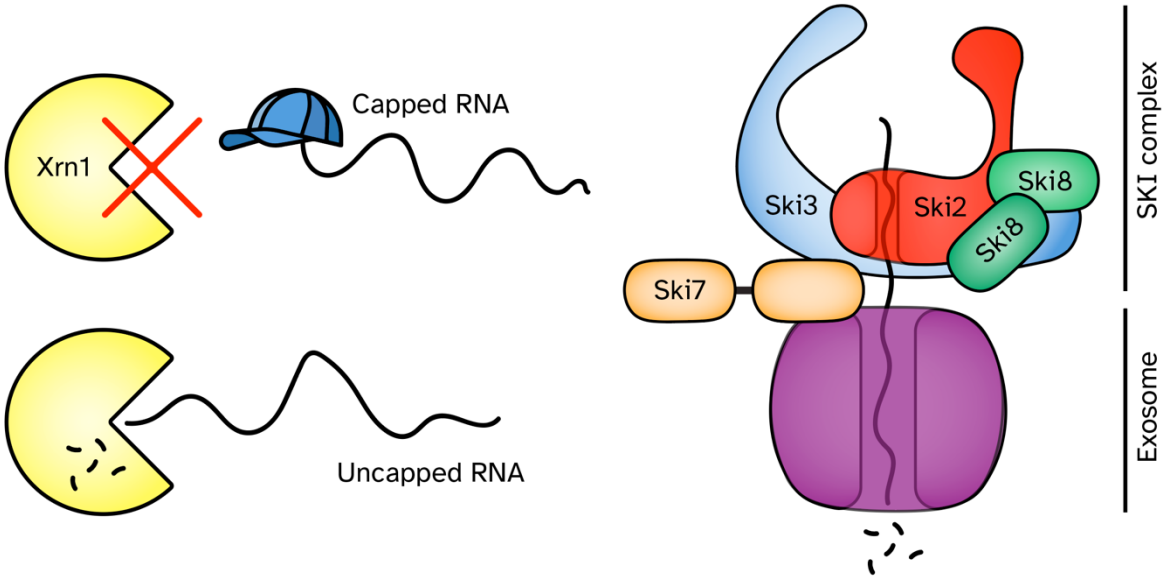

Figure 1.6: The Xrn1-Ski-exosome RNA surveillance pathway.
Decapped RNAs are digested 5’-3’ by Xrn1. Deadenylated RNAs are threaded by the Ski complex into the exosome and digested into mononucleotides.

The SKI (superkiller) genes get their name from the phenotype that results from their deletion or disruption because L-A and M proliferate to a much higher degree, resulting in increased production of killer toxin compared to other killer yeast cells[176–178]. The Ski complex is a heterotetramer comprising one monomer each of Ski2 and Ski3 and two monomers of Ski8 (Fig 1.6)[163,179–181]. Ski2 is a putative helicase that uses ATP hydrolysis to unwind RNA secondary structure and to dissociate bound proteins[164,182]. It also plays a role in suppressing the translation of uncapped mRNAs[183,184]. The exosome comprises nine non-catalytic subunits that are arranged in two layers and form a torus and Rrp44, the enzymatic subunit responsible for digesting RNAs into mononucleotides[185–187]. There is evidence to suggest that the exosome is ancient, as structurally homologous complexes have been found in bacteria and archaea[188–194]. Other proteins may interact with and regulate the exosome, depending on the cellular compartment[163,195,196]. The SKI complex is linked to the exosome via Ski7 and threads deadenylated mRNAs into the exosome core. During no-go decay, the SKI complex binds the small ribosomal subunit and recruits Ski7 and the exosome to mediate RNA degradation[180].

1.4.2 *XRN1* is a species-specific restriction factor in yeasts

Dr. Paul A. Rowley and his colleagues discovered that *XRN1* is a species-specific restriction factor in yeasts[197]. That is, *XRN1* blocks viral replication and propagation. They hypothesized that *XRN1* and components of the SKI complex and exosome have undergone coevolution with L-A as speciation has occurred. And if it had, that it would be under significant constraint since *XRN1* is a crucial component in host RNA metabolism and other processes. Host protein-host protein interactions can be distinguished from host protein-viral protein interactions by comparing the rates of synonymous and nonsynonymous mutations[198]. The former typically have a ratio of ≈1, while the latter will produce a ratio >1, also referred to as positive selection. A ratio <1 is referred to as negative, or purifying, selection. It is important to point out that proteins undergoing positive selection are not necessarily the most important ones in controlling viral replication. Instead, signatures of positive selection identify those proteins that physically

interact with viruses and are “flexible” enough to evolve in response to selective pressure from viruses. These proteins either are required by the virus for its replication or are engaged by the virus to evade the immune system.

The researchers compared sequence data for *XRN1* and SKI and exosome components from *S. cerevisiae, S. paradoxus, S. mikatae, S. kudriavzevii, S. arboricolus,* and *S. bayanus* and used four statistical tests to identify signatures of positive selection. Most of the genes analyzed passed at least one test, but only *XRN1* and *RRP40*, the catalytic component of the exosome, were indicated by all four tests, strongly suggesting that these genes are undergoing positive selection. The role of *XRN1* in L-A restriction was well recognized, so it was analyzed further.

To test whether *XRN1* has undergone rapid coevolution, the researchers first confirmed that L-A copy number decreases when a null strain is complemented with a plasmid-mounted *XRN1* gene under its native promoter. Catalytically dead variants of *XRN1* did not reduce L-A copy number. And complementation with *XRN1* from *S. mikatae, S. kudriavzevii*, and *S. bayanus* (SmXrn1, SkXrn1, and SbXrn1, respectively) did not reduce L-A to the same extent as *S. cerevisiae XRN1* (ScXrn1). To corroborate this, the researchers utilized the satellite dsRNA called M1 that depends upon L-A for its replication and encapsidation. It encodes the K1 killer toxin and produces zones of growth inhibition when grown on a lawn of sensitive yeast. The size of the zone of growth inhibition can be used to infer the degree to which an *XRN1* variant is restricting L-A and/or M1. Transforming *S. cerevisiae xrn1Δ* with SmXrn1, SkXrn1, or SbXrn1 resulted in larger growth inhibition zones compared to the ScXrn1 transformation, indicating relatively greater killer toxin production and thus less restriction of L-A and M. In a third assay, the researchers overexpressed *XRN1* orthologs to test their ability to cure clones of killer toxin production. The heterospecific orthologs cured only 8-12% of clones, while ScXrn1 cured 49% of clones. Loss of L-A and M was confirmed by RT-PCR. These data suggested that *XRN1* has evolved to specifically inhibit the replication of L-A and M and that arms race dynamics have led to signatures of positive selection.

The researchers then examined the other functions of *XRN1*. An *xrn1Δ* strain has a severe growth defect, which was fully recovered when complemented with any *XRN1* ortholog. Each ortholog also confers equal resistance to benomyl, an antifungal drug that destabilizes microtubules. They also produce similar amounts of cytotoxicity when overexpressed. *XRN1* promotes the replication of retrotransposons. No difference in retrotransposition was observed between the *XRN1* orthologs. These data suggested that *XRN1* has the flexibility to coevolve with L-A to restrict its replication and to maintain its ability to perform its other functions.

The researchers then correlated the signatures of positive selection to regions of Xrn1 responsible for species-specific virus restriction. No ScXrn1 structure is available, so the researchers generated one using Phyre, based on its homology with *Kluyveromyces lactis* Xrn1, for which there is a structure. However, it lacks structural data for residues 354-503, 979-1109, and 1240-1528 (ScXrn1 numbering). The statistical tests identified signatures of positive selection in 17 codons, 14 of which fell in the unmodeled region, which has 83% amino acid identity across the *Saccharomyces* genus, compared to the catalytic domain, which has 96% amino acid identity. The remaining three codons are in or near the D1 domain, are surface-exposed, and far removed from the active site. The researchers created Xrn1 chimeras by replacing portions of SkXRN1 with the corresponding portions from ScXRN1. Using the same killer curing assay as above, they found that species-specificity correlates primarily to the D1 domain (residues 731-914) and secondarily to the D2 (915-960 and 1134-1151) and D3 domains (978-1108). The chimeras were functionally equivalent to all Xrn1 orthologs regarding their cellular functions. These data suggest that the interaction domain of Xrn1, including D1-D3, has evolved to direct Xrn1's exonucleolytic activity against L-A.

To test whether Xrn1 interacts with L-A Gag to target uncapped viral RNAs, Xrn1 and Gag were tagged for use in coimmunoprecipitation assays. ScXrn1 and SkXrn1 immunoprecipitated Gag, and Gag immunoprecipitated ScXrn1 and SkXrn1. This interaction was not mediated by ssRNAs, as RNase A digestion had no effect. Repeating the assay with antibodies specific to Gag produced similar results. These results were

surprising because it was expected that positive selection is being driven by interactions between host and viral proteins; therefore, interactions between Xrn1 and Gag may be affected. The researchers had three hypotheses to explain the conflicting results between the different assays. First, it is possible that, instead of Gag being the species-specific target of Xrn1, Gag is antagonizing Xrn1. Second, the species-specificity in the Xrn1-Gag interaction is due to a third component. Third, perhaps coimmunoprecipitation assays are not sensitive enough to distinguish the difference in binding between Gag and Xrn1 orthologs.

To test *XRN1* species-specificity in other yeast species, the researchers searched for and discovered a totivirus in *S. kudriavzevii* and named it SkV-L-A1. It has a similar genome organization to L-A and is more closely related to L-A than to L-BC. The researchers expressed each Xrn1 ortholog and measured the effect on L-A replication. SkV-L-A1 curing was not observed in any clone for any ortholog, even SkXrn1, perhaps because the high-copy plasmids were designed for use in *S. cerevisiae* and cannot express Xrn1 to a high enough level. Using RT-qPCR, they found that SkXrn1 reduced SkV-L-A1 levels by 40%; SmXrn1 and SbXrn1 reduced levels by 13% and 15%, and ScXrn1 reduced SkV-L-A1 levels by 27%. This relatively high restriction makes sense considering the close relatedness of ScV-L-A and SkV-L-A1.

It is still unknown whether the interaction between Xrn1 and Gag is direct or indirect. The researchers speculate the possibility of three scenarios: (1) Xrn1 targets uncapped viral RNAs and competes with Gag as the viral transcripts are extruded into the cytoplasm; (2) Xrn1 targets L-A RNA but is redirected by Gag, and (3) Xrn1 is recruited to sites of viral particle assembly by interacting with Gag monomers[199–201]. Future studies should also determine whether Xrn1 has similarly coevolved with other L-A and M variants that are less laboratory-adapted and more stress tolerant[96,202].

1.4.3 Diverse antiviral systems prevent lethal pathogenesis caused by L-A

Much work done to understand the relationship between *S. cerevisiae* and L-A and M is done by members of the lab of Dr. Marc Meneghini. They first studied the role of

Nuc1 during sporulation[30,203]. Nuc1 is localized to the mitochondria but is released during programmed cell death (PCD), which is triggered in the remnant of the mother cell during meiosis[204,205]. Nuc1 is a highly conserved nuclease and digests DNA into nucleosomal ladders during PCD[206,207].

Deleting both copies of *NUC1* did not affect PCD in yeast, so they hypothesized that it had other targets, such as L-A and M. A significant accumulation of the K1 killer toxin was observed in sporulated *nuc1Δ/nuc1Δ* strains, as well as *ski3Δ/ski3Δ* strains. Unlike the *NUC1* deletions, the *ski3Δ/ski3Δ* strains produce ≈100% inviable spores. This phenotype can be rescued by evicting, or curing, M. The same was observed with *nuc1Δ ski3Δ* spores. The researchers determined that attenuation of M by Nuc1 is due to its nuclease activity because overexpression of the catalytically dead Nuc1-H138A did not rescue the M-dependent *nuc1Δ ski3Δ* synthetic lethality. Interestingly, they found that *ski3Δ* spore clones from *SKI3/ski3Δ* strains were viable (with a slight growth defect), but those from *ski3Δ/ski3Δ* strains were not. This suggested that Ski3 proteins inherited from the mother cell attenuated M. To investigate the role of maternal vs spore autonomous Nuc1 and Ski3, they created *MAK3* deletions. Mak3 is required to maintain M only during mitosis, not sporogenesis, so M will persist until the spores germinate and start undergoing mitosis. A *MAK3* deletion was able to rescue *nuc1Δ ski3Δ* synthetic lethality from *NUC1/nuc1Δ SKI3/ski3Δ* strains in 90% of spores. However, it did not rescue *nuc1Δ ski3Δ* synthetic lethality from *nuc1Δ/nuc1Δ SKI3/ski3Δ* strains. This reveals that maternal Nuc1 and Ski3 are sufficient to attenuate M but Ski3 is not and that both maternal and spore autonomous Nuc1 is important in attenuating killer. The researchers hypothesized that the M-attenuating activity of Nuc1 was required only during sporulation, so they sporulated a *NUC1/nuc1Δ SKI3/ski3Δ* strain containing a plasmid expressing *NUC1*. Mitotically proliferating *nuc1Δ ski3Δ* spore clones readily lost the *NUC1* plasmid but retained M, which was consistent with the hypothesis. Taken together, these data suggest that Nuc1 and the SKI complex act in parallel pathways to prevent M-dependent lethality during sporulation (Fig 1.7).

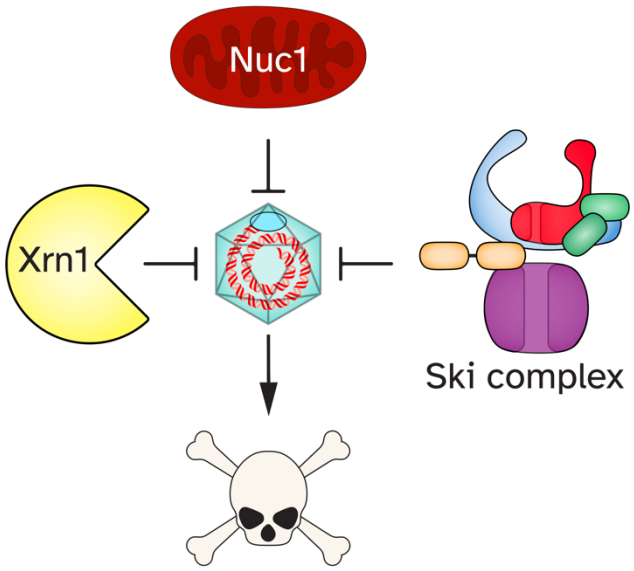

Figure 1.7: Parallel antiviral systems in S. *cerevis*iae.

The researchers also found that, in vegetatively growing haploid yeast cells (i.e., cells replicating by mitosis) containing L-A, single deletions of *NUC1*, *SKI3*, or *XRN1* result in subtle growth defects, observable only at 37°C and when grown on glycerol, which requires functional mitochondria to use as a carbon source[208,209]. However, *nuc1Δ ski3Δ* or *nuc1Δ xrn1Δ* double deletions are conditionally lethal at 37°C, regardless of carbon source. This phenotype could be rescued by evicting L-A. On the other hand, a *ski3Δ xrn1Δ* double mutant is inviable, regardless of temperature, carbon source, or presence of L-A. Overexpression of *XRN1* rescued the conditionally lethal phenotype caused by the *nuc1Δ ski3Δ* genotype.

To identify additional antiviral factors, the researchers searched a genetic interaction database for gene deletions that cause a synthetic growth defect when combined with a *NUC1* deletion. They found 16 candidates, including the 3'-5' RNA exonucleases *REX2* and *MYG1*, both of which have homologs in bacteria and humans. Like the *nuc1Δ ski3Δ* double mutant, the *nuc1Δ rex2Δ* double mutant is associated with growth defects and synthetic lethality at high temperature. The *nuc1Δ ski3Δ rex2Δ* triple mutant was inviable. The *nuc1Δ myg1Δ* genotype had a growth defect but did not cause synthetic lethality at high temperature. The *nuc1Δ ski3Δ myg1Δ* triple mutant was synthetic lethal

at high temperature. Synthetic growth phenotypes were rescued in strains lacking L-A, suggesting that *REX2* and *MYG1* are antiviral factors.

To discover other genes capable of rescuing the *nuc1Δ ski3Δ* growth defect, the researchers performed a suppression screen. That is, they screened for genes whose overexpression suppress, or reverse, the phenotype conferred by *nuc1Δ ski3Δ*. The genes *SRO9, SLF1,* and *PAB1* were identified. Each encodes an RNA-binding protein that associates with the ribosome. *SRO9* and *SLF1* are paralogs and have a homolog in humans that has a recognized role in innate immunity. *PAB1* encodes poly(A) binding protein, a common target of viral inhibition in humans. Overexpression of *SRO9* and *PAB1* reduces levels of Gag, suggesting that they suppress the *nuc1Δ ski3Δ* growth defect by attenuating the replication of L-A. *SLF1* overexpression did not reduce Gag levels, suggesting that it protects the cell from the pathogenic effects of L-A replication.

A previous study noted that deletion of *NUC1* or *SKI* genes resulted in induction of genes involved in the proteostatic stress response, and the researchers hypothesized that it was due to elevated Gag levels. They verified this by fusing GFP to a reporter gene in a flow cytometry assay. Additionally, they found that overexpression of *SRO9* or *PAB1* but not *SLF1* reversed the proteostatic stress response. In a fluorescence microscopy experiment, the researchers then observed foci of protein aggregates in *nuc1Δ ski3Δ* cells. Taken together, these data suggest that the lethal effects of L-A in vegetatively growing cells are due to proteostatic stress.

1.5 Viral subversions of RNA surveillance

Since viral genomes and transcripts lack many host-encoded modifications and are aberrant from the host's perspective, viruses have evolved diverse mechanisms to evade or actively interfere with RNA surveillance mechanisms to protect their transcripts and genomes from degradation[210]. The influenza polymerase endonucleolytically cleaves a host mRNA 10-13 bp downstream of the 5' cap and takes the capped fragment, using it to prime RNA synthesis[211,212]. Flaviviruses, including West Nile virus,

yellow fever virus, and dengue virus, hijack host RNA degradation enzymes to cause pathogenicity. During flavivirus infection, the genomic RNA (gRNA) is introduced into the cytoplasm, whereupon it is attacked by Xrn1. Xrn1 is a highly processive enzyme and digests ≈10 kb of RNA before it is halted by strong secondary structure elements located in the 3' UTR[213–215]. The remaining fragment is called a small flaviviral RNA (sfRNA) and functions in pathogenesis[216–220]. sfRNAs interfere with several immune responses, including RNA silencing, RNA quality control mechanisms, and the type 1 interferon response[214,221–224]. Members of the alphaherpesviruses, gammaherpesviruses, and betacoronaviruses encode proteins that localize to translation complexes and promote host mRNA cleavage and degradation by Xrn1[225–229]. This has the effect of globally decreasing host gene expression, thus reducing the activation of immune pathways. Knockdown and chemical inhibition of *SKI* genes inhibits the replication of influenza A virus, Middle East respiratory syndrome coronavirus, Ebola virus, and Marburg virus, indicating that these viruses hijack the Ski complex and use it to enhance their replication[230]. And a virus could even hypothetically protect its genome by encasing it in a polysome[231].

When it was first observed that L-A and L-BC Gag covalently bind m^7GMP moieties derived from host mRNA 5' caps, it was hypothesized that the decapped mRNA would act as a decoy against Xrn1, allowing the viral transcripts to be translated or packaged[232–237]. However, later evidence showed that Xrn1 requires that its substrates be monophosphorylated[238]; therefore, the diphosphorylated mRNA fragments would be poor decoys. Furthermore, L-A and L-BC deliberately synthesize their transcripts with 5' diphosphates, no matter whether the reaction is primed with nucleotide monophosphates or nucleotide triphosphates[124,238]. Upon their extrusion through pores in the capsid, some viral transcripts receive the 5' cap cleaved from a host mRNA, which are then translated, while transcripts that did not receive a 5' cap are packaged[232–235,239]. Viral 3' termini lack a poly(A) tail[77]. It remains unknown whether the phosphate-metabolizing enzymatic activity is mediated by the totivirus RdRP or a host protein recruited into virus particles. There is evidence that suggests that *S. cerevisiae*

possesses an enzyme with diphosphatase activity that removes the beta phosphate, leaving a 5’ monophosphate[238].

Resistance by 20S and 23S to Xrn1 overexpression was discovered after the researchers noted that transcripts from the launch vector had the native 5’ sequence, even though there were dozens of base pairs between the transcription start site and the start of the 20S or 23S sequence[240]. However, when an *xrn1Δ* strain was transformed with the launch vector, the vector did not generate virus, even though the strain supported the replication of 20S and 23S when introduced by cytoduction. This evidence suggested that Xrn1 was responsible for degrading the initial sequence transcribed from the vector but was impeded by the 5’ stem-loop.

CHAPTER 2: NOVEL VIRUSES OF THE FAMILY *PARTITIVIRIDAE* DISCOVERED IN *SACCHAROMYCES CEREVISIAE*

This chapter has led to one peer reviewed publication: Taggart NT, Crabtree AM, Creagh JW, Bizarria R Jr., Li S, de la Higuera I, Barnes JE, Shipley MA, Boyer JM, Stedman KM, Ytreberg FM, Rowley PA. (2023) Novel viruses of the family *Partitiviridae* discovered in *Saccharomyces cerevisiae*. PLoS Pathog. 19(6): e1011418.

2.1 Introduction

The objectives of the work in this chapter were (1) to determine the prevalence and diversity of *Saccharomyces cerevisiae* partitiviruses, (2) to determine their genome sequence and protein structures, and (3) to determine their relationship to other partitiviruses, with the aim of employing them as a model system for the study of agriculturally and clinically relevant partitiviruses.

Saccharomyces cerevisiae is a very versatile organism and is widely used in commercial applications: in brewing and winemaking, in coffee and cacao bean fermentations, as a leavening agent in baking, as a source of nutrition or probiotic, as a source of CO_2 for aquatic plants, and even as a delivery vehicle for a biopesticide[241–244]. *S. cerevisiae* is also a principal model organism in the study of eukaryotic cell biology and metabolism. Attractive features include its relatively small genome, rapid growth, ease of manipulation, very low pathogenicity, and its similarity to cells of higher eukaryotes, including plants and animals[245,246]. This allows it to host viruses relevant to human health and agriculture, and it has been used to study viral replication, localization of viral proteins, interactions with host proteins, and cellular effects on the host[76,77,247,248]. *S. cerevisiae* also has its own viruses and parasitic genetic elements, including RNA viruses, DNA plasmids, and retrotransposons[76].

Modern RNA sequencing technologies allow the rapid discovery of many novel mycoviruses, including members of the virus family *Partitiviridae* in *S. cerevisiae*, among others[93,95,97,249,250]. Partitiviruses (PVs) are unenveloped icosahedral viruses comprising two linear, double-stranded RNA (dsRNA) genome segments that are 1.4-2.4 kbp

and are packaged into separate viral particles[62]. The longer segment, dsRNA1, encodes an RNA dependent RNA polymerase (RdRP), and the shorter segment, dsRNA2, encodes the capsid protein (CP)[251]. PV particles measure 25-40 nm and have T = 1 symmetry, composed of 60 homodimeric subunits and contain one to two copies of the RdRP[63]. The 3D structures of five PVs have been solved, and each has protrusions (P-domain) projecting from the shell (S-domain) of the particle and forms intermolecular interactions between CP monomers[64–68,252] (Fig 1.4A).

PVs have been found within both Ascomycete and Basidiomycete fungi, as well as plants and protozoans and perhaps insects[72–75]. In late 2021, Crucitti et al. reported the discovery of a novel partitivirus species using a high-throughput RNA sequencing approach[253]. Due to its high identity to CSpV1, a virus in the genus *Cryspovirus* that infects the mammal-pathogenic protozoa *Cryptosporidium parvum*, the authors called the virus species Saccharomyces cerevisiae cryspovirus 1 (ScCV1). PVs have no known natural vector and are transmitted intracellularly[76,77]. Many PVs are cryptic and have no apparent effects on their host. However, some fungal PVs cause altered morphology, a reduced growth rate, reduced conidial formation, and disrupted sexual reproduction[51,80–83]. PVs can also cause hypo- or hypervirulence in pathogenic hosts[70,79,81,84,85]. There have been a few studies investigating how partitiviruses alter host physiology, but the family *Partitiviridae* is, by and large, understudied, and there is little to no understanding of how these viruses subvert or evade host antiviral systems. A large factor in this knowledge gap is the lack of a robust model system. This work describes three species of partitivirus discovered in *S. cerevisiae*, including their independence of the killer yeast phenotype, position within the *Partitiviridae* phylogenetic tree, genome organization, and predicted structures of their RdRPs and CPs, and sets the foundation for establishing *Saccharomyces cerevisiae* partitiviruses as a novel model system for the study of partitivirus biology.

2.2 Results

2.2.1 Partitiviruses identified in S. *cerevisiae*.

To survey the *S. cerevisiae* virome without bias, dsRNAs were extracted from a random selection of 520 strains sourced from the 1,002 Yeast Genomes Project collection and analyzed by short-read sequencing[254]. 110 contigs with significant sequence similarity to known virus families were identified (Fig 2.1A)[133,255]. Contigs with sequence similarity to the *Totiviridae* were the most abundant, followed by satellite dsRNAs (including the *S. cerevisiae* killer toxins K1, K2, and Klus and *S. paradoxus* killer toxins K66 and K21), and the *Partitiviridae*[63]. Other virus families were represented by three or fewer contigs and were not investigated further. One of these was a narnavirus that was detected and described by Mardanov et al[249]. This experiment was performed by Angela M. Crabtree.

To determine the prevalence and diversity of PVs in *S. cerevisiae*, 161 strains from the 1,002 Yeast Genomes Project collection, 146 strains from the collection of Ludlow et al., and three additional strains were screened using cellulose spin chromatography to extract dsRNAs (Appendix C) (with contributions from Josephine M. Boyer, Camden D. Doering, Mason A. Shipley, Nic Hoffman, and Darby Fox)[242,254]. PVs were identified by their characteristic electrophoretic mobility. 44 strains (≈14%) contained PVs, chiefly from the collection of Ludlow et al. (Table 2.1). For example, strains YO858 and Y-5509 each contain three dsRNAs (Fig 2.1B), which were verified to be dsRNAs by RNase III digestion (Fig 2.1C) (performed by Mason A. Shipley). They likely represent a ≈4.6 kbp monopartite totivirus genome and a ≈1.5 kbp bipartite partitivirus genome encoding an RdRP (dsRNA1) and CP (dsRNA2). Reverse transcription-PCR (RT-PCR) was used to verify the presence of PVs in total nucleic acid extracts (Fig 2.1D). RT-PCR without the RT enzyme added failed to amplify PV sequences, and the yeast chromosomal gene *UBC6* was amplified in all samples. *S. cerevisiae* strain BJH001 does not contain PVs and was included as a negative control[255].

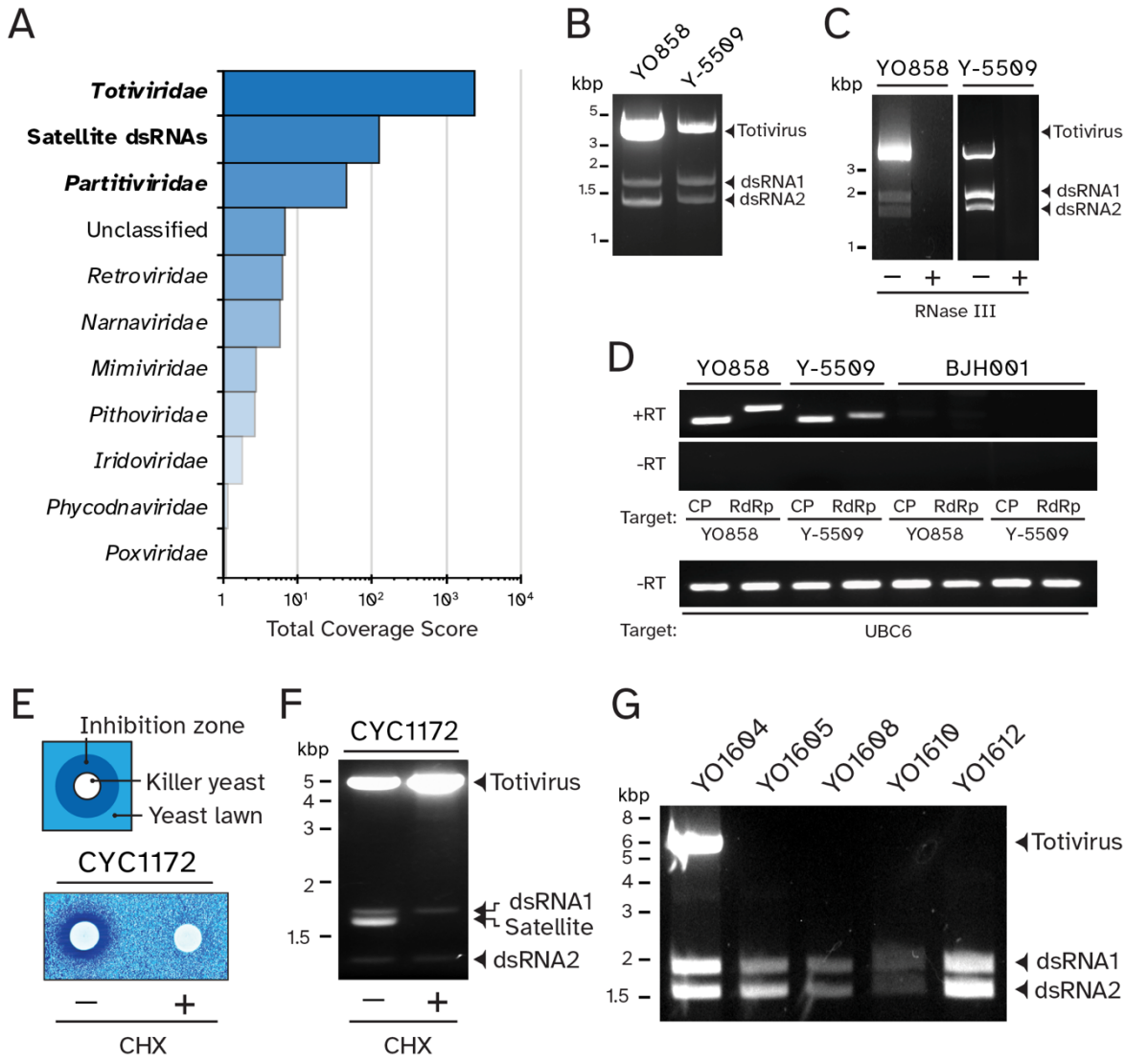

Figure 2.1: The identification of PVs in *S. cerevisiae*.
(**A**) Virus contigs were assembled from the sequencing of dsRNAs extracted from 52Ø strains of *S. cerevisiae*. (**B**) Agarose gel electrophoresis analysis of dsRNAs extracted from two PV-infected strains of *S. cerevisiae*. (**C**) dsRNAs extracted in panel B were subjected to incubation at 37°C with and without RNase III, and the resulting products were analyzed by agarose gel electrophoresis. (**D**) Two-step RT-PCR of total nucleic acids extracted from *S. cerevisiae* targeting the CP or RdRP genes with (+RT) or without (-RT) reverse transcriptase. Strain BJH00Ø was used as a negative control as it does not harbor PVs. Primers targeting the yeast gene *UBC6* were used as a PCR-positive control for genomic DNA. (**E**) *Top* Schematic of a killer toxin production by a killer yeast strain with a zone of growth inhibition. *Bottom* Killer activity of strain CYC1172 before and after treatment with cycloheximide (**F**) Electrophoretic mobilities of dsRNAs extracted from CYC1172 before and after treatment with cycloheximide. (**G**) Agarose gel electrophoresis of dsRNAs extracted from selected strains of *S. cerevisiae* that contained either a totivirus and PV (lane 1) or only a PV (lanes 2–5).

Table 2.1: The prevalence of viruses in 310 strains of *S. cerevisiae*.

Type of dsRNA	Number of strains	% prevalence
Totiviruses	129	42
Satellites	63	20
Partitiviruses	44	14
ScPV1*	25	57
ScPV2*	32	73
ScPV3*	2	5

* Total number of ScPVs is higher than the number of *S. cerevisiae* strains due to virus coinfection.

dsRNAs smaller than ≈4 kbp have historically been associated with dsRNA satellites, which often encode toxins capable of killer other yeast cells[76,77]. A totivirus and three low molecular weight dsRNAs were discovered in *S. cerevisiae* strain CYC1172 (Fig 2.1F), suggesting co-infection of a totivirus, a dsRNA satellite, and a partitivirus. The putative partitivirus was verified not to be a satellite by treating CYC1172 with cycloheximide, a protein synthesis inhibitor that can cause the selective loss of satellite dsRNAs (Fig 2.1E) (performed by Josephine M. Boyer)[256]. Colonies that did not produce a zone of growth inhibition in a killer assay lost one of the low molecular weight dsRNAs, but the other two remained (Fig 2.1F). Furthermore, 15 yeast strains (4.4%) were later discovered that contained partitiviruses but not totiviruses, supporting the independence of partitiviruses from totiviruses and the killer yeast phenotype (Fig. 2.1G). ScPVs were especially abundant in coffee strains (25/44 (57%), Fisher's exact test $p<0.01$) and cacao strains (16/44 (36%), Fisher's exact test $p<0.01$) (Fig 2.2A) (Appendix C). Only three ScPV+ strains (Y-55009, CYC1172, and ICV D254 Lalvin) had other origins (coconut pods and grape must).

2.2.2 S. *cerevisiae* PVs are most closely related to Cryptosporidium parvum virus 1.

Short-read sequencing was used to produce the complete RdRP and CP ORFs of 14 ScPVs (Fig B.1 and Appendix E). The length of the genome segments and proteins of each partitivirus is within a range characteristic of its genus, and ScPV proteins were the smallest of all PVs, except the RdRPs of genus *Deltapartitivirus* (Fig 2.2B). RdRP

sequences from 14 ScPVs and 45 representative PVs, including two from unofficial *Partitiviridae* genera, were aligned to generate a phylogenetic tree, using maximum likelihood (performed by Dr. Paul A. Rowley). The ScPVs were clustered in a monophyletic group, with the protozoan *C. parvum* partitivirus as its most closely related outgroup (Fig 2.2C). The percent amino acid identity between ScPV and CSpV1 RdRPs ranged from 33 to 38%, and the CPs ranged from 17 to 23% (Appendix F).

Individual ScPVs clustered into three clades, suggestive of three distinct species, which were named Saccharomyces cerevisiae partitivirus 1, -2, and -3, represented by the ScPVs infecting strains Y-55009 (ScPV1-55009), YO858 (ScPV2-858), and CYC1172 (ScPV3-1172). The RdRP and CP percent amino acid identities between the species is far less than 90%, supporting their categorization as distinct species (Appendix F)[75].

ScPV3-1172 bears a 98.78% amino acid sequence identity to the partially sequenced PV species called Saccharomyces cerevisiae cryspovirus 1 (ScCV1). ScCV1 was discovered by Crucitti et al. in two European winemaking strains: ICV D254 Lalvin (D254) and Uvaferm 43 (U43)[253]. While their publication predates that of Taggart et al., 2023, partitiviruses had been discovered in *S. cerevisiae* several years previously by members of the Rowley lab, which had been presented at conferences[69,257]. In this work, when dsRNAs were extracted from strains D254 and U43 and electrophoresed to verify the data of Crucitti et al., none were observed in U43. D254 contained a band associated with totiviruses, two bands associated with partitiviruses, and perhaps a band associated with satellite dsRNAs, as expected (Fig 2.3).

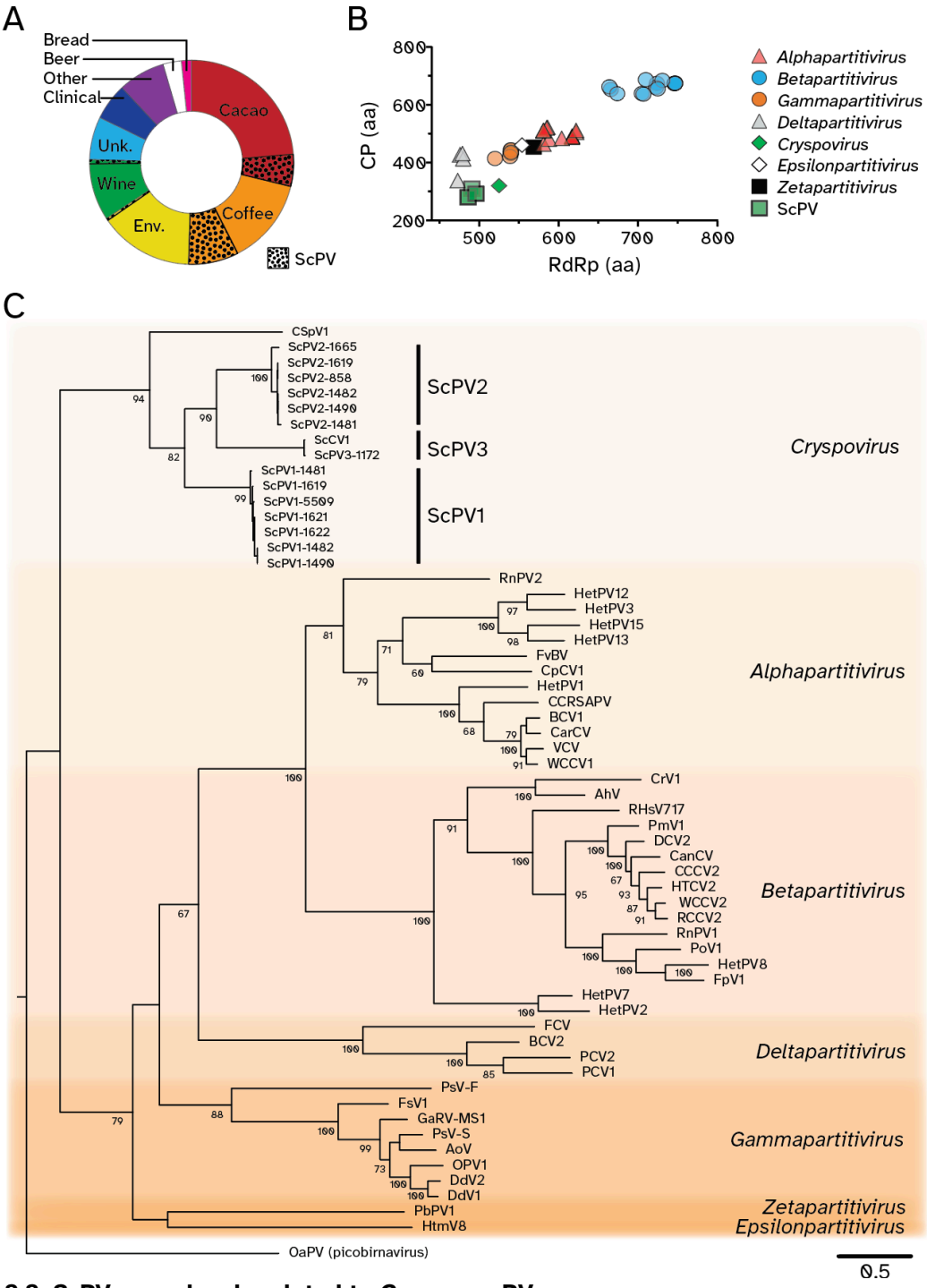

Figure 2.2: ScPVs are closely related to *C. parvum* PVs.

(**A**) Strains of *S. cerevisiae* isolated from different sources and the proportion infected with ScPVs (dotted regions). (**B**) Comparing the protein lengths of RdRPs and CPs of diverse PVs to ScPV1-5509, SCPV2-858, and ScPV3-1172. (**C**) A PhyML maximum likelihood phylogenetic model of the relatedness of PVs based on the amino acid sequence of the RdRP[330]. The RdRP from the picobirnavirus OaPV was used as an outgroup. The numbers at each node are the bootstrap values from 1000 iterations. The scale bar represents the distance of one amino acid substitution per site. The amino acid sequences in the phylogeny are from the viruses listed in S7 Table.

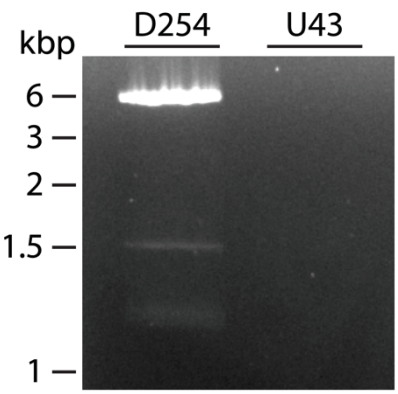

Figure 2.3: Electrophoresis of dsRNAs extracted from *S. cerevisiae* strains D254 and U43.

Furthermore, Crucitti et al. claimed to have submitted all sequences to NCBI (GenBank accession numbers OK412913-OK412915), but the primer sequences, in combination with the full sequence for ScPV3-1172 reported in Taggart et al., 2023 and close attention to detail, reveal that they omitted some data[69]. The primers used to sequence dsRNA1 amplify a 1639 bp sequence, yet the submitted sequences are 1586 bp and 1553 bp for the ScCV1-D254 and ScCV1-U43 isolates, respectively. And the submitted sequences for dsRNA2 are 1048 bp and 1052 bp vs the 1073 bp PCR amplicon. Excerpts of a multiple sequence alignment of the primers, ScCV1-D254, ScCV1-U43, and ScPV3-1172 are found in Figure 2.4. 55 nucleotides from four out of 12 primers hybridize within those missing bases. Furthermore, an additional 9 nucleotides from two primers match neither ScCV1-D254 nor ScCV1-U43. 59 of the total 64 anomalous nucleotides match the sequence of ScPV3-1172.

```
Primer              ScCV1-RdRp-I-f           ScCV1-RdRp-REV
Virus-primer id     !!!!!!!!!!!!!!!!!!!!     ***-**-**************
Primer sequence     CAGATACCATGTTATTTTCCGG    GCCTGTCACACCTGCTATTG
ScCV1-D254-dsRNA1   ----------------------    GCCTGTCACACCTGCTATTG
ScCV1- U43-dsRNA1   ----------------------    GCCCGTTACACCTGCTATTG
ScPV3-1172-dsRNA1   cagataccatgttattttccgg    GCCCGTTACACCTGCTATTG
Virus id                                        -  -
Position            28                        552

Primer              ScCV1-RdRp-II-f          ScCV1-RdRp-II-r
Virus-primer id     -*************!*!!!!!!    *********-!!!!!!!!!!!!
Primer sequence     GTTAATGGATCTTTGTTCGTCG    cagtgcgtaatccttaaagacg
ScCV1-D254-dsRNA1   GTTAATGGATCTTTCTGATCTT    cagtgcgtatc-----------
ScCV1- U43-dsRNA1   ATTAATGGATCTTTCTGATCTT    ----------------------
ScPV3-1172-dsRNA1   ATTAAT GGATCTTTCCGATCT    cagtgcgtaatccttaaagacg
Virus id            -              -
Position            858                       1645

Primer              ScCV1-CP-I-f             ScCV1-CP-FW
Virus-primer id     !!!!!!!!!!!!*********    ***!****************
Primer sequence     ATTTGCAGTTATTCAGTAGCG    CCTGCCTCAAATCCTCCTGG
ScCV1-D254-dsRNA2   -------------cagtagcg    CCTACCTCAAATCCTCCTGG
ScCV1- U43-dsRNA2   ------------tcagtagcg    CCTACCTCAAACCCTCCTGG
ScPV3-1172-dsRNA2   atttgcagttattcagtagcg    CCTGCCTCAAATCCTCCTGG
Virus id                                        -       -
Position            127                       814

Primer              ScCV1-CP-II-r
Virus-primer id     **************!!!!!!!!!!
Primer sequence     CGTACAACGAAGTAACGAAGAGTG
ScCV1-D254-dsRNA2   cgtacaacgaa-------------
ScCV1- U43-dsRNA2   cgtacaacgaagta----------
ScPV3-1172-dsRNA2   cgtacaacgaagtaacgaagagtg
Virus id                      -------------
Position            1176
```

Figure 2.4: Multiple sequence alignment of ScCV1-D254, ScCV1-U43, ScPV3-1172, and primers from Crucitti et al.
Mismatches between ScCV1-D254, ScCV-U43, or ScPV3-1172 are denoted by '-'. For ease of reading, matches are not denoted. Mismatches between either ScCV1-D254 or ScCV-U43 and a primer are denoted by '-'. Matches between ScCV1-D254, ScCV-U43, and a primer are denoted by '*'. Mismatches between a primer and both ScCV1-D254 and ScCV-U43 are denoted by '!' and are bolded. Lowercase letters in the virus sequence indicate an untranslated region, and uppercase letters indicate an open reading frame. Primers with no mismatches have been omitted.

2.2.3 ScPVs have similar genome organization to other partitiviruses

After identifying 44 ScPV+ *S. cerevisiae* strains using dsRNA extractions, short-read sequencing and RT-PCR were used to determine which ScPV species each strain contained (Table 2.1 and Appendix G). Eight strains contained only ScPV1; 16 strains contained only ScPV2, and 16 strains were coinfected with ScPV1 and ScPV2. ScPV3 was

found only in two European wine strains. ScPV1 and ScPV2 coinfection was confirmed by resolving doublets of dsRNA1 in high percentage agarose (Fig 2.5).

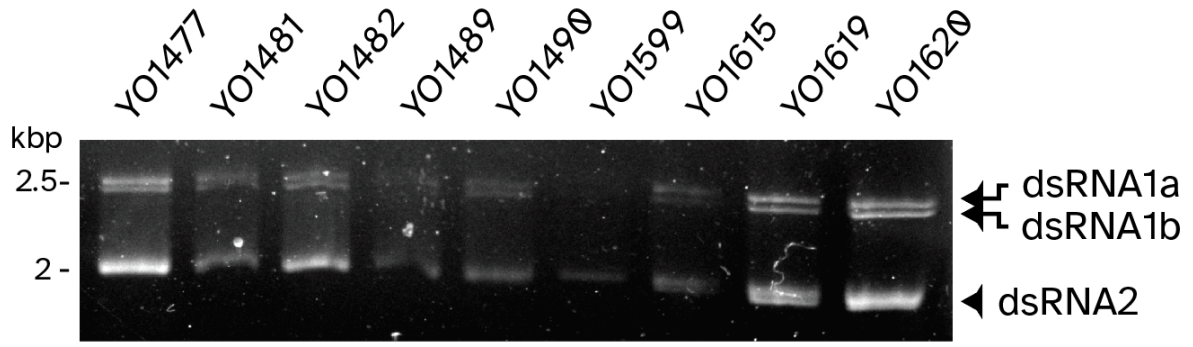

Figure 2.5: Gel electrophoresis of dsRNAs isolated from strains of S. *cerevisiae* that are coinfected with ScPVs.
To corroborate the results of the multiplex RT-PCR screen, dsRNAs from nine strains were extracted and electrophoresed in a 3.2% agarose gel slab at 140V for 245 min and stained with 0.5 µg/mL ethidium bromide for 40 min.

The complete sequences of ScPV1-5509, ScPV2-858, and ScPV3-1172 were obtained using 5' rapid amplification of cDNA ends (5' RACE) (Fig 2.6A and Appendix A) (performed in large part by Angela M. Crabtree)[258,259]. ScPV genomes are organized similarly to CSpV1 and have similar length ORFs and untranslated regions (UTRs). Analysis of the ScPV 3' UTRs using mFold revealed extensive secondary structure in dsRNA2 (Fig B.2) (performed by Dr. Paul A. Rowley). Each virus has a unique sequence element (CSE) in their 3' UTRs that are conserved between the segments (Fig 2.6B)[260]. The CSEs of CSpV1, ScPV1-5509, and ScPV2-858 are 39 bp, 32 bp, and 40 bp, respectively, and all are 100% identical between each segment. ScPV3-1172's CSE is 36 bp but has only 84% identity between each segment. The CSEs of each species have no homology to each other, but they are all predicted to form small stem-loop structures that may be involved in viral RNA replication or packaging. Additionally, the 5' UTRs have extensive secondary structure (Fig 2.6A and Fig B.2).

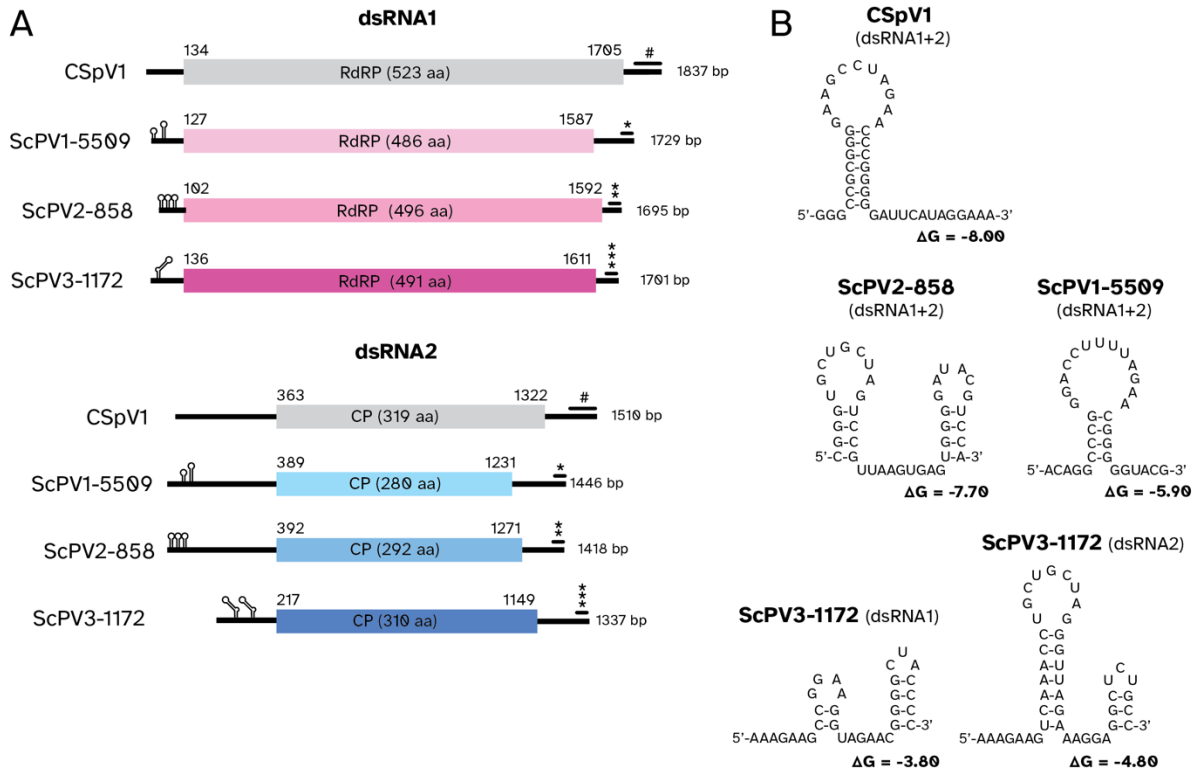

Figure 2.6: Genome organization of PVs from *S. cerevisiae*.
(A) Schematic representation of dsRNA1 and dsRNA2 of three species of PV from *S. cerevisiae* as well as CSpV1. The ORFs are represented as rectangles that encode the RdRP and CP. Stem-loop structures are annotated to represent similar structures in the 5' UTRs of each species (S3 Fig). #/*/**/*** represent the pairs of CSE sequences in the terminal 3' UTRs (B) Secondary structure of RNA sequence present in the 3' CSE of dsRNA1 and dsRNA2 of CSpV1, ScPV1-5509, ScPV2-858, and ScPV3-1172.

2.2.4 ScPVs assemble spherical particles with structural similarity to the PV shell domain.

To verify that ScPVs assemble viral particles, viral particles were purified by PEG precipitation and sucrose gradient fractionation from an *S. cerevisiae* infected with only ScPVs. Smooth, spherical virus-like particles with a diameter of ≈30 nm were observed under TEM (Fig 2.7A). Dr. Shunji Li aided with the particle purification, and Dr. Ignacio de la Higuera (Center for Life in Extreme Environments, Portland State University) performed the microscopy.

Tertiary structure predictions of ScPV and CSpV1 CP monomers were generated ab initio using AlphaFold2, with confidence of up to 80% but sharply declining after ≈150 residues (Fig B.3). Low confidence in the C-terminus may be explained by intrinsic

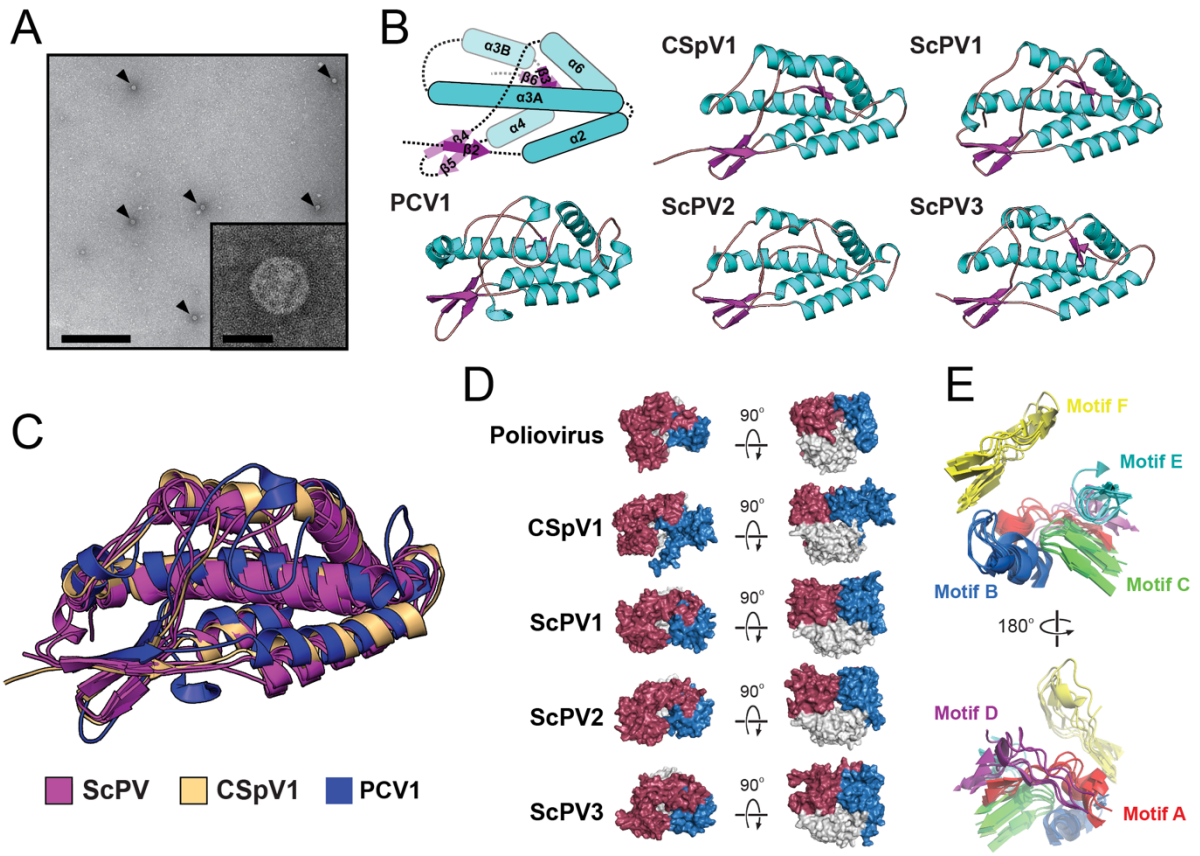

Figure 2.7: The ScPV CP and RdRP share structural similarities with PVs and poliovirus. (**A**) Visualization of ScPV1 and ScPV2 particles by TEM as indicated by arrowheads. Scale bars are 500 nm (main image) and 25 nm (inset). (**B**) Molecular modeling using AlphaFold2 and energy minimization of the S-domain of three species of ScPV and CSpV1 compared to the solved structure of PCV1 (PDB:7ncr). The α-helices (blue rectangles) and β-sheets (magenta arrows) are labeled according to their common positioning within the S-domains. (**C**) An overlay of the five structures represented in panel B. (**D**) Molecular models of CSpV1, ScPV1, ScPV2, and ScPV3 RdRPs generated by comparison to poliovirus 1 RdRP (PDB:1ra6). Red, fingers domain; Blue, thumb domain; White, palm domain. (**E**) A superimposition of the RdRP conserved catalytic motifs A-F of poliovirus 1, CSpV1, ScPV1, ScPV2, and ScPV3. Red, motif A; Blue, motif B; Green, motif C; Purple, motif D; Cyan, motif E; Yellow, motif F.

disorder (ID), or the absence of stable secondary and tertiary structure under physiological conditions (Table 2.2 and Fig 2.8). The probability of each residue being disordered was calculated using NetSurfP–3.0[261]. In contrast, the RdRPs have only 1-4 residues with a >50% probability of being disordered.

Table 2.2: Number and proportion of disordered and basic residues in PV capsids.

Virus	Len	N-term ID aa	C-term ID aa	Max probability	Overall % basic aa	% basic aa amongst ID aa
CSpV1	319	2	9	78%	21.0	32.0
ScPV1-5509	280	6	18	75%	18.2	33.3
ScPV2-858	292	1	38	94%	19.4	28.2
ScPV3-1172	310	4	42	96%	20.4	21.7

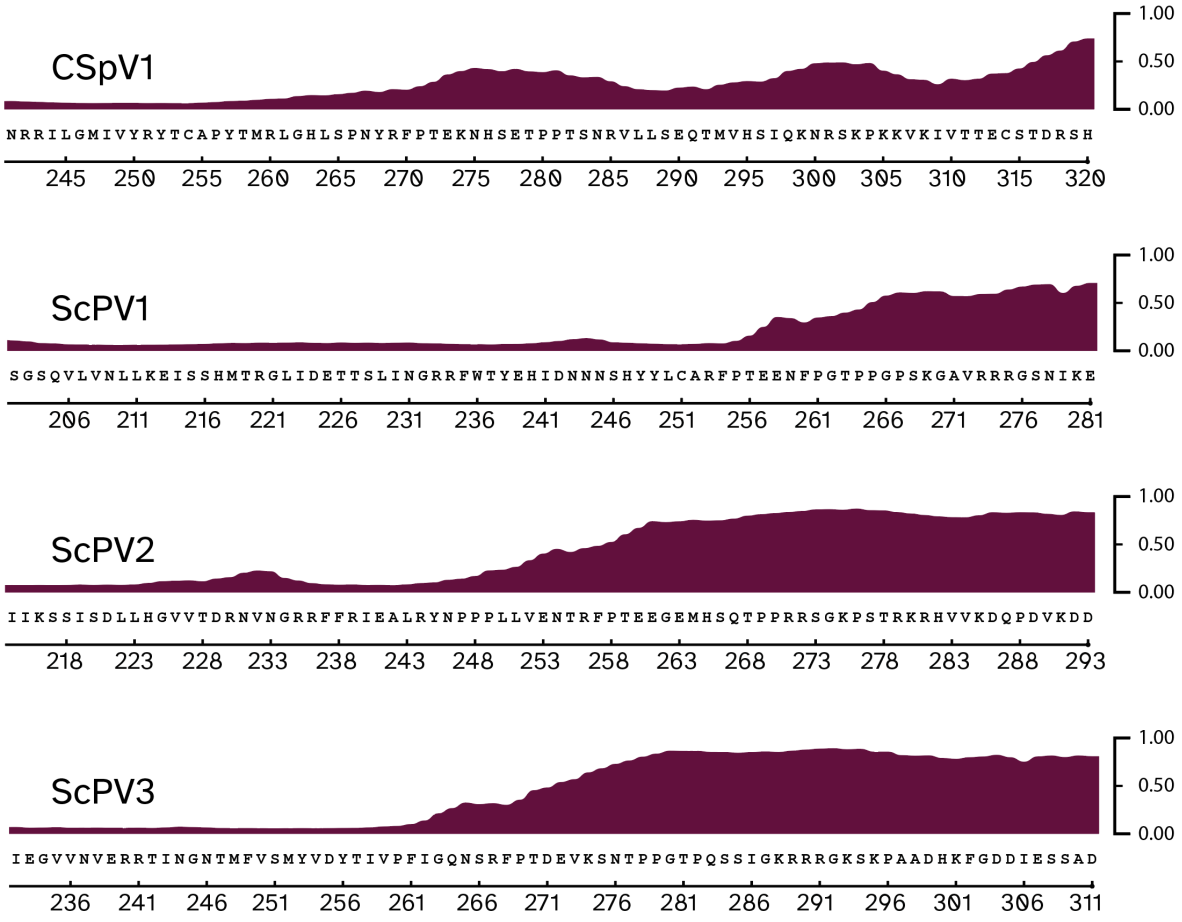

Figure 2.8: Probability of disordered residues in PV capsid 3' termini.
The last 80 residues of the capsid of CSpV1, ScPV1-5509, ScPV2-858, and ScPV3-1172 are plotted. Thickness of the maroon line is the probability of that residue being disordered.

Energy minimization yielded an average 81.7% Ramachandran-favored residues and a 2.2 Å average molprobity (Fig B.4 and Appendix I). The N-terminal domain comprised mostly α-helices and was typical of PVs: four short α-helices, (α2, α4, α5, and α6),

cradled a longer α3-helix, forming a rhomboid shell domain (S-domain) (Fig 2.7B). DALI searches indicated that the ScPV CP has structural similarity to the CP of pepper cryptic virus 1 (PCV-1; PDB:7ncr), having an average root mean squared deviation (RMSD) of 4.34 Å (Fig 2.7C). Superimposition of a ScPV CP monomer on a PCV1 particle indicates that the majority of the particle structure may be composed of the ScPV S-domains (Fig B.5). Due to the low confidence modeling prediction for the C-terminal domain, it is unclear whether ScPVs capsids have P-domains. Protein structure models were produced by Jack W. Creagh.

2.2.5 ScPV RdRPs share structural homology with that of poliovirus.

Tertiary structure predictions of the RdRPs of ScPV1-3 and CSpV1 were generated using the same method as above (performed by Jack W. Creagh). All models had at least a 95% confidence score across their entire sequence (Fig B.3). Energy minimization yielded an average 93.5% Ramachandran favored residues and a 1.20 Å average molprobity (Fig B.4 and Appendix I). Each model included the fingers, palm, and thumb domains that are characteristic of viral RdRPs, and the tertiary structures were similar to the RdRP of human poliovirus (PDB:2ijd-1 and PDB:1ra6, average RMSD <3.1 Å) (Fig 2.7D)[262–265]. Furthermore, motifs A-F aligned well between ScPV1-3, CSpV1, and poliovirus (Fig 2.7E and Fig B.6). The similarity between ScPV and poliovirus RdRPs supports the common ancestry of *Partitiviridae* and *Picornaviridae* within the *Pisuviricota* phylum.

2.3 Discussion

In summary, three species of partitivirus were discovered in *S. cerevisiae* (Fig 2.1) and were named Saccharomyces cerevisiae partitivirus 1, -2, and -3 (Fig 2.2C). ScPV1 and ScPV2 are predominantly found in yeasts from coffee and cacao fermentations, while ScPV3 is found in winemaking strains (Fig 2.2A). ScPVs are most closely related to Cryptosporidium parvum virus 1 (CSpV1) (Fig 2.2C) in genus *Cryspovirus* and have similar genome organization to other partitiviruses (Fig 2.6A). ScPVs have significant predicted secondary structure, which is hypothesized to play roles in packaging and

replication (Fig 2.6B). Viral particles were purified and imaged by electron microscopy, which revealed a capsid surface lacking obvious protrusions (Fig 2.7A). The N-terminus of the CP is predicted to have similar folds to those of other partitiviruses (Fig 2.7B and 2.7C), and the C-terminus is predicted to be intrinsically disordered (Fig 2.8). The models of the ScPV RdRPs are structurally homologous to those of other RNA viruses and contain the conserved domains and catalytic motifs (Fig 2.7D and 2.7E).

This study marks the first detailed characterization of novel dsRNA viruses found within *S. cerevisiae* in nearly half a century[114]. These viruses belong to the *Partitiviridae* family and are the first discovered in yeasts[253,257]. *Saccharomyces cerevisiae* partitiviruses (ScPVs) are almost always found in coffee and cacao strains from four genetically different yeast populations (South American and African cacao, South American and African coffee). Evidence suggests that admixture has occurred between these populations due to human migrations and agricultural practices[242]. ScPV3 stands out because it has solely been identified in European winemaking strains, suggesting either a separate lineage of ScPVs or crossbreeding and introduction from coffee and cacao strains. The fermentation of coffee and cacao beans by diverse yeast and bacterial species, including genetically diverse *S. cerevisiae* strains, is employed to break down the carbohydrates and proteins in the bean mucilage, which may facilitate the introduction of viruses into new yeast populations, owing to more frequent outcrossing[243,266]. However, the prevalence of ScPVs may also owe to the advantages they confer to *S. cerevisiae* during the fermentation process. Commercially available coffee and cacao beans result from successful fermentation and possess desirable flavor profiles, making it intriguing to investigate failed fermentations to determine the effects of ScPV infection. On the other hand, it is plausible that coffee and cacao strains are simply more susceptible to viral infection than other yeast lineages[30,182,197,267–270].

ScPVs are most closely related to PVs of the genus *Cryspovirus* but meet several of the criteria set by ICTV to classify them in a genus distinct from *Cryspovirus*. First, CSpV1 infects a protozoan, and ScPVs infect a yeast. Second, ScPV genome segments (dsRNA1: 1995-1729 bp; dsRNA2: 1337-1446 bp) and proteins (RdRP: 486-496 aa; CP:

280-310 aa) are shorter than those of CSpV1 (dsRNA1: 1837 bp; dsRNA2; 1510bp; RdRP: 523 aa; CP: 319 aa). Third, ScPV RdRPs form a phylogenetic group separate from the CSpV1 RdRP, even though the amino acid sequence identities are 32.7-37.7%, which is above the 24% cutoff stipulated by ICTV[75]. So, it is possible that the taxonomic organization of *Partitiviridae* changes following the discovery of ScPVs. Indeed, *Cryspovirus* was initially proposed to distinguish it from plant infecting *Partitiviridae* genera[271].

This close relationship is suggestive of horizontal transfer of PVs between yeasts and protozoa. *Cryptosporidium* spp. can produce chronic infections and have been in close connection with humans and livestock for several millennia[272]. And yeast propagates to high cell densities during fermentation. Thus, the mammalian gut could have provided an environment that brought protozoa and yeast together, enabling horizontal virus transfer. Furthermore, despite PVs lacking genes involved in mobilization, extracellular transmission has been observed under laboratory conditions in both fungi, plants, and protozoa[48,54,273–276]. Further endeavors aimed at characterizing viruses found in fungi and protozoa will be essential for gaining insights into the evolutionary roots of partitiviruses and the extent to which they are transmitted across different biological kingdoms.

ScPV capsids have high structural homology to those of PVs, especially PCV-1, despite lacking obvious P-domains, having no sequence homology, and being the smallest PV capsids[64]. The S-domains of other CPs are larger, owing to extended loops between helices. P-domains can either interrupt the continuity of the S-domain or compose C-terminal extensions[65–68]. ScPV CPs are ≈100 residues in length, which would be enough to form a P-domain, which are ≈80 residues long, if it were not for the fact that many of the C-terminal residues are predicted to be intrinsically disordered (Fig 2.8). This is supported by the observation of a smooth particle morphology (Fig 2.7A).

Unlike host proteins, which evolve in response to the selective pressure of thermodynamic stability, viral proteins evolve in response to the selective pressure exerted by

host antiviral systems. They must be versatile and capable of adapting to changes in their environment[277]. One solution is intrinsic disorder (ID), or the absence of stable secondary and tertiary structure under physiological conditions. ID has a recognized role in protein interactions with other proteins, nucleic acids, and other biological molecules, as well as enzyme catalysis, and is abundant in viral proteins[277–279]. For instance, ID is associated with particle assembly and stability, packaging of genomic segments, and particle maturation[277].

X-ray crystallography and cryo-electron microscopy experiments have revealed the capsid structures of five partitivirus capsids to date. Three have disordered N-termini, including 28-41 residues[64–66]. The cryo-EM structure of Penicillium stoloniferum virus-F (PsV-F) shows that its 41 N-terminal residues form a domain that is inserted into the capsid and interacts with the viral genome. Pepper cryptic virus-1 (PCV-1) has an additional disordered region that includes residues 329-378. This contrasts with ScPVs, which have very few N-terminal residues with a >50% probability of being disordered and instead have disordered C-termini. The disordered regions of ScPV1 and ScPV2 are enriched in basic residues relative to the entire protein but not to the same extent as PsV-F (24% vs 11%). The ScPV3 disordered region is not enriched in basic residues. The authors speculate that the basic residues allow the N-terminus to interact with RNA and facilitate packaging of genomic segments. Ostensibly, FpV1 and SsPV1 lack disordered regions, since the authors did not mention any; however, neither structure was deposited in the Protein Data Bank, so it is impossible to verify[68,70].

ID allows viral proteins to moonlight and to perform multiple functions. Such moonlighting activity has been observed in the capsids of many dsRNA viruses, such as the cap-snatching activity of L-A and L-BC[112,232,233,235,280,281]. This frees the virus of the burden of encoding a separate protein for each function it must perform. Considering this, it is tempting to speculate that the capsids of ScPVs have evolved to acquire enzymatic functions that participate in evading or subverting host antiviral systems or otherwise influencing host metabolism[112,232–235,280,282–284]. However, empirical data is

required to determine the structure of ScPV C-termini and whether they play any important roles.

The objective of Crucitti et al. was to identify viruses that could potentially influence the technological attributes of both *Saccharomyces* and non-*Saccharomyces* yeast strains. However, the authors provide no rationale for how a virus could produce advantageous technological attributes. Indeed, they only describe viruses that are *not* desirable in winemaking. For instance, killer yeast contamination can cause stuck fermentations[285]. And they claim that they succeeded in identifying such viruses. However, most of the viruses identified in their approach have already been described.

The authors additionally report the discovery of the first partitivirus infecting *S. cerevisiae* wine strains ICV D254 Lalvin (D254) and Uvaferm 43 (U43) and called it Saccharomyces cerevisiae cryspovirus 1 (ScCV1). The presence of a PV was confirmed in this work in D254 but not U43. ScCV1 was determined to be the same species as ScPV3-1172 characterized in Taggart et al., 2023. Crucitti et al. neglected to publish their entire sequence of ScCV1, which is frustrating since they stated that they would clarify the phylogenetic relationship of ScCV1 within the *Partitiviridae* family by conducting a more in-depth analysis of the 5' and 3' termini. However, the publication of the full ScPV3-1172 sequence by Taggart et al. makes it a moot point, and the frustration is alleviated since this work is the first to utilize *S. cerevisiae* partitiviruses as a model for partitivirus biology.

CHAPTER 3: *SACCHAROMYCES CEREVISIAE* PARTITIVIRUSES VS HOST ANTIVIRAL SYSTEMS

3.1 Introduction

The objectives of the work in this chapter were (1) to determine whether ScPVs segregate to meiotic progeny and can be efficiently transmitted horizontally, (2) to determine whether they are susceptible or resistant to Xrn1, and (3) to determine the effect of knocking out genes involved in RNA turnover on ScPV replication. These are pursuant to the establishment of *S. cerevisiae* and ScPVs as a model system for the study of *Partitiviridae*. The hypothesis was that ScPVs have evolved mechanisms to evade RNA turnover and quality control mechanisms.

S. cerevisiae possesses several robust mechanisms for detecting and degrading aberrant RNAs, such as those lacking a 5' cap and/or a poly(A) tail, which includes viral RNAs[30,176,182,197,208,236,240]. The best studied of these are *XRN1*, *NUC1*, and the SKI complex and exosome. Xrn1 is a 5'-3' exoribonuclease that digests uncapped mRNAs. Nuc1 is a mitochondrial protein that can enter the cytoplasm through the mitochondrial porins during stress[204]. The SKI complex funnels deadenylated mRNAs into the exosome, where they are digested[155,286]. During mitosis, Xrn1, Nuc1, and the SKI complex, among several other proteins, function in parallel pathways to prevent the proteostatic stress, mitochondrial dysfunction, and even lethality that would otherwise result from the unchecked replication of L-A[287]. During meiosis and sporogenesis, these pathways attenuate L-A and M to reduce the massive intracellular accumulation of killer toxin caused by rerouting of secretory pathways[30,203,205,288].

Viruses have evolved mechanisms to evade or interfere with host immunity to protect their transcripts and genomes from degradation. Narnaviruses employ strong stem-loop structures that prevent degradation by Xrn1[240]. The polymerases of L-A and L-BC synthesize transcripts with a diphosphorylated 5' end, which is a poor substrate for Xrn1[124,238], and the capsid proteins have cap-snatching activity, cleaving the cap moiety from host mRNAs and ligating it to its transcripts[225,232,236].

3.2 Results

3.2.1 ScPVs maintain stable infections in *S. cerevisiae* under laboratory conditions and are efficiently transmitted vertically via meiosis.

Before *S. cerevisiae* can be used as a model system to study partitiviruses, it first had to be determined whether ScPVs could maintain a stable infection of their host under laboratory conditions. Four strains of *S. cerevisiae* were grown on YPD agar at either ambient temperature or 4°C for six weeks. Electrophoresis of extracted dsRNAs indicated the sustained presence of ScPVs in all four strains (Fig 3.1A). Some partitiviruses are known to inefficiently segregate to meiotic progenies during spore formation, if at

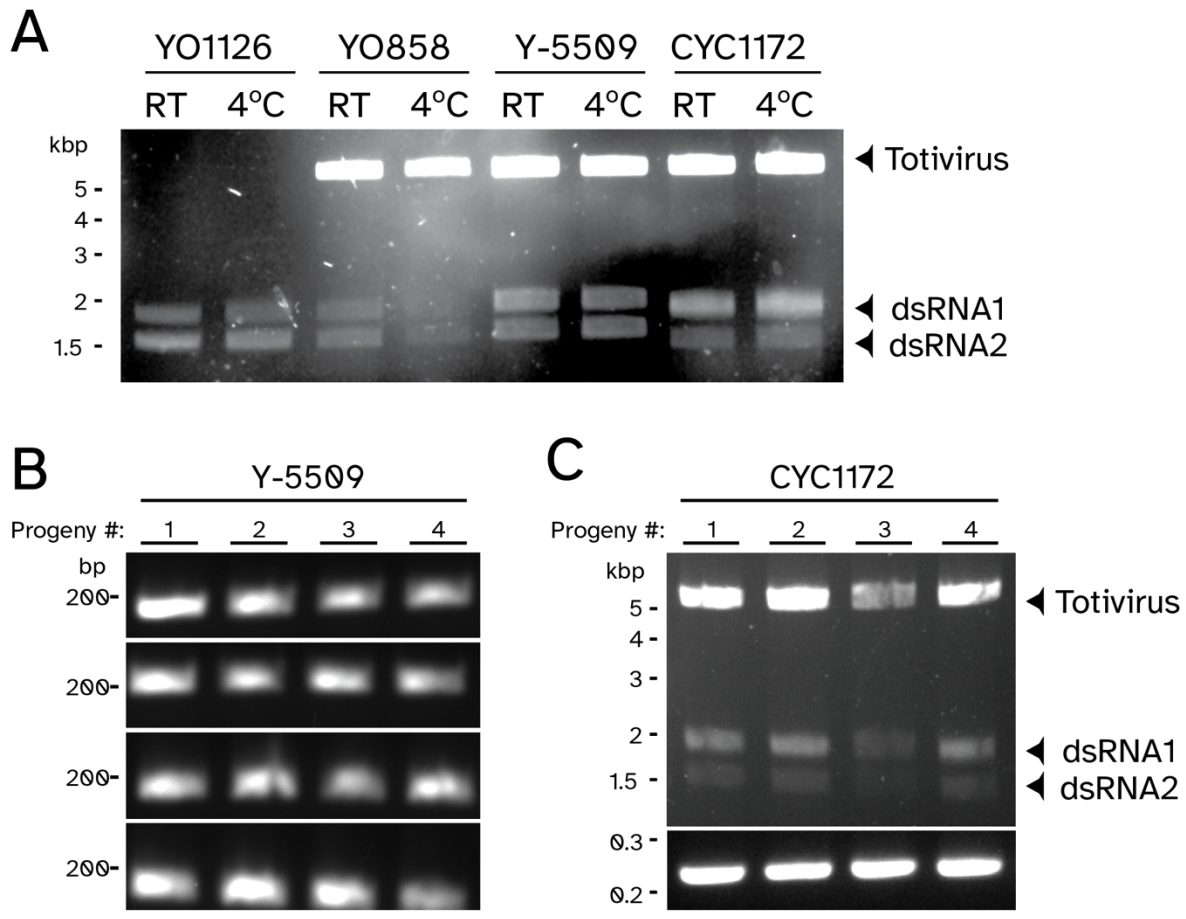

Figure 3.1: ScPVs maintain stable infections in *S. cerevisiae* under laboratory conditions and are efficiently transmitted through meiosis.
(**A**) The presence of ScPV was measured by dsRNA extraction after maintenance on agar plates incubated at either room temperature or 4°C for 6 weeks. Detection of ScPV using RT-PCR in the haploid progeny of four dissected asci of (**B**) Y-5509 and (**C**) *bottom panel* CYC1172. (**C**) Detection of ScPV3 in the haploid progeny of a dissected ascus of CYC1172 by extracting dsRNAs.

all[75]. Two *S. cerevisiae* strains containing ScPVs were sporulated (with aid from Dr. Jill Johnson), and 4-16 spore colonies were inspected for virus by extracting dsRNAs and by RT-PCR. ScPVs successfully segregated to all meiotic progenies (Fig 3.1B and 3.1C). This bodes well for the use of *S. cerevisiae* and ScPVs as a model system.

3.2.2 Cytoduction of ScPVs into laboratory strains of *S. cerevisiae*

The goal of this study was to transfer an ScPV into a strain of *S. cerevisiae* with a well-understood genomic background. The first method used to attempt to transfer ScPVs into laboratory strains of *S. cerevisiae* was cytoduction. There is no marker for ScPV infection, so mitochondria, which also reside in the cytoplasm, were chosen as a proxy. Mitochondria enable respiratory proficiency, or the ability to utilize nonfermentable carbon sources such as glycerol and ethanol. In the cytoduction scheme, a wild ScPV+ *URA3* haploid is mated with a respiratory deficienct (rho$^-$) *kar1 ura3Δ0* lab strain (Fig 3.2)[289,290]. The *kar1* mutation prevents karyogamy, or nuclear fusion, whereas plasmogamy, or mixing of the cytoplasm, is unaffected[291]. The product of mating is thus called a heterokaryon, which produces haploid progeny with the genome of either the wild yeast strain or the lab yeast strain and cytoplasmic components from both parent strains, including mitochondria and ScPVs.

The gene product of *URA3*, orotidine-5'-monophosphate decarboxylase, is involved in the biosynthesis of pyrimidines[292,293]. It converts 5-fluorootic acid (5-FOA) into 5-fluorouracil, which inhibits DNA synthesis[294–298]. 5-fluorouracil is also incorporated into RNAs; thus, it also inhibits protein synthesis. These properties have made 5-FOA a useful drug in yeast genetics and in the treatment of cancer[299]. Therefore, 5-FOA is used to counterselect *URA3* cells; that is, it kills wild parental cells, the heterokaryons, and the heterokaryon progenies that received the wild genotype. The lab parental yeast is counterselected by growing the cells on ethanol and glycerol, which are nonfermentable carbon sources and cannot be utilized by rho$^-$ cells.

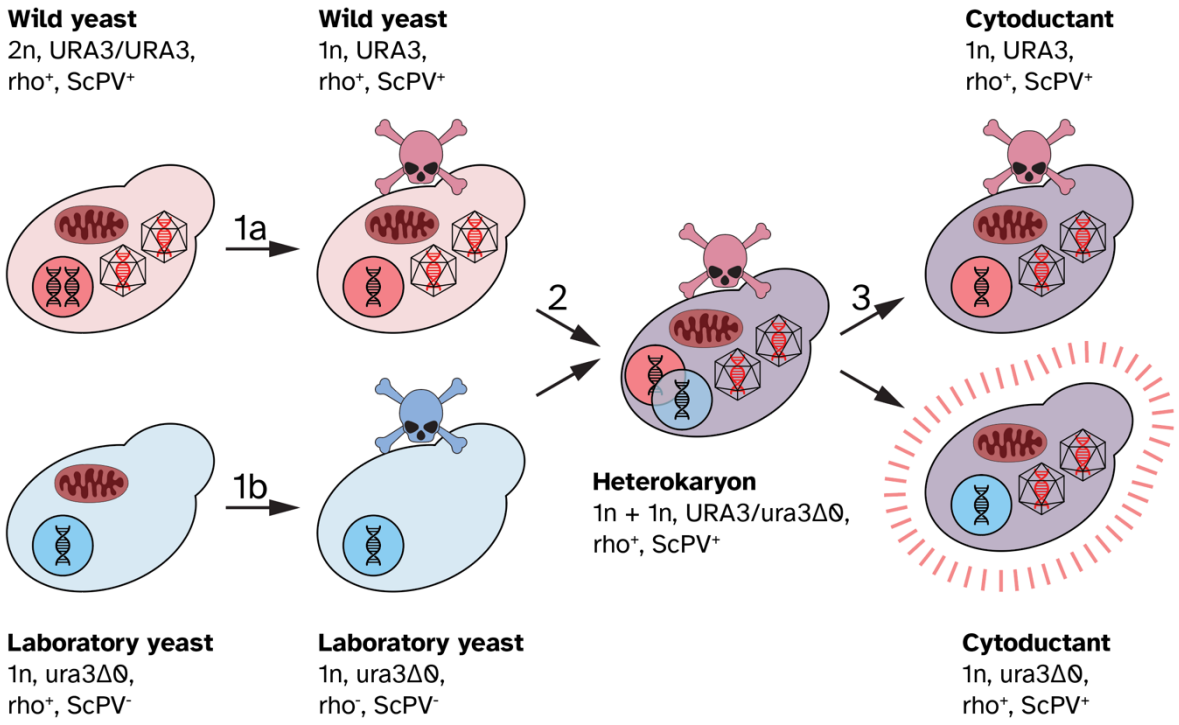

Figure 3.2: An overview of the cytoduction scheme.
(**1a**) Stable, domesticated haploids are derived from wild, diploid yeast infected with ScPVs. (**1b**) Laboratory yeast cells are treated with ethidium bromide to impair mitochondrial function. (**2**) ScPV+ haploids are mated with *kar1* rho$^-$ haploids and form a heterokaryon. Plasmogamy occurs, indicated by a purple cytoplasm, but nucleogamy does not. (**3**) Heterokaryons produce haploid progeny with either the genome of the wild yeast or of the laboratory yeast. Respiratory proficiency has been restored in cells with the laboratory yeast genotype, which is a proxy for ScPVs. Pink skulls indicate selection by 5-FOA; blue skulls indicate inability to grow on ethanol and glycerol.

Cells of the *S. cerevisiae* lab strain 1368 (*MATα his4 kar1 ura3Δ0* [L-A-HNB M1]) were incubated in ethidium bromide to induce respiratory deficiency by impairing mitochondrial function[289,300–304]. ScPV3+ CYC1172 cells were sporulated, but, since the author did not yet possess the yeast tetrad dissection skills, the asci were digested with Zymolyase and sonicated to release the ascospores. Rho$^-$ 1368 cells were added to a small amount of the digested ascus suspension and selected on YPEG and 5-FOA.

Any colony that grows on YPEG and 5-FOA should have the same genetic background as the laboratory strain 1368 and carry ScPVs. Putative cytoductants were probed for the RdRP and CP of ScPV3 by RT-PCR, and one was identified (Fig 3.3A). To determine

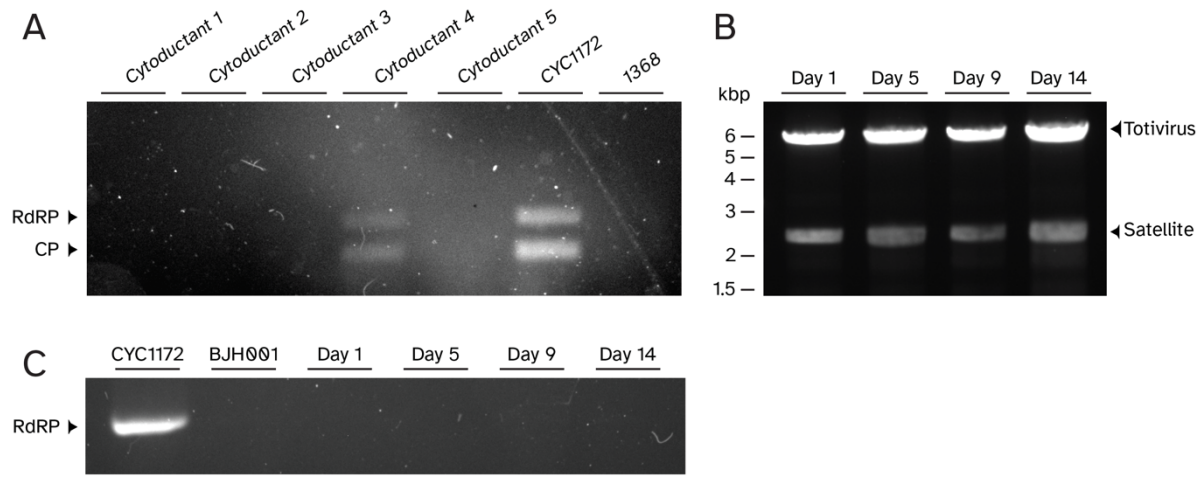

Figure 3.3: Verifying ScPV3 presence in cytoductants.
(**A**) Cytoductants were probed for ScPV3 RdRP and CP. (**B**) dsRNA extractions from different time points of the stability assay. Units are in kilobases. (**C**) The same time points were probed for ScPV3 RdRP.

whether ScPV3 could maintain a stable infection in its new host, cytoductant #4 was serially passaged daily for two weeks. dsRNAs were extracted from the cultures from days 1, 5, 9, and 14 and electrophoresed (Fig 3.3B). Only bands associated with totiviruses and satellite dsRNAs were observed. To verify that the copy number of ScPV3 was not extremely low, the same time points were probed for the RdRP by RT-PCR (Fig 3.3C). No PCR amplicons were observed for any time point. These data suggest that ScPVs are neither efficiently nor stably transmitted via cytoduction, so a new approach was taken.

3.2.3 Horizontal transmission of ScPVs by strain hybridization

The goal of this study was to determine whether ScPVs can be efficiently transmitted horizontally by strain hybridization. The ScPV-infected yeast strains are homothallic, meaning they can switch mating types (see Appendix A for an in-depth overview), so stable haploids had to be obtained. This was accomplished by disrupting the *HO* locus with the *ho::HygMX* cassette, which was amplified from strains from the collection generated by Cubillos et al, followed by sporulation and tetrad dissection[305–307]. Efficiency of horizontal ScPV transfer was tested by mating ScPV+ strains with the *S. cerevisiae* laboratory strain BY4741 *xrn1Δ::KanMX* to create a ScPV+ hybrid strain (Fig 3.4A and 3.4B).

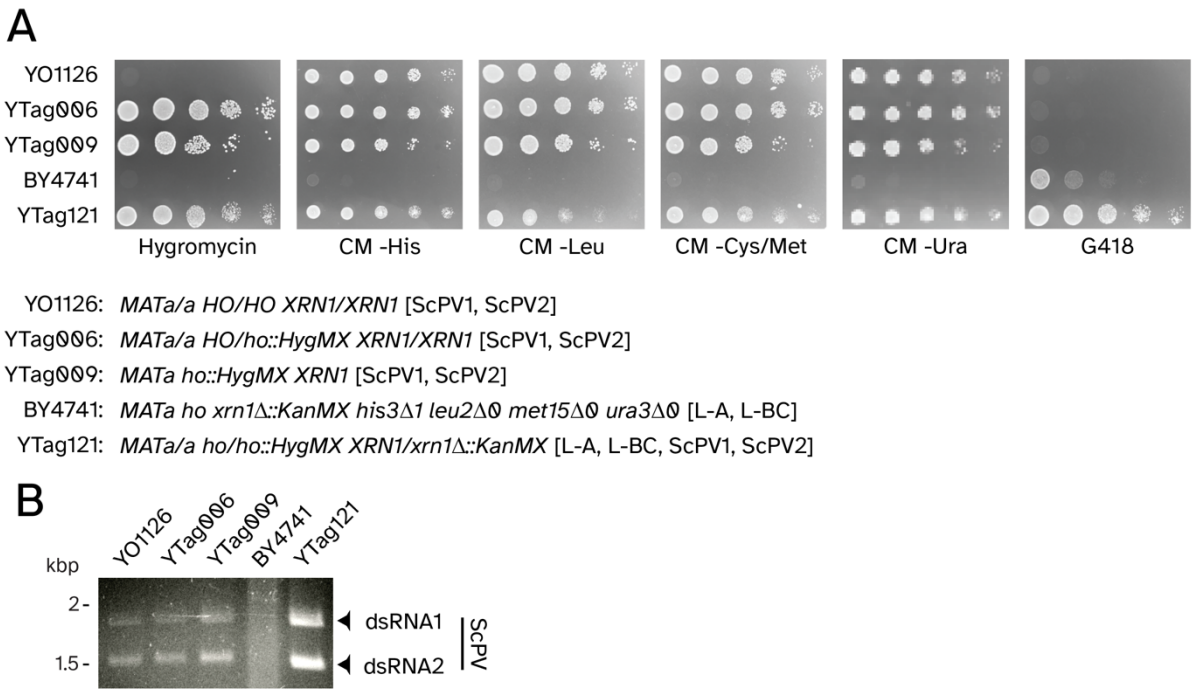

Figure 3.4: ScPVs are efficiently transmitted horizontally by mating.
(**A**) Confirmation of expected genotypes using selective growth media. (**B**) Confirmation of the inheritance of ScPVs during strain construction by cellulose chromatography and gel electrophoresis.

3.2.4 ScPVs are resistant to the antiviral effects of Xrn1

To determine if ScPVs are susceptible to attack by Xrn1p, a high copy plasmid encoding *XRN1* was used to transform YTag021, an *S. cerevisiae* strain that harbors totiviruses (L-A and L-BC) and partitiviruses (ScPV1-1126 and ScPV2-1126). 96 clones were examined by RT-PCR for the loss of ScPV1-1126, ScPV2-1126, L-A, and L-BC; the cure rates are listed in Table 3.1.

Table 3.1: Cure rates of L-A, L-BC, ScPV1, and ScPV2 upon Xrn1 overexpression.

Virus	# Clones cured	% Cured clones
ScPV1-1126	1	1
ScPV2-1126	15	15.6
L-A	19	19.8
L-BC	19	19.8

Eight clones were chosen to corroborate the RT-PCR data by extracting and electrophoresing dsRNAs (Table 3.2). dsRNAs associated with totiviruses—L-A and L-BC are

approximately the same size and cannot be distinguished—and two PVs were observed in all 8 clones, which contradicts the results from the RT-PCR assay.

Table 3.2: Corroboration of multiplex RT-PCR results by purifying and electrophoresing dsRNAs.

Strain	Expected amplicon(s) (bp)	Observed amplicon(s) (bp)	Agrees with RT-PCR?
BY4741	L-A, L-BC	TV	-
YO1126	ScPV1, ScPV2	2 PVs	-
Clone E1	L-BC, ScPV1, ScPV2	TV, 2 PVs	Possibly
Clone G1	L-A, ScPV1, ScPV2	TV, 2 PVs	Possibly
Clone H2	ScPV1, ScPV2	TV, 2 PVs	No
Clone E6	ScPV1	TV, 2 PVs	No
Clone A7	ScPV1	TV, 2 PVs	No
Clone H8	None	TV, 2 PVs	No
Clone C10	L-A, L-BC, ScPV1, ScPV2	TV, 2 PVs	Yes
Clone E11	ScPV1	TV, 2 PVs	No

This calls into question whether *XRN1* was successfully being expressed to begin with. Rather than perform a relatively expensive Western blot, 19 colonies supposedly cured of L-A and five uncured colonies were probed for L-A by RT-PCR (Table 3.3). 17 of the "cured" colonies yielded an L-A amplicon and one of the "uncured" colonies did not. This suggests a 12.5% cure rate of L-A, which is less than expected[197], so a different approach to assaying the susceptibility of ScPVs to Xrn1 was taken.

Table 3.3: Probing Xrn1 overexpression clones for L-A by RT-PCR.

Strain	L-A expected?	L-A observed?	Strain	L-A expected?	L-A observed?
BY4741	Y	Y	B7	Y	Y
YO1126	-	-	H7	-	-
B1	Y	Y	E8	-	Y
E1	-	Y	H8	-	Y
H1	-	Y	B9	-	Y
C2	-	Y	D9	-	Y
H2	-	Y	D10	-	Y
B3	Y	Y	B11	Y	-
F4	-	Y	D11	-	Y
H4	-	Y	E11	-	Y

Table 3.3 con't					
B5	Y	Y	H11	-	Y
E6	-	Y	B12	-	Y
A7	-	Y	D12	-	-

YTag084, a strain containing L-A-lus, L-BC, the satellite dsRNA M2, and ScPV3 was transformed with the same *XRN1*-encoding high copy plasmid as above. Loss of killer toxin production is an easily screened proxy for loss of M2 or L-A-lus due to *XRN1* overexpression, as described in Chapter 1[197]. 50% of clones lost K2 toxin production (Fig 3.5A), which is comparable to the loss of K1 toxin production observed by Rowley et al. (57%)[197]. 5 killers and 15 non-killers were probed by RT-PCR for L-A-lus and L-BC; 100% of clones carried both L-A-lus and L-BC. Extraction and electrophoresis of dsRNAs confirmed that killer yeasts retained M2, and non-killer yeasts lost M2 (Fig 3.5B). Totiviruses and ScPV3 were observed in all clones, demonstrating that ScPV3 is resistant to Xrn1.

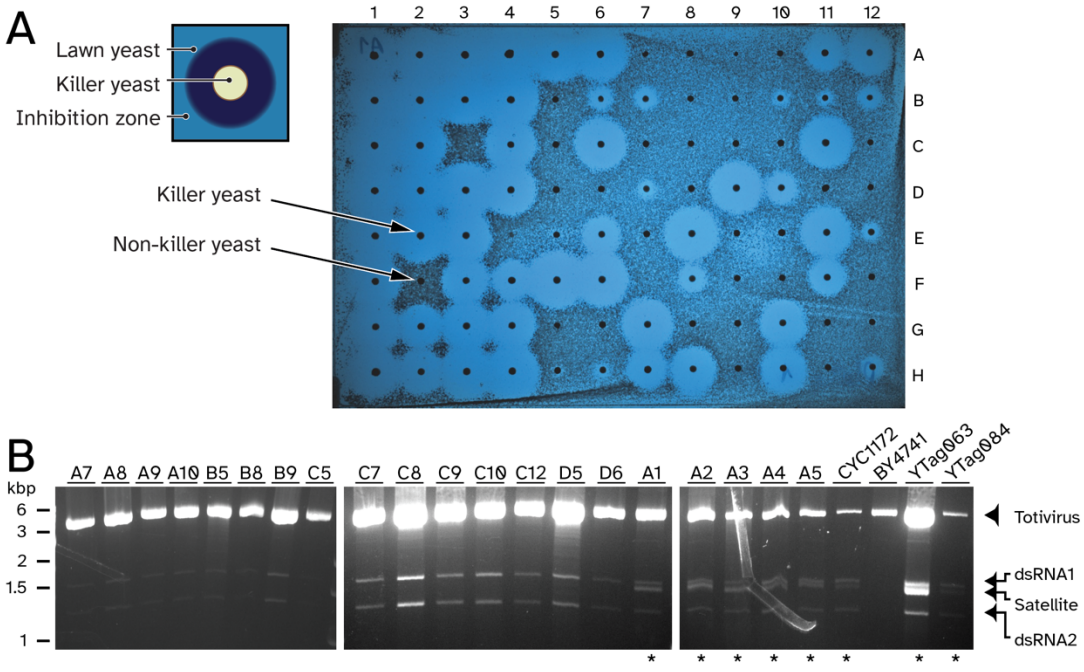

Figure 3.5: ScPVs are insensitive to the overexpression of Xrn1.
(**A**) Curing of the M2 satellite dsRNA from strain YTag084 by *XRN1* expression as assayed by an agar plate killer assay (**B**) Extraction of dsRNAs from killer (*) and non-killer yeasts isolated from the plate in panel A. CYC1172 and YTag063 (killer yeast strains) and BY4741 (non-killer yeast strain) were included as controls for the presence or absence of a satellite dsRNA.

3.2.5 The effect of yeast innate immunity gene knock outs on ScPV copy number

The goal of this study was to determine the effect of knocking out genes involved in RNA turnover on ScPV replication, including *NUC1, SKI2, SKI3, SKI7, SKI8, and XRN1*. As a preliminary study, ScPV+ yeast strains with *NUC1*, *SKI2*, and *SKI7* deletions were created by hybridizing YTag009 *MAT***a** *ho::HygMX* [ScPV1-1126, ScPV2-1126] with strains from the deletion collection[308]. PCR verification determined that the *SKI3* and *XRN1* deletion mutants did not carry the *KanMX* deletion cassette at the expected locus, despite being resistant to G418, so those null mutants were acquired from collaborators. And the *ski8Δ* strain was not a haploid, as expected. Therefore, it would have to be sporulated before it could be hybridized with a ScPV-infected strain, but it never did and so was not pursued further. All hybrids retained ScPV1 and ScPV2. The *NUC1/nuc1Δ*, *SKI2/ski2Δ*, *SKI3/ski3Δ*, and *SKI7/ski7Δ* hybrids readily sporulated, but the *XRN1/xrn1Δ* hybrid was rho$^-$ and incapable of sporulation, and it was not pursured further. Because many haploid progeny of yeast hybrids form dispersal-resistant flocs[309–311], cells were normalized by weight prior to dsRNA extractions to visually inspect the change in ScPV copy number. There was no obvious relationship between ScPV copy number and deletion of either *NUC1* or *SKI7* (Fig 3.6). The *SKI2* deletion correlated with an increase in band intensity, suggesting that Ski2 acts to restrict ScPV replication. No bands were visible for any spore clones from the *SKI3/ski3Δ* hybrid. To verify that the apparent loss of ScPV from all four spore clones was not an error, 16 additional spore clones were probed for ScPV by RT-PCR; none contained either ScPV1-1126 or ScPV2-1126.

Two more approaches at determining the effect of gene knock outs on ScPV copy number were also applied. First, *SKI2* and *SKI3* knock outs were to be studied in a wild background. The strain chosen for this approach was YO815 because it carries only ScPV2-815. *SKI2* and *SKI3* were knocked out by amplifying the deletion cassettes from the original strains in the deletion collection and transforming YO815. Several complications were encountered. First, the transformation efficiency was extremely

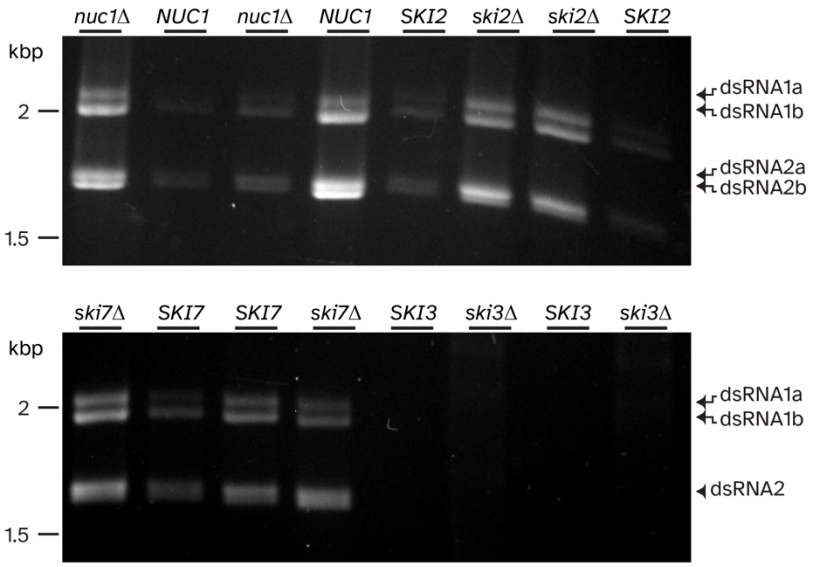

Figure 3.6: The effect of *NUC1*, *SKI2*, *SKI3*, and *SKI7* deletion on copy number of ScPV1 and ScPV2 in the meiotic progenies of hybrid strains.
ScPV-infected yeast strains were hybridized with null mutants from the deletion collection. Presence of ScPV1 and ScPV2 was confirmed prior to sporulation and tetrad dissection. Cells were normalized, and dsRNAs were extracted and electrophoresed.

low, yielding two colonies for the *SKI2* deletion and one for the *SKI3* deletion. These were re-streaked to ensure they were monoclonal. To verify successful knockout, the *SKI2* and *SKI3* loci were probed by PCR (Table 3.4). Heterozygous transformants were obtained for *SKI2* and *SKI3*.

Table 3.4: Probing the *SKI2* and *SKI3* loci to verify successful knockout.

Strain	Target	Expected amplicon(s) (bp)	Observed amplicon(s) (bp)	Genotype
BY4741 *SKI2*	*SKI2*	5283	5000	*SKI2*
BY4741 *ski2Δ::KanMX*	“	3000	3000	*ski2Δ::KanMX*
Transformant 1	“	5283, 3000	5000, 3000	*SKI2/ski2Δ::KanMX*
Transformant 2	“	5283, 3000	5000, 3000	*SKI2/ski2Δ::KanMX*
Transformant 3	“	5283, 3000	5000, 3000	*SKI2/ski2Δ::KanMX*
Transformant 4	“	5283, 3000	5000	*SKI2/SKI2*
BY4741 *SKI3*	*SKI3*	5984	6000	*SKI3*
BY4741 *ski3Δ::KanMX*	“	3266	3000	*ski3Δ::KanMX*
Transformant 5	“	5984, 3266	6000, 3000	*SKI3/ski3Δ::KanMX*
Transformant 6	“	5984, 3266	3000	*ski3Δ::KanMX/ski3Δ::KanMX*

Interestingly, one of the *SKI2* transformants produced only an amplicon associated with *SKI2* and not *ski2Δ::KanMX*, suggesting it was not knocked out. For curiosity's sake, this transformant was not discarded. And one of the *SKI3* transformants produced only an amplicon associated with *ski3Δ::KanMX*, suggesting both copies were knocked out. The transformants were then probed for ScPV2-815 (Table 3.5).

Table 3.5: Probing *SKI2* and *SKI3* deletion transformants for ScPV2.

Strain	Genotype	Target	Expected amplicon(s) (bp)	Observed amplicon(s) (bp)
BY4741	*SKI2*	ScPV2-815 CP	0	0
YO815	*SKI2*	"	1333	1333
Transformant 1	*SKI2/ ski2Δ::KanMX*	"	1333	0
Transformant 2	*SKI2/ ski2Δ::KanMX*	"	1333	0
Transformant 3	*SKI2/ ski2Δ::KanMX*	"	1333	0
Transformant 4	*SKI2/SKI2*	"	1333	1333
Transformant 5	*SKI3/ ski3Δ::KanMX*	"	1333	0
Transformant 6	*ski3Δ::KanMX/ ski3Δ::KanMX*	"	1333	0

Interestingly, ScPV2-815 was cured from all successful knockouts. The transformants were also sporulated and dissected, and the spore colonies were selected on G418. However, G418 resistance did not segregate 2:2 for all asci (Table 3.6). These issues have not yet been resolved.

Table 3.6: Expected of G418-resistant spore clones, based on Table 3.5, vs observed rates.

Strain	Genotype	# of spores	Exptected G418-resistant spore clones	Observed G418-resistant spore clones
Transformant 1	*SKI2/ ski2Δ::KanMX*	80	50%	51.3%
Transformant 2	*SKI2/ ski2Δ::KanMX*	80	50%	50%
Transformant 3	*SKI2/ ski2Δ::KanMX*	76	50%	50%
Transformant 4	*SKI2/SKI2*	88	0%	100%
Transformant 5	*SKI3/ ski3Δ::KanMX*	80	50%	85%
Transformant 6	*ski3Δ::KanMX/ ski3Δ::KanMX*	72	100%	77.8%

The second new approach to study *SKI2* and *SKI3* knockouts was to back-cross YO815 with lab strains carrying or lacking totiviruses to produce an ScPV+ strain with a genetic background more like that of BY4741. This approach is also useful because L-A and L-BC could interact with ScPV1 and ScPV2 in a synergistic or antagonistic manner to mediate host and/or virus phenotypes, a phenomenon that has been observed in plants, fungi, and animals[312–315]. Three L-A-o L-BC-o strains were acquired from Dr. Marc Meneghini with various genotypes. These included SCY846 (*MAT***a**/α *NUC1/nuc1Δ::NatMX MAK3/mak3Δ::KanMX*), SCY877 (*MAT***a**/α *XRN1/xrn1Δ::KanMX MAK3/mak3Δ::HygMX NUC1/nuc1Δ::NatMX*), and SCY898 (*MAT***a** *ski3Δ::HygMX*) and were constructed by Sabrina Chau. These strains were assured to sporulate very efficiently. However, no degree of sporulation was observed, even after eight weeks. So, the genotypes and phenotypes were verified (Tables 3.7 and 3.8 and Fig 3.7A-E).

Table 3.7: Verifying genotypes of L-A-o L-BC-o strains.

Strain	Genotype	Target	Expected amplicon(s) (bp)	Observed amplicon(s) (bp)
BY4741	*MAK3*	*MAK3*	882	900
YTag106	*Mak3Δ::KanMX*	"	1932	2000
SCY846	*MAK3/mak3Δ::KanMX*	"	1932, 882	2000, 900
SCY877	*MAK3/mak3Δ::HygMX*	"	1927, 882	2500, 900
SCY898	*MAK3*	"	882	900
BY4741	*NUC1*	*NUC1*	1457	1450
SCY846	*NUC1/nuc1Δ::NatMX*	"	1457, 1590	1450, 1600
SCY877	*NUC1/nuc1Δ::NatMX*	"	1457, 1590	1450, 1600
SCY898	*NUC1*	"	1457	1450
BY4741	*SKI3*	*SKI3*	5984	6000
SCY846	*SKI3*	"	5984	6000
SCY877	*SKI3*	"	5984	6000
SCY898	*Ski3Δ::HygMX*	"	3266	3000
YTag008	*MAT***a**	*MAT*	544	540
YTag009	*MAT*α	"	404	400
SCY846	*MAT***a**/α	"	544, 404	540, 400
SCY877	MATa/α	"	544, 404	540, 400
SCY898	*MAT***a**	"	544	540

Table 3.7 con't				
BY4741	*XRN1*	*XRN1*	4975	5000
BY4741	*xrn1Δ::KanMX*	"	1969	2000
SCY846	*XRN1/XRN1*	"	4975	5000
SCY877	*XRN1/xrn1Δ::KanMX*	"	4975, 1969	5000, 2000
SCY898	*XRN1*	"	4975	5000

Table 3.8: Verifying phenotypes of L-A-o L-BC-o strains.

Strain	Antibiotic/carbon source	Growth expected?	Growth observerd?
YTag106	G418	Y	Y
BY4741	"	N	N
SCY846	"	Y	N
SCY877	"	Y	Y
SCY898	"	N	N
BY4741	Streptothricin	N	N
SCY846	"	Y	Y
SCY877	"	Y	Y
SCY898	"	N	N
YTag008	Hygromycin	Y	Y
BY4741	"	N	N
SCY846	"	N	N
SCY877	"	Y	Y
SCY898	"	Y	N
BY4741	Ethanol, glycerol	Y	Y
YTag011	"	N	N
SCY846	"	Y	Y
SCY877	"	Y	Y
SCY898	"	Y	Y

Results were mixed. While all strains produced PCR amplicons of the expected sizes (except for SCY846's *MAK3* amplicon, which was larger than what was expected for either *MAK3* or *mak3Δ*) (Fig 3.7B-E), only SCY877 grew on all expected antibiotics (Fig 3.7A). SCY846 failed to grow on G418, and SCY898 failed to grow on hygromycin. These issues have not yet been resolved. Fortunately, all strains were of the expected mating type (Fig 3.7E).

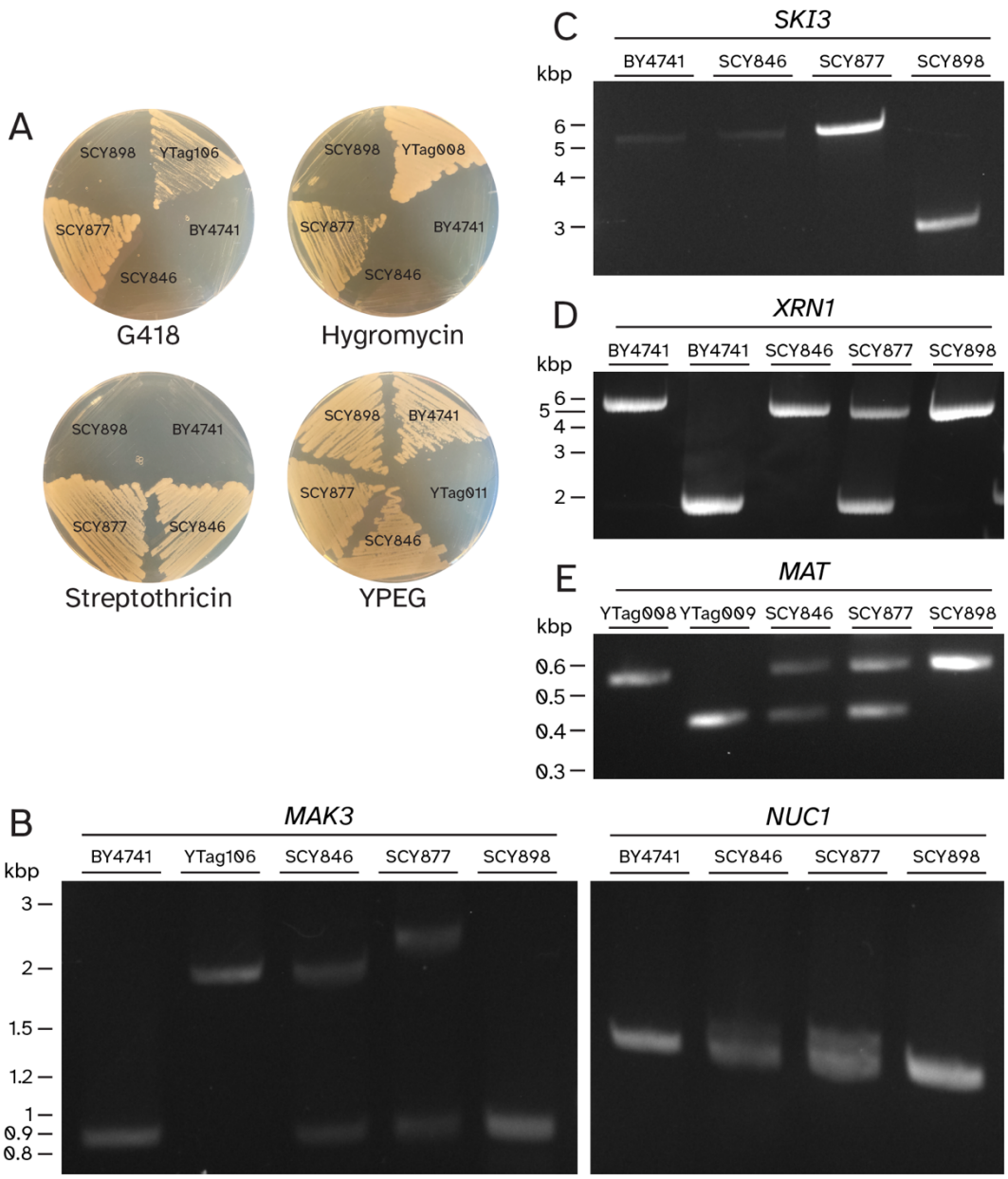

Figure 3.7: Verifying phenotypes and genotypes of L-A-o L-BC-o strains.
(**A**) Verifying antibiotic resistance and respiratory proficiency of strains provided by Dr. Meneghini. The (**B**) *MAK3, NUC1,* (**C**) *SKI3,* (**D**) *XRN1,* and (**E**) *MAT* loci were probed by PCR.

3.3 Discussion

In summary, *Saccharomyces cerevisiae* partitiviruses maintain stable infections and are efficiently transmitted vertically through meiosis and horizontally by strain hybridization. ScPVs are resistant to Xrn1 overexpression, and *SKI2* deletion is associated with increased copy number. Sporulation of a *SKI3/ski3Δ* strain is associated with loss

of ScPVs from all meiotic progenies. There is no obvious relationship between ScPV copy number and deletion of either *NUC1* or *SKI7*.

ScPVs maintain stable infections in *S. cerevisiae* under laboratory conditions and, unlike other partitiviruses, are efficiently transmitted vertically via meiosis[75]. These observations will enable the utilization of various genetic tools and *S. cerevisiae* strain collections to explore host-virus interactions, antiviral systems, and partitivirus replication and infection.

Cytoduction was chosen to transfer ScPVs into an *S. cerevisiae* strain with a well-understood genetic background. However, the cytoduction approach, as described above, produced very few colonies that recovered respiratory proficiency and grew on 5-FOA-containing media. There are several potential factors explaining this. First, the author did not yet possess the skills of yeast tetrad dissection. Thus, the ScPV+ cells mated with the respiratory deficient lab strain was a mixture of diploids, *MAT***a** ascospores, and *MAT*α ascospores. Second, the YPG recipe utilized in cytoduction (0% ethanol, 30% glycerol) is inferior to the YPEG recipe used to test the respiratory proficiency of the L-A-o L-BC-o strains (2% ethanol, 3% glycerol), and cells grew at a prohibitively slow rate. Finally, except for the first batch, successfully preparing media containing 5-FOA repeatedly eluded the author. The agar would either have a very soft consistency, disallowing cells to be streaked on its surface, or it would not successfully select for *ura3* cells, instead allowing *URA3* cells to grow as well. These are the principal reasons that the strain hybridization approach was chosen. Initially, the cytoduction method did successfully transmit an ScPV to a laboratory strain of *S. cerevisiae*. However, the virus was immediately and spontaneously cured. On the other hand, attempts to transfer ScPVs horizontally by strain hybridization were successful (Fig 3.4B), which enabled the study of how ScPVs interact with *S. cerevisiae* antiviral systems, including *XRN1*, the SKI complex, and *NUC1*.

ScPVs appear resistant to the antiviral effects of Xrn1. This suggests that these viruses employ mechanisms to protect their RNAs from degradation by the host. It is tempting

to speculate on what these mechanisms might be. One likely method is secondary structure in viral transcripts, which is a very common method for evading or subverting Xrn1, including in the *S. cerevisiae* viruses 20S and 23S[210,213–224,240]. Other methods could include 5' end modification, catalyzed either by the polymerase or the capsid, which would mask the transcript's viral nature and protect it from Xrn1[124,232–235,238,280,281,316,317]. Interestingly, many different sizes of zone of growth inhibition were observed (Fig 3.5A), perhaps owing to varying levels of Xrn1 expression.

Some genes that potentially interact with ScPVs were identified by deleting genes known to be important in restricting other *S. cerevisiae* viruses[203,206,208]. Ski2 appears to be important in restricing ScPV replication. Since Ski2 is involved with the exosome, the susceptibility of ScPVs suggests that they lack mechanisms to furnish their transcripts with poly(A) tails[185–187]. And a *SKI3* deletion, which permitted ScPV infection in a heterozygote, resulted in complete loss of ScPV1 and ScPV2 following sporulation, regardless of the genotype of the spore clone. More research is required to investigate this fascinating phenomenon.

On the other hand, *NUC1* and *nuc1Δ* genotypes did not correlate with a significant change in the copy number of ScPV1 or ScPV2, nor did the *SKI7 and ski7Δ* genotypes. However, band intensity of the former did correlate with flocculation. That is, the first (*nuc1Δ)* and fourth (*NUC1*) spore clones (Fig 3.6), which had higher band intensity compared to the second and third spore clones, were flocculent, while the second and third spore clones were not. So, it is possible that weighing cell pellets is a flawed method to normalize number of cells. Further experiments are required to verify this hypothesis. However, this line of experimentation requires an optimized method of dispersing flocs, which are resistant to EDTA, sulfuric acid, sonication, and even yeast lytic enzyme.

Two interesting phenomena were observed when *SKI2* and *SKI3* were knocked out in the wildtype *S. cerevisiae* background. The first was that all *ski2Δ::KanMX* and *ski3Δ::KanMX* transformants were cured of ScPV2-815. This is especially interesting

because it is in contrast with the hybrid deletion mutants, all of which retained ScPV1-1126 and ScPV2-1126. The second phenomenon observed was that susceptibilty and resistance to G418 did not always segregate 2:2. One parsimonious explanation is that the *KanMX* cassette integrated into more than one locus in the genome, despite both cassettes having over 1000 base pairs of homology to the *SKI2* and *SKI3* and UTRs, which should have ensured fidelous recombination. This may also be the reason that the *XRN1* and *SKI3* deletion mutants are not true deletions. Further experimentation is required to resolve this enigma.

It is interesting that the diploid L-A-o L-BC-o strains provided by Dr. Marc Meneghini did not sporulate. It is true that no single sporulation protocol is conducive for the sporulation of all *S. cerevisiae* strains; however, the diploid L-A-o L-BC-o strains did not sporulate when the sporulation protocol utilized in Dr. Meneghini's lab was tried (inoculating 2 mL 1% potassium acetate, 0.05% raffinose with cells taken from a YPD agar plate and incubating at 30°C (or 25°C, rarely)). Further investigation is required.

Taken together, these studies point the direction in which further research may be most fruitful.

3.4 Future directions

The long-term future goal of this line of research is to gain an understanding of partitivirus biology and their interctions with yeast antiviral systems such that *S. cerevisiae* can be utilized more effectively as a model organism for studying partitiviruses and other relevant RNA viruses. The overall objective of future research is to answer basic questions regarding partitivirus biology: (1) what host genes are important in either supporting or restricting viral replication, and (2) how do partitiviruses protect their genomes and transcripts from host RNA turnover and quality control pathways? The central hypothesis is that ScPVs have similar interactions with host antiviral systems as other *S. cerevisiae* viruses, and the rationale is that the knowledge gained by studying the biology of ScPVs will translate to other PVs, whose hosts are pathogenic or difficult to study. This will, in turn, inform the development of treatments against

relevant agricultural and human diseases. The overall outcome of this aim will be a detailed understanding of the mechanisms by which partitiviruses evade or subvert the innate immunity of their host. This is expected to be significant because it will inform the increased use of *S. cerevisiae* as a model organism for the study of eukaryotic RNA viruses.

3.4.1 Specific aim 1: Genetic study of genes known to be important for viral replication in yeast

Components of yeast RNA metabolism and innate immunity important for ScPV infection will be identified by knocking out and overexpressing genes known to be important for the infection of other yeast viruses[30,69,76,203,208]. The hypothesis is that ScPVs have evolved mechanisms similar to totiviruses and narnaviruses to evade RNA metabolic processes, including Xrn1 and components of the SKI complex and cytoplasmic exosome. The objective of this aim will be to identify components of RNA metabolism interacting with ScPVs, and the approach will be to assess the effects of RNA metabolism gene knock-out and overexpression on viral replication. The rationale is that these processes are important for virus attenuation in other yeasts and in higher eukaryotes.

Study 1.1: RNA metabolism and innate immunity gene *KO* project.

To identify the genes important for the replication or restriction of ScPVs, ScPV-infected strains will be crossed with deletion mutants and sporulated. Strains carrying double gene knockouts will be constructed in the same manner[318]. Changes in viral copy number will be assessed by extracting and electrophoresing dsRNAs, which may be followed up with RT-qPCR. Changes to host growth rate will be assessed by growing *S. cerevisiae* strains at different temperatures and on fermentable or non-fermentable carbon sources.

Unrestricted viral proliferation is expected to cause proteostatic stress, resulting in a conditionally lethal phenotype. Hsf1 (heat shock transcription factor) is a sensor of proteostatic stress and transactivates genes involved in the proteostatic stress

response[319–322]. Thus, proteostatic stress may be visualized by fusing GFP to Hsf1 and analyzing by microscopy or flow cytometry. Additionally, protein aggregates associated with proteostatic stress can be visualized by fusing GFP with Hsp104 (heat shock protein), which colocalizes with protein aggregates[319].

Other protein-protein interactions between *S. cerevisiae* and ScPV may be identified by utilizing a yeast two-hybrid library, using the capsid protein as the bait, or by purifying virions and assessing by mass spectroscopy for the presence of other host proteins.

The first approach to verify ScPV-host protein interactions will be to overexpress the identified host genes and assess change in ScPV copy number. If a gene deletion results in an increase in viral copy number, overexpression of the same gene is expected to result in a decrease in viral copy number, and vice versa. ScPV-host protein interactions will also be corroborated by fusing affinity tags to the proteins and attempting to coimmunoprecipitate virions. Conversely, virions will be purified and probed for the host proteins in a Western blot. To determine whether identified interations are mediated by RNAs, RNases will be added to the reaction tubes prior to Western blotting.

3.4.2 Specific aim 2: Investigation of the mechanisms of antiviral escape.

The objective of this aim will be to shed light on how ScPVs protect their genomes and their transcripts from being degraded by yeast mechanisms of RNA surveillance. The hypothesis is that ScPVs employ secondary structure to protect the integrity of their transcripts from host degradation. The approach will be to assess the influence of the ScPV untranslated region (UTR) on the stability of mRNAs and to challenge viral transcripts with Xrn1. The rationale is that narnaviruses employ secondary structure to protect their genomes and transcripts and that the 5’ UTRs of ScPVs contain extensive secondary structure motifs[213,238,240].

Study 2.1: Determine the effect of ScPV UTRs on the stability of transcripts.

Fragments of ScPV UTRs will be inserted upstream of a GFP gene under the control of a galactose-inducible promoter[323]. Cells will be harvested at different time points following shut-off of transcription. RNAs will be extracted, and a Northern blot will be performed with probes specific to the GFP gene. The decay rate of the transcript will be calculated and compared to narnavirus and cellular UTRs that are known to affect RNA stability[155,324,325]. This may be followed-up with RT-qPCR. If necessary, instead of expressing the ScPV UTR-GSP construct under a galactose-inducible promoter, an alternative approach will be taken, in which the experiment will be performed in a strain encoding a thermally labile RNA pol II[324].

Study 2.2: Determine whether ScPV transcripts are susceptible to Xrn1.

Transcripts representing the 5' UTRs of different species of ScPVs with a poly (G) tract will be transcribed in vitro from a DNA construct and labeled with short-lived fluorophores. To determine the effectiveness of Xrn1 at degrading ScPV transcripts, these transcripts will be challenged with purified Xrn1[213]. The kinetics of RNA degradation will be assessed with gel electrophoresis. Mutagenesis experiments will be performed to determine what parts of the UTR stabilize the ScPV transcripts.

REFERENCES

1. Qu, Z. *et al.* Exploring the Symbiotic Mechanism of a Virus-Mediated Endophytic Fungus in Its Host by Dual Unique Molecular Identifier–RNA Sequencing. *Msystems* **6**, e00814-21 (2021).

2. Case, N. T. *et al.* The future of fungi: threats and opportunities. *G3: GenesGenomesGenet.* **12**, (2022).

3. Rossman, A. Y. Ecological Impacts of Non-Native Invertebrates and Fungi on Terrestrial Ecosystems. 97–107 (2008) doi:10.1007/978-1-4020-9680-8_7.

4. Fisher, M. C. *et al.* Emerging fungal threats to animal, plant and ecosystem health. *Nature* **484**, 186–194 (2012).

5. Goka, K. *et al.* Amphibian chytridiomycosis in Japan: distribution, haplotypes and possible route of entry into Japan. *Mol. Ecol.* **18**, 4757–4774 (2009).

6. Cunningham, A. A. *et al.* Emergence of amphibian chytridiomycosis in Britain. *Vet. Rec.* **157**, 386 (2005).

7. Garner, T. W. J. *et al.* The emerging amphibian pathogen *Batrachochytrium dendrobatidis* globally infects introduced populations of the North American bullfrog, Rana catesbeiana. *Biol. Lett.* **2**, 455–459 (2006).

8. Crawford, A. J., Lips, K. R. & Bermingham, E. Epidemic disease decimates amphibian abundance, species diversity, and evolutionary history in the highlands of central Panama. *Proc. Natl. Acad. Sci.* **107**, 13777–13782 (2010).

9. Stuart, S. N. *et al.* Status and Trends of Amphibian Declines and Extinctions Worldwide. *Science* **306**, 1783–1786 (2004).

10. Garcia-Solache, M. A. & Casadevall, A. Global Warming Will Bring New Fungal Diseases for Mammals. *Mbio* **1**, e00061-10 (2010).

11. Myburg, H. *et al.* DNA sequence data and morphology define *Cryphonectria* species in Europe, China, and Japan. *Can. J. Bot.* **82**, 1730–1743 (2004).

12. Lee, S. H., Park, J. Y., Kim, K. H. & Lee, J. K. Characteristics of hypovirulent strains of chestnut blight fungus, *Cryphonectria parasitica* isolated in Korea. *Acta Hortic.* 611–616 (2004) doi:10.17660/actahortic.2005.693.81.

13. Elliott, K. J. & Swank, W. T. Long-term changes in forest composition and diversity following early logging (1919–1923) and the decline of American chestnut (*Castanea dentata*). *Plant Ecol.* **197**, 155–172 (2008).

14. Bellini, E. The chestnut and its resources: Images and considerations. *Acta Horticulture* 85–96 (2004) doi:10.17660/actahortic.2005.693.8.

15. Bounous, G. The chestnut: A multipurpose resource for the new millennium. *Acta Hortic.* 33–40 (2004) doi:10.17660/actahortic.2005.693.1.

16. Hepting, G. H. Death of the American Chestnut. *J. For. Hist.* **18**, 60–67 (1974).

17. Prospero, S., Conedera, M., Heiniger, U. & Rigling, D. Saprophytic Activity and Sporulation of *Cryphonectria parasitica* on Dead Chestnut Wood in Forests with Naturally Established Hypovirulence. *Phytopathology* **96**, 1337–1344 (2006).

18. Meyer, J. B., Gallien, L. & Prospero, S. Interaction between two invasive organisms on the European chestnut: does the chestnut blight fungus benefit from the presence of the gall wasp? *FEMS Microbiol. Ecol.* **91**, (2015).

19. Havir, E. A. & Anagnostakis, S. L. Oxalate production by virulent but not by hypovirulent strains of *Endothia parasitica*. *Physiol. Plant Pathol.* **23**, 369–376 (1983).

20. Ringling, D., Heiniger, U. & Hohl, H. R. Reduction of laccase activity in dsRNA-containing hypovirulent strains of *Cryphonectria (Endothia) parasitica*. *Physiology and Biochemistry* (1989).

21. Kotta-Loizou, I. Mycoviruses and their role in fungal pathogenesis. *Curr Opin Microbiol* **63**, 10–18 (2021).

22. Cortesi, P. & Milgroom, M. G. Genetics of Vegetative Incompatibility in *Cryphonectria parasitica*. *Appl. Environ. Microbiol.* **64**, 2988–2994 (1998).

23. Choi, G. H. *et al.* Molecular Characterization of Vegetative Incompatibility Genes That Restrict Hypovirus Transmission in the Chestnut Blight Fungus *Cryphonectria parasitica*. *Genetics* **190**, 113–127 (2012).

24. Zhang, D.-X., Spiering, M. J., Dawe, A. L. & Nuss, D. L. Vegetative Incompatibility Loci with Dedicated Roles in Allorecognition Restrict Mycovirus Transmission in Chestnut Blight Fungus. *Genetics* **197**, 701–714 (2014).

25. Biella, S., Smith, M. L., Aist, J. R., Cortesi, P. & Milgroom, M. G. Programmed cell death correlates with virus transmission in a filamentous fungus. *Proc. R. Soc. Lond. Ser. B: Biol. Sci.* **269**, 2269–2276 (2002).

26. Caten, C. E. Vegetative Incompatibility and Cytoplasmic Infection in Fungi. *Microbiology* **72**, 221–229 (1972).

27. Myers, J. M. *et al.* Survey of Early-Diverging Lineages of Fungi Reveals Abundant and Diverse Mycoviruses. *mBio* **11**, (2020).

28. Lau, S. K. P. *et al.* Novel Partitivirus Enhances Virulence of and Causes Aberrant Gene Expression in *Talaromyces marneffei* crossm. *mBio* (2018).

29. Schmitt, M. J. & Breinig, F. Yeast viral killer toxins: lethality and self-protection. *Nat Rev Microbiol* **4**, (2006).

30. Gao, J. *et al.* Meiotic viral attenuation through an ancestral apoptotic pathway. *Proc National Acad Sci* **116**, 16454–16462 (2019).

31. Hollings, M. Viruses Associated with A Die-Back Disease of Cultivated Mushroom. *Nature* **196**, 962–965 (1962).

32. Márquez, L. M., Redman, R. S., Rodriguez, R. J. & Roossinck, M. J. A Virus in a Fungus in a Plant: Three-Way Symbiosis Required for Thermal Tolerance. *Science* **315**, 513–515 (2007).

33. Zhang, H. *et al.* A 2-kb Mycovirus Converts a Pathogenic Fungus into a Beneficial Endophyte for *Brassica* Protection and Yield Enhancement. *Mol Plant* **13**, 1420–1433 (2020).

34. Nuss, D. L. Hypovirulence: Mycoviruses at the fungal–plant interface. *Nat. Rev. Microbiol.* **3**, 632–642 (2005).

35. Castanho, B., Butler, E. E. & Shepherd, R. J. The Association of Double-Stranded RNA with *Rhizoctonia* Decline. *Phytopathology* (1978).

36. Chu, Y.-M. *et al.* Double-Stranded RNA Mycovirus from *Fusarium graminearum*. *Appl. Environ. Microbiol.* **68**, 2529–2534 (2002).

37. Nerva, L. *et al.* Mycoviruses mediate mycotoxin regulation in *Aspergillus ochraceus*. *Environ Microbiol* **21**, 1957–1968 (2019).

38. Khan, H. A., Nerva, L. & Bhatti, M. F. The good, the bad and the cryptic: The multi-faceted roles of mycoviruses and their potential applications for a sustainable agriculture. *Virology* **585**, 259–269 (2023).

39. Obbard, D. J., Gordon, K. H. J., Buck, A. H. & Jiggins, F. M. The evolution of RNAi as a defence against viruses and transposable elements. *Philosophical Transactions of the Royal Society B: Biological Sciences* **364**, 99–115 (2009).

40. Aulia, A. *et al.* Identification of an RNA Silencing Suppressor Encoded by a Symptomless Fungal Hypovirus, Cryphonectria Hypovirus 4. *Biology* **10**, 100 (2021).

41. Segers, G. C., Wezel, R. van, Zhang, X., Hong, Y. & Nuss, D. L. Hypovirus Papain-Like Protease p29 Suppresses RNA Silencing in the Natural Fungal Host and in a Heterologous Plant System. *Eukaryot. Cell* **5**, 896–904 (2006).

42. Drinnenberg, I. A., Fink, G. R. & Bartel, D. P. Compatibility with Killer Explains the Rise of RNAi-Deficient Fungi. *Science* **333**, 1592–1592 (2011).

43. Drinnenberg, I. A. *et al.* RNAi in Budding Yeast. *Science* **326**, 544–550 (2009).

44. Li, B. *et al.* Coinfection of Two Mycoviruses Confers Hypovirulence and Reduces the Production of Mycotoxin Alternariol in *Alternaria alternata* f. sp. *mali*. *Front Microbiol* **13**, 910712 (2022).

45. Song, X. *et al.* Extending the Host Range of Fusarium Poae Virus 1 from *Fusarium poae* to other *Fusarium* Species in the Field. *Viruses* **14**, 2246 (2022).

46. Guo, J. *et al.* Hypovirulence caused by mycovirus in *Colletotrichum fructicola*. *Front Plant Sci* **13**, 1038781 (2022).

47. Cornejo, C., Hisano, S., Bragança, H., Suzuki, N. & Rigling, D. A new double-stranded RNA mycovirus in *Cryphonectria naterciae* is able to cross the species barrier and is deleterious to a new host. *Preprint* doi:10.20944/preprints202109.0325.v1.

48. Andika, I. B. *et al.* Phytopathogenic fungus hosts a plant virus: A naturally occurring cross-kingdom viral infection. *Proc National Acad Sci* **114**, 12267–12272 (2017).

49. Zheng, L., Zhang, M., Chen, Q., Zhu, M. & Zhou, E. A novel mycovirus closely related to viruses in the genus *Alphapartitivirus* confers hypovirulence in the phytopathogenic fungus *Rhizoctonia solani*. *Virology* **456**, 220–226 (2014).

50. Kanematsu, S. *et al.* A Reovirus Causes Hypovirulence of *Rosellinia necatrix*. *Phytopathology* **94**, 561–8 (2004).

51. Kanematsu, S., Sasaki, A., Onoue, M., Oikawa, Y. & Ito, T. Extending the Fungal Host Range of a Partitivirus and a Mycoreovirus from *Rosellinia necatrix* by Inoculation of Protoplasts with Virus Particles. *Phytopathology* **100**, 922–930 (2010).

52. Sasaki, A., Kanematsu, S., Onoue, M., Oyama, Y. & Yoshida, K. Infection of *Rosellinia necatrix* with purified viral particles of a member of *Partitiviridae* (RnPV1-W8). *Arch Virol* **151**, 697–707 (2006).

53. Sasaki, A., Miyanishi, M., Ozaki, K., Onoue, M. & Yoshida, K. Molecular characterization of a partitivirus from the plant pathogenic ascomycete *Rosellinia necatrix*. *Arch Virol* **150**, 1069–1083 (2005).

54. Nerva, L., Varese, G. C., Falk, B. W. & Turina, M. Mycoviruses of an endophytic fungus can replicate in plant cells: evolutionary implications. *Sci Rep* **7**, 1908 (2017).

55. Marzano, S.-Y. L. & Domier, L. L. Novel mycoviruses discovered from metatranscriptomics survey of soybean phyllosphere phytobiomes. *Virus Res.* **213**, 332–342 (2016).

56. Gilbert, K. B., Holcomb, E. E., Allscheid, R. L. & Carrington, J. C. Hiding in plain sight: New virus genomes discovered via a systematic analysis of fungal public transcriptomes. *Plos One* **14**, e0219207 (2019).

57. Larios, D. C. V. *et al.* Exploring the Mycovirus Universe: Identification, Diversity, and Biotechnological Applications. *J. Fungi* **9**, 361 (2023).

58. Hough, B., Steenkamp, E., Wingfield, B. & Read, D. Fungal Viruses Unveiled: A Comprehensive Review of Mycoviruses. *Viruses* **15**, 1202 (2023).

59. Wolf, Y. I. *et al.* Origins and Evolution of the Global RNA Virome. *Mbio* **9**, e02329-18 (2018).

60. Ghabrial, S. A., Castón, J. R., Jiang, D., Nibert, M. L. & Suzuki, N. 50-plus years of fungal viruses. *Virology* **479**, 356–368 (2015).

61. Son, M., Yu, J. & Kim, K.-H. Five Questions about Mycoviruses. *PLoS Pathog.* **11**, e1005172 (2015).

62. Buck, K. W. & Kempson-Jones, G. F. Biophysical Properties of Penicillium stoloniferum Virus S. *J Gen Virol* **18**, 223–235 (1973).

63. Nibert, M. L. *et al.* Taxonomic reorganization of family *Partitiviridae* and other recent progress in partitivirus research. *Virus Res* **188**, 128–141 (2014).

64. Byrne, M., Kashyap, A., Esquirol, L., Ranson, N. & Sainsbury, F. The structure of a plant-specific partitivirus capsid reveals a unique coat protein domain architecture with an intrinsically disordered protrusion. *Commun Biology* **4**, 1155 (2021).

65. Pan, J. *et al.* Atomic structure reveals the unique capsid organization of a dsRNA virus. *P Natl Acad Sci Usa* **106**, 4225–30 (2009).

66. Tang, J. *et al.* Backbone Trace of Partitivirus Capsid Protein from Electron Cryomicroscopy and Homology Modeling. *Biophysical Journal* **99**, (2010).

67. Ochoa, W. F. *et al.* Partitivirus Structure Reveals a 120-Subunit, Helix-Rich Capsid with Distinctive Surface Arches Formed by Quasisymmetric Coat-Protein Dimers. *Structure* **16**, (2008).

68. Tang, J. *et al.* Structure of Fusarium poae virus 1 shows conserved and variable elements of partitivirus capsids and evolutionary relationships to picobirnavirus. *Journal of Structural Biology* **172**, (2010).

69. Taggart, N. T. *et al.* Novel viruses of the family *Partitiviridae* discovered in *Saccharomyces cerevisiae*. *PLOS Pathog.* **19**, e1011418 (2023).

70. Xiao, X. *et al.* A Novel Partitivirus That Confers Hypovirulence on Plant Pathogenic Fungi. *J Virol* **88**, 10120–10133 (2014).

71. Buck, K. W. Replication of double-stranded RNA in particles of Penicillium stoloniferum virus S. *Nucleic Acids Res* **2**, 1889–1902 (1975).

72. Shi, M. *et al.* Redefining the invertebrate RNA virosphere. *Nature* **540**, 539–543 (2016).

73. Cross, S. T. *et al.* Partitiviruses Infecting *Drosophila melanogaster* and *Aedes aegypti* Exhibit Efficient Biparental Vertical Transmission. *Journal of Virology* **94**, (2020).

74. Cross, S. T. *et al.* Galbut Virus Infection Minimally Influences *Drosophila melanogaster* Fitness Traits in a Strain and Sex-Dependent Manner. *Viruses* **15**, 539 (2023).

75. Vainio, E. J. *et al.* ICTV Virus Taxonomy Profile: *Partitiviridae*. *J Gen Virol* **99**, 17–18 (2017).

76. Rowley, P. A. The frenemies within: viruses, retrotransposons and plasmids that naturally infect *Saccharomyces* yeasts. *Yeast* **34**, 279–292 (2017).

77. Wickner, R. B., Fujimura, T. & Esteban, R. Viruses and Prions of *Saccharomyces cerevisiae*. *Adv Virus Res* **86**, 1–36 (2013).

78. Nerva, L. *et al.* Transmission of Penicillium aurantiogriseum partiti-like virus 1 to a new fungal host (*Cryphonectria parasitica*) confers higher resistance to salinity and reveals adaptive genomic changes. *Environ Microbiol* **19**, 4480–4492 (2017).

79. Jiang, Y. *et al.* Molecular Characterization of a Debilitation-Associated Partitivirus Infecting the Pathogenic Fungus *Aspergillus flavus*. *Front Microbiol* **10**, 626 (2019).

80. Vainio, E. J. *et al.* Heterobasidion Partitivirus 13 Mediates Severe Growth Debilitation and Major Alterations in the Gene Expression of a Fungal Forest Pathogen. *J. Virol.* **92**, (2018).

81. Bhatti, M. F. *et al.* The effects of dsRNA mycoviruses on growth and murine virulence of *Aspergillus fumigatus*. *Fungal Genet Biol* **48**, 1071–1075 (2011).

82. Magae, Y. & Sunagawa, M. Characterization of a mycovirus associated with the brown discoloration of edible mushroom, *Flammulina velutipes*. *Virol. J.* **7**, 342 (2010).

83. Thapa, V. *et al.* Using a Novel Partitivirus in *Pseudogymnoascus destructans* to Understand the Epidemiology of White-Nose Syndrome. *PLoS Pathog.* **12**, e1006076 (2016).

84. Liu, H. *et al.* Mycoviral gene integration converts a plant pathogenic fungus into a biocontrol agent. *Proc National Acad Sci* **119**, e2214096119 (2022).

85. Mahillon, M. *et al.* Genomic and biological characterization of a novel partitivirus infecting *Fusarium equiseti*. *Virus Res* **297**, 198386 (2021).

86. Lau, S. K. P. *et al.* Novel Partitivirus Enhances Virulence of and Causes Aberrant Gene Expression in *Talaromyces marneffei*. *mBio* **9**, e00947-18 (2018).

87. Narayanasamy, S. *et al.* A global call for talaromycosis to be recognised as a neglected tropical disease. *Lancet Glob. Heal.* **9**, e1618–e1622 (2021).

88. Jenkins, M. C. *et al.* Fecundity of *Cryptosporidium parvum* is correlated with intracellular levels of the viral symbiont CPV. *Int J Parasitol* **38**, 1051–1055 (2008).

89. Ghabrial, S. A. & Suzuki, N. Viruses of Plant Pathogenic Fungi. *Phytopathology* **47**, 353–84 (2009).

90. Roossinck, M. J. Evolutionary and ecological links between plant and fungal viruses. *New Phytol* **221**, 86–92 (2019).

91. Fauver, J. R. *et al.* West African *Anopheles gambiae* mosquitoes harbor a taxonomically diverse virome including new insect-specific flaviviruses, mononegaviruses, and totiviruses. *Virology* **498**, 288–299 (2016).

92. Hartley, M.-A., Ronet, C., Zangger, H., Beverley, S. M. & Fasel, N. Leishmania RNA virus: when the host pays the toll. *Front Cell Infect Mi* **2**, 99 (2012).

93. Lee, M. D. *et al.* The Characterization of a Novel Virus Discovered in the Yeast *Pichia membranifaciens*. *Viruses* **14**, 594 (2022).

94. Konovalovas, A., Serviené, E. & Serva, S. Genome Sequence of *Saccharomyces cerevisiae* Double-Stranded RNA Virus L-A-28. *Genome Announc* **4**, e00549-16 (2016).

95. Ramírez, M., Velázquez, R., Maqueda, M. & Martínez, A. Genome Organization of a New Double-Stranded RNA LA Helper Virus From Wine *Torulaspora delbrueckii* Killer

Yeast as Compared With Its *Saccharomyces* Counterparts. *Front Microbiol* **11**, 593846 (2020).

96. Rodríguez-Cousiño, N., Gómez, P. & Esteban, R. L-A-lus, a New Variant of the L-A Totivirus Found in Wine Yeasts with Klus Killer Toxin-Encoding Mlus Double-Stranded RNA: Possible Role of Killer Toxin-Encoding Satellite RNAs in the Evolution of Their Helper Viruses. *Appl Environ Microb* **79**, 4661–4674 (2013).

97. Rodríguez-Cousiño, N., Gómez, P. & Esteban, R. Variation and Distribution of L-A Helper Totiviruses in *Saccharomyces* sensu stricto Yeasts Producing Different Killer Toxins. *Toxins* **9**, 313 (2017).

98. Diamond, M. E. *et al.* Overlapping genes in a yeast double-stranded RNA virus. *J Virol* **63**, 3983–3990 (1989).

99. Dinman, J. D., Icho, T. & Wickner, R. B. A -1 ribosomal frameshift in a double-stranded RNA virus of yeast forms a gag-pol fusion protein. *Proc National Acad Sci* **88**, 174–178 (1991).

100. Fujimura, T. & Wickner, R. B. Gene overlap results in a viral protein having an RNA binding domain and a major coat protein domain. *Cell* **55**, 663–671 (1988).

101. Dinman, J. D. & Wickner, R. B. Ribosomal frameshifting efficiency and gag/gag-pol ratio are critical for yeast M1 double-stranded RNA virus propagation. *J. Virol.* **66**, 3669–3676 (1992).

102. Tercero, J. C., Dinman, J. D. & Wickner, R. B. Yeast MAK3 N-acetyltransferase recognizes the N-terminal four amino acids of the major coat protein (gag) of the L-A double-stranded RNA virus. *J Bacteriol* **175**, 3192–3194 (1993).

103. Tercero, J. C., Riles, L. E. & Wickner, R. B. Localized mutagenesis and evidence for post-transcriptional regulation of MAK3. A putative N-acetyltransferase required for double-stranded RNA virus propagation in *Saccharomyces cerevisiae*. *J. Biol. Chem.* **267**, 20270–20276 (1992).

104. Tercero, J. C. & Wickner, R. B. MAK3 encodes an N-acetyltransferase whose modification of the L-A gag NH2 terminus is necessary for virus particle assembly. *J. Biol. Chem.* **267**, 20277–20281 (1992).

105. Park, C.-M., Lopinski, J. D., Masuda, J., Tzeng, T.-H. & Bruenn, J. A. A Second Double-Stranded RNA Virus from Yeast. *Virology* **216**, 451–454 (1996).

106. Sommer, S. S. & Wickner, R. B. Yeast L dsRNA consists of at least three distinct RNAs; evidence that the non-mendelian genes [HOK], [NEX] and [EXL] are on one of these dsRNAs. *Cell* **31**, 429–441 (1982).

107. Wesolowski, M. & Wickner, R. B. Two New Double-Stranded RNA Molecules Showing Non-Mendelian Inheritance and Heat Inducibility in *Saccharomyces cerevisiae*. *Mol Cell Biol* **4**, 181–187 (1984).

108. Wickner, R. B. Plasmids controlling exclusion of the K2 killer double-stranded RNA plasmid of yeast. *Cell* **21**, 217–226 (1980).

109. Wickner, R. B. & Toh-E, A. [HOK], a new yeast non-mendelian trait, enables a replication-defective killer plasmid to be maintained. *Genetics* **100**, 159–174 (1981).

110. Castón, J. R. *et al.* Structure of L-A Virus: A Specialized Compartment for the Transcription and Replication of Double-stranded RNA. *J. Cell Biol.* **138**, 975–985 (1997).

111. Esteban, R. & Wickner, R. B. Three different M1 RNA-containing viruslike particle types in *Saccharomyces cerevisiae*: in vitro M1 double-stranded RNA synthesis. *Mol Cell Biol* **6**, 1552–1561 (1986).

112. Naitow, H., Tang, J., Canady, M., Wickner, R. B. & Johnson, J. E. L-A virus at 3.4 Å resolution reveals particle architecture and mRNA decapping mechanism. *Nat Struct Mol Biol* **9**, 725–728 (2002).

113. Fujimura, T., Esteban, R. & Wickner, R. B. In vitro L-A double-stranded RNA synthesis in virus-like particles from *Saccharomyces cerevisiae*. *Proceedings of the National Academy of Sciences* **83**, 4433–4437 (1986).

114. Herring, A. J. & Bevan, E. A. Virus-like Particles Associated with the Double-stranded RNA Species Found in Killer and Sensitive Strains of the Yeast *Saccharomyces cerevisiae*. *J Gen Virol* **22**, 387–394 (1974).

115. Nakayashiki, T., Kurtzman, C. P., Edskes, H. K. & Wickner, R. B. Yeast prions [URE3] and [PSI+] are diseases. *Proc. Natl. Acad. Sci.* **102**, 10575–10580 (2005).

116. Crabtree, A. M., Taggart, N. T., Lee, M. D., Boyer, J. M. & Rowley, P. A. The prevalence of killer yeasts and double-stranded RNAs in the budding yeast *Saccharomyces cerevisiae*. *FEMS Yeast Res.* (2023) doi:10.1093/femsyr/foad046.

117. Bostian, K. A., Jayachandran, S. & Tipper, D. J. A glycosylated protoxin in killer yeast: Models for its structure and maturation. *Cell* **32**, 169–180 (1983).

118. Cooper, A. & Bussey, H. Characterization of the Yeast KEX1 Gene Product: a Carboxypeptidase Involved in Processing Secreted Precursor Proteins. *Mol. Cell. Biol.* **9**, 2706–2714 (1989).

119. Leibowitz, M. J. & Wickner, R. B. A chromosomal gene required for killer plasmid expression, mating, and spore maturation in *Saccharomyces cerevisiae*. *Proc. Natl. Acad. Sci.* **73**, 2061–2065 (1976).

120. Schmitt, M. J. & Tipper, D. J. K28, a unique double-stranded RNA killer virus of *Saccharomyces cerevisiae*. *Mol Cell Biol* **10**, 4807–4815 (1990).

121. Magliani, W., Conti, S., Gerloni, M., Bertolotti, D. & Polonelli, L. Yeast killer systems. *Clin Microbiol Rev* **10**, 369–400 (1997).

122. Bostian, K. A., Sturgeon, J. A. & Tipper, D. J. Encapsidation of yeast killer double-stranded ribonucleic acids: dependence of M on L. *J Bacteriol* **143**, 463–70 (1980).

123. El-Sherbeini, M., Tipper, D. J., Mitchell, D. J. & Bostian, K. A. Virus-like particle capsid proteins encoded by different L double-stranded RNAs of *Saccharomyces cerevisiae*: their roles in maintenance of M double-stranded killer plasmids. *Mol Cell Biol* **4**, 2818–2827 (1984).

124. Fujimura, T. & Esteban, R. Diphosphates at the 5′ end of the positive strand of yeast L-A double-stranded RNA virus as a molecular self-identity tag. *Mol Microbiol* **102**, 71–80 (2016).

125. Esteban, R. & Wickner, R. B. A Deletion Mutant of L-A Double-Stranded RNA Replicates Like M1 Double-Stranded RNA. *Journal of Virology* (1987).

126. Hutchins, K. & Bussey, H. Cell wall receptor for yeast killer toxin: involvement of (1,6)-beta-D-glucan. *J Bacteriol* **154**, 161–9 (1983).

127. Breinig, F., Tipper, D. J. & Schmitt, M. J. Kre1p, the Plasma Membrane Receptor for the Yeast K1 Viral Toxin. *Cell* **108**, 395–405 (2002).

128. Reiter, J., Herker, E., Madeo, F. & Schmitt, M. J. Viral killer toxins induce caspase-mediated apoptosis in yeast. *J Cell Biology* **168**, 353–358 (2005).

129. Ivanovska, I. & Hardwick, J. M. Viruses activate a genetically conserved cell death pathway in a unicellular organism. *J Cell Biology* **170**, 391–399 (2005).

130. Schmitt, M. J., Klavehn, P., Wang, J., Schönig, I. & Tipper, D. J. Cell cycle studies on the mode of action of yeast K28 killer toxin. *Microbiology+* **142**, 2655–2662 (1996).

131. Eisfeld, K., Riffer, F., Mentges, J. & Schmitt, M. J. Endocytotic uptake and retrograde transport of a virally encoded killer toxin in yeast. *Mol. Microbiol.* **37**, 926–940 (2000).

132. Becker, B. & Schmitt, M. J. Yeast Killer Toxin K28: Biology and Unique Strategy of Host Cell Intoxication and Killing. *Toxins* **9**, 333 (2017).

133. Fredericks, L. R. *et al.* The Species-Specific Acquisition and Diversification of a K1-like Family of Killer Toxins in Budding Yeasts of the Saccharomycotina. *Plos Genet* **17**, e1009341 (2021).

134. Young, T. W. & Yagiu, M. A comparison of the killer character in different yeasts and its classification. *Antonie Van Leeuwenhoek* **44**, 59–77 (1978).

135. Woods, D. R. & Bevan, E. A. Studies on the Nature of the Killer Factor Produced by *Saccharomyces cerevisiae*. *Microbiology* **51**, 115–126 (1968).

136. Bussey, H. Effects of Yeast Killer Factor on Sensitive Cells. *Nat. N. Biol.* **235**, 73–75 (1972).

137. Kadowaki, K. & Halvorson, H. O. Appearance of a New Species of Ribonucleic Acid During Sporulation in *Saccharomyces cerevisiae*. *J. Bacteriol.* **105**, 826–830 (1971).

138. Widner, W. R., Matsumoto, Y. & Wickner, R. B. Is 20S RNA Naked? *Mol. Cell. Biol.* **11**, 2905–2908 (1991).

139. García-Cuéllar, M. P., Esteban, L. M., Fujimura, T., Rodríguez-Cousiño, N. & Esteban, R. Yeast Viral 20 S RNA Is Associated with Its Cognate RNA-dependent RNA Polymerase (∗). *J Biol Chem* **270**, 20084–20089 (1995).

140. Solórzano, A., Rodríguez-Cousiño, N., Esteban, R. & Fujimura, T. Persistent Yeast Single-stranded RNA Viruses Exist in Vivo as Genomic RNA·RNA Polymerase Complexes in 1:1 Stoichiometry*. *J Biol Chem* **275**, 26428–26435 (2000).

141. Vega, L., Sevillano, L., Esteban, R. & Fujimura, T. Resting complexes of the persistent yeast 20S RNA Narnavirus consist solely of the 20S RNA viral genome and its RNA polymerase p91. *Mol Microbiol* **93**, 1119–1129 (2014).

142. Esteban, L. M., Rodriguez-Cousiño, N. & Esteban, R. T double-stranded RNA (dsRNA) sequence reveals that T and W dsRNAs form a new RNA family in *Saccharomyces cerevisiae*. Identification of 23 S RNA as the single-stranded form of T dsRNA. *J Biol Chem* **267**, 10874–10881 (1992).

143. Rodriguez-Cousiño, N., Esteban, L. M. & Esteban, R. Molecular cloning and characterization of W double-stranded RNA, a linear molecule present in *Saccharomyces cerevisiae*. Identification of its single-stranded RNA form as 20 S RNA. *J Biol Chem* **266**, 12772–12778 (1991).

144. Esteban, R. & Fujimura, T. Launching the yeast 23S RNA Narnavirus shows 5' and 3' cis-acting signals for replication. *Proc National Acad Sci* **100**, 2568–2573 (2003).

145. Esteban, R., Vega, L. & Fujimura, T. Launching of the Yeast 20S RNA Narnavirus by Expressing the Genomic or Antigenomic Viral RNA in Vivo. *J Biol Chem* **280**, 33725–33734 (2005).

146. Fujimura, T. & Esteban, R. Bipartite 3′-Cis-acting Signal for Replication in Yeast 23 S RNA Virus and Its Repair*. *J Biol Chem* **279**, 13215–13223 (2004).

147. Fujimura, T. & Esteban, R. The Bipartite 3′-cis-Acting Signal for Replication Is Required for Formation of a Ribonucleoprotein Complex in Vivo between the Viral Genome and Its RNA Polymerase in Yeast 23 S RNA Virus*. *J Biol Chem* **279**, 44219–44228 (2004).

148. Vijayraghavan, S., Kozmin, S. G., Xi, W. & McCusker, J. H. A novel narnavirus is widespread in *Saccharomyces cerevisiae* and impacts multiple host phenotypes. *G3 Genes Genomes Genetics* **13**, (2022).

149. Strope, P. K. *et al.* 2μ plasmid in *Saccharomyces* species and in *Saccharomyces cerevisiae*. *FEMS Yeast Res.* **15**, (2015).

150. Strope, P. K. *et al.* The 100-genomes strains, an S. *cerevisiae* resource that illuminates its natural phenotypic and genotypic variation and emergence as an opportunistic pathogen. *Genome Res* **25**, 762–774 (2015).

151. Vijayraghavan, S. *et al.* Mitochondrial Genome Variation Affects Multiple Respiration and Nonrespiration Phenotypes in *Saccharomyces cerevisiae*. *Genetics* **211**, 773–786 (2018).

152. Parker, R. & Song, H. The enzymes and control of eukaryotic mRNA turnover. *Nat Struct Mol Biol* **11**, 121–127 (2004).

153. Muhlrad, D. & Parker, R. Mutations affecting stability and deadenylation of the yeast MFA2 transcript. *Genes Dev.* **6**, 2100–2111 (1992).

154. Decker, C. J. & Parker, R. A turnover pathway for both stable and unstable mRNAs in yeast: evidence for a requirement for deadenylation. *Genes Dev.* **7**, 1632–1643 (1993).

155. Anderson, J. S. J. & Parker, R. The 3' to 5' degradation of yeast mRNAs is a general mechanism for mRNA turnover that requires the SKI2 DEVH box protein and 3' to 5' exonucleases of the exosome complex. *The EMBO Journal* (1998).

156. Hsu, C. L. & Stevens, A. Yeast cells lacking 5'-->3' exoribonuclease 1 contain mRNA species that are poly(A) deficient and partially lack the 5' cap structure. *Mol Cell Biol* **13**, 4826–4835 (1993).

157. Muhlrad, D., Decker, C. J. & Parker, R. Deadenylation of the unstable mRNA encoded by the yeast MFA2 gene leads to decapping followed by 5'-->3' digestion of the transcript. *Genes Dev.* **8**, 855–866 (1994).

158. Dunckley, T. & Parker, R. The DCP2 protein is required for mRNA decapping in *Saccharomyces cerevisiae* and contains a functional MutT motif. *EMBO J.* **18**, 5411–5422 (1999).

159. Dijk, A. A. van, Makeyev, E. V. & Bamford, D. H. Initiation of viral RNA-dependent RNA polymerization. *J Gen Virol* **85**, 1077–1093 (2004).

160. Steiger, M., Carr-Schmid, A., Schwartz, D. C., Kiledjian, M. & Parker, R. Analysis of recombinant yeast decapping enzyme. *RNA* **9**, 231–238 (2003).

161. Johnson, A. W. Rat1p Nuclease. in vol. 342 260–268 (Academic Press, 2001).

162. Johnson, A. W. Rat1p and Xrn1p are functionally interchangeable exoribonucleases that are restricted to and required in the nucleus and cytoplasm, respectively. *Mol Cell Biol* **17**, 6122–6130 (1997).

163. Halbach, F., Reichelt, P., Rode, M. & Conti, E. The Yeast Ski Complex: Crystal Structure and RNA Channeling to the Exosome Complex. *Cell* **154**, 814–826 (2013).

164. Parker, R. RNA Degradation in *Saccharomyces cerevisae*. *Genetics* **191**, 671–702 (2012).

165. Sato, H. & Singer, R. H. Cellular variability of nonsense-mediated mRNA decay. *Nat Commun* **12**, 7203 (2021).

166. Muhlrad, D. & Parker, R. Recognition of Yeast mRNAs as "Nonsense Containing" Leads to Both Inhibition of mRNA Translation and mRNA Degradation: Implications for the Control of mRNA Decapping. *Mol Biol Cell* **10**, 3971–3978 (1999).

167. Son, M. & Wickner, R. B. Nonsense-mediated mRNA decay factors cure most [PSI+] prion variants. *Proc National Acad Sci* **115**, 201717495 (2018).

168. Karousis, E. D. & Mühlemann, O. The broader sense of nonsense. *Trends Biochem Sci* **47**, 921–935 (2022).

169. Lejeune, F. Nonsense-Mediated mRNA Decay, a Finely Regulated Mechanism. *Biomed* **10**, 141 (2022).

170. Doma, M. K. & Parker, R. Endonucleolytic cleavage of eukaryotic mRNAs with stalls in translation elongation. *Nature* **440**, 561–564 (2006).

171. Frischmeyer, P. A. *et al.* An mRNA surveillance mechanism that eliminates transcripts lacking termination codons. *Science* (2002).

172. Hoof, A. van, Frischmeyer, P. A., Dietz, H. C. & Parker, R. Exosome-Mediated Recognition and Degradation of mRNAs Lacking a Termination Codon. *Science* **295**, 2262–2264 (2002).

173. Aviv, T., Lin, Z., Ben-Ari, G., Smibert, C. A. & Sicheri, F. Sequence-specific recognition of RNA hairpins by the SAM domain of Vts1p. *Nat. Struct. Mol. Biol.* **13**, 168–176 (2006).

174. Rendl, L. M., Bieman, M. A. & Smibert, C. A. *S. cerevisiae* Vts1p induces deadenylation-dependent transcript degradation and interacts with the Ccr4p-Pop2p-Not deadenylase complex. *RNA* **14**, 1328–1336 (2008).

175. Buchan, J. R. & Parker, R. Eukaryotic Stress Granules: The Ins and Outs of Translation. *Mol Cell* **36**, 932–941 (2009).

176. Ball, S. G., Tirtiaux, C. & Wickner, R. B. Genetic control L-A and L-(BC) dsRNA copy number in killer systems of *Saccharomyces cerevisiae*. *Genetics* (1984).

177. Ridley, S. P., Sommer, S. S. & Wickner, R. B. Superkiller Mutations in *Saccharomyces cerevisiae* Suppress Exclusion of M2 Double-Stranded RNA by L-A-HN and Confer Cold Sensitivity in the Presence of M and L-A-HN. *Mol. Cell. Biol.* **4**, 761–770 (1984).

178. Sweeney, T. K., Tate, A. & Fink, G. R. A study of the transmission and structure of double-stranded RNAs associated with the killer phenomenon in *Saccharomyces cerevisiae*. *Genetics* (1976).

179. Brown, J. T., Bai, X. & Johnson, A. W. The yeast antiviral proteins Ski2p, Ski3p, and Ski8p exist as a complex in vivo. *RNA* (2000).

180. Schmidt, C. *et al.* The cryo-EM structure of a ribosome–Ski2-Ski3-Ski8 helicase complex. *Science* **354**, 1431–1433 (2016).

181. Wang, L., Lewis, M. S. & Johnson, A. W. Domain interactions within the Ski2/3/8 complex and between the Ski complex and Ski7p. *Rna* **11**, 1291–1302 (2005).

182. Widner, W. R. & Wickner, R. B. Evidence that the SKI Antiviral System of *Saccharomyces cerevisiae* Acts by Blocking Expression of Viral mRNA. *Mol. Cell. Biol.* **13**, 4331–4341 (1993).

183. Widner, W. R. & Wickner, R. B. Evidence that the SKI Antiviral System of *Saccharomyces cerevisiae* Acts by Blocking Expression of Viral mRNA. *Molecular and Cellular Biology* (1993).

184. Johnson, A. W. & Kolodner, R. D. Synthetic Lethality of sep1 (xrn1) ski2 and sep1 (xrn1) ski3 Mutants of *Saccharomyces cerevisiae* Is Independent of Killer Virus and Suggests a General Role for These Genes in Translation Control. *Mol. Cell. Biol.* **15**, 2719–2727 (1995).

185. Mitchell, P., Petfalski, E., Shevchenko, A., Mann, M. & Tollervey, D. The Exosome: A Conserved Eukaryotic RNA Processing Complex Containing Multiple 3′→5′ Exoribonucleases. *Cell* **91**, 457–466 (1997).

186. Chlebowski, A., Tomecki, R., López, M. E. G., Séraphin, B. & Dziembowski, A. RNA Exosome. *Adv. Exp. Med. Biol.* **702**, 63–78 (2011).

187. Chlebowski, A., Lubas, M., Jensen, T. H. & Dziembowski, A. RNA decay machines: The exosome. *Biochimica Et Biophysica Acta Bba - Gene Regul Mech* **1829**, 552–560 (2013).

188. Lorentzen, E., Dziembowski, A., Lindner, D., Seraphin, B. & Conti, E. RNA channelling by the archaeal exosome. *EMBO Rep.* **8**, 470–476 (2007).

189. Koonin, E. V., Wolf, Y. I. & Aravind, L. Prediction of the Archaeal Exosome and Its Connections with the Proteasome and the Translation and Transcription Machineries by a Comparative-Genomic Approach. *Genome Res.* **11**, 240–252 (2001).

190. Symmons, M. F., Jones, G. H. & Luisi, B. F. A Duplicated Fold Is the Structural Basis for Polynucleotide Phosphorylase Catalytic Activity, Processivity, and Regulation. *Structure* **8**, 1215–1226 (2000).

191. Ramos, C. R. R., Oliveira, C. L. P., Torriani, I. L. & Oliveira, C. C. The *Pyrococcus* Exosome Complex. *J. Biol. Chem.* **281**, 6751–6759 (2006).

192. Lorentzen, E. & Conti, E. Structural Basis of 3′ End RNA Recognition and Exoribonucleolytic Cleavage by an Exosome RNase PH Core. *Mol. Cell* **20**, 473–481 (2005).

193. Lorentzen, E. *et al.* The archaeal exosome core is a hexameric ring structure with three catalytic subunits. *Nat. Struct. Mol. Biol.* **12**, 575–581 (2005).

194. Büttner, K., Wenig, K. & Hopfner, K.-P. Structural Framework for the Mechanism of Archaeal Exosomes in RNA Processing. *Mol. Cell* **20**, 461–471 (2005).

195. Lykke-Andersen, S., Brodersen, D. E. & Jensen, T. H. Origins and activities of the eukaryotic exosome. *J. Cell Sci.* **122**, 1487–1494 (2009).

196. Briggs, M. W., Burkard, K. T. D. & Butler, J. S. Rrp6p, the Yeast Homologue of the Human PM-Scl 100-kDa Autoantigen, Is Essential for Efficient 5.8 S rRNA 3′ End Formation*. *J. Biol. Chem.* **273**, 13255–13263 (1998).

197. Rowley, P. A., Ho, B., Bushong, S., Johnson, A. & Sawyer, S. L. *XRN1* Is a Species-Specific Virus Restriction Factor in Yeasts. *PLOS Pathogens* 1–27 (2016).

198. Booker, T. R., Jackson, B. C. & Keightley, P. D. Detecting positive selection in the genome. *Bmc Biol* **15**, 98 (2017).

199. Chahar, H. S., Chen, S. & Manjunath, N. P-body components LSM1, GW182, DDX3, DDX6 and XRN1 are recruited to WNV replication sites and positively regulate viral replication. *Virology* **436**, 1–7 (2013).

200. Reineke, L. C. & Lloyd, R. E. Diversion of stress granules and P-bodies during viral infection. *Virology* **436**, 255–267 (2013).

201. Dougherty, J. D., White, J. P. & Lloyd, R. E. Poliovirus-Mediated Disruption of Cytoplasmic Processing Bodies. *J Virol* **85**, 64–75 (2011).

202. Rodríguez-Cousiño, N. *et al.* A New Wine *Saccharomyces cerevisiae* Killer Toxin (Klus), Encoded by a Double-Stranded RNA Virus, with Broad Antifungal Activity Is Evolutionarily Related to a Chromosomal Host Gene. *Appl Environ Microb* **77**, 1822–1832 (2011).

203. Gao, J., Chau, S. & Meneghini, M. D. Viral attenuation by Endonuclease G during yeast gametogenesis: insights into ancestral roles of programmed cell death? *Microbial Cell* (2019) doi:10.15698/mic2020.02.705.

204. Büttner, S. *et al.* Endonuclease G Regulates Budding Yeast Life and Death. *Mol Cell* **25**, 233–246 (2007).

205. Li, L. Y., Luo, X. & Wang, X. Endonuclease G is an apoptotic DNase when released from mitochondria. *Nature* **412**, 95–99 (2001).

206. Eastwood, M. D., Cheung, S. W. T., Lee, K. Y., Moffat, J. & Meneghini, M. D. Developmentally Programmed Nuclear Destruction during Yeast Gametogenesis. *Dev Cell* **23**, 35–44 (2012).

207. Eastwood, M. D., Cheung, S. W. T. & Meneghini, M. D. Programmed nuclear destruction in yeast. *Autophagy* (2012).

208. Chau, S. *et al.* Diverse yeast antiviral systems prevent lethal pathogenesis caused by the L-A mycovirus. *Proceedings of the National Academy of Sciences* (2023).

209. Liu, Y. X. & Dieckmann, C. L. Overproduction of yeast viruslike particles by strains deficient in a mitochondrial nuclease. *Mol Cell Biol* **9**, 3323–3331 (1989).

210. Narayanan, K. & Makino, S. Interplay between viruses and host mRNA degradation. *Biochimica Et Biophysica Acta Bba - Gene Regul Mech* **1829**, 732–741 (2013).

211. Boivin, S., Cusack, S., Ruigrok, R. W. H. & Hart, D. J. Influenza A Virus Polymerase: Structural Insights into Replication and Host Adaptation Mechanisms*. *J. Biol. Chem.* **285**, 28411–28417 (2010).

212. Plotch, S. J., Bouloy, M., Ulmanen, I. & Krug, R. M. A unique cap (m7GpppXm)-dependent influenza virion endonuclease cleaves capped RNAs to generate the primers that initiate viral RNA transcription. *Cell* **23**, 847–858 (1981).

213. Chapman, E. G., Moon, S. L., Wilusz, J. & Kieft, J. S. RNA structures that resist degradation by Xrn1 produce a pathogenic Dengue virus RNA. *Elife* **3**, e01892 (2014).

214. Schuessler, A. *et al.* West Nile Virus Noncoding Subgenomic RNA Contributes to Viral Evasion of the Type I Interferon-Mediated Antiviral Response. *Journal of Virology* (2012).

215. Silva, P. A. G. C., Pereira, C. F., Dalebout, T. J., Spaan, W. J. M. & Bredenbeek, P. J. An RNA Pseudoknot Is Required for Production of Yellow Fever Virus Subgenomic RNA by the Host Nuclease XRN1. *J. Virol.* **84**, 11395–11406 (2010).

216. Naeve, C. W. & Trent, D. W. Identification of Saint Louis encephalitis virus mRNA. *J. Virol.* **25**, 535–545 (1978).

217. Takeda, H., Oya, A., Hashimoto, K., Yasuda, T. & Yamada, M.-A. Association of Virus Specific Replicative Ribonucleic Acid with Nuclear Membrane in Chick Embryo Cells Infected with Japanese Encephalitis Virus. *J. Gen. Virol.* **38**, 281–291 (1978).

218. Wengler, G., Wengler, G. & Gross, H. J. Studies on virus-specific nucleic acids synthesized in vertebrate and mosquito cells infected with flaviviruses. *Virology* **89**, 423–437 (1978).

219. Urosevic, N., Maanen, M. van, Mansfield, J. P., Mackenzie, J. S. & Shellam, G. R. Molecular characterization of virus-specific RNA produced in the brains of flavivirus-susceptible and -resistant mice after challenge with Murray Valley encephalitis virus. *J. Gen. Virol.* **78**, 23–29 (1997).

220. Pijlman, G. P. *et al.* A Highly Structured, Nuclease-Resistant, Noncoding RNA Produced by Flaviviruses Is Required for Pathogenicity. *Cell Host Microbe* **4**, 579–591 (2008).

221. Liu, R. *et al.* Identification and characterization of small sub-genomic RNAs in dengue 1–4 virus-infected cell cultures and tissues. *Biochem. Biophys. Res. Commun.* **391**, 1099–1103 (2010).

222. Schnettler *et al.* Noncoding Flavivirus RNA Displays RNA Interference Suppressor Activity in Insect and Mammalian Cells. *Journal of Virology* (2012).

223. Moon, S. L. *et al.* A noncoding RNA produced by arthropod-borne flaviviruses inhibits the cellular exoribonuclease XRN1 and alters host mRNA stability. *RNA* **18**, 2029–2040 (2012).

224. Chang, R.-Y. *et al.* Japanese encephalitis virus non-coding RNA inhibits activation of interferon by blocking nuclear translocation of interferon regulatory factor 3. *Vet. Microbiol.* **166**, 11–21 (2013).

225. Gaglia, M. M., Covarrubias, S., Wong, W. & Glaunsinger, B. A. A Common Strategy for Host RNA Degradation by Divergent Viruses. *J Virol* **86**, 9527–9530 (2012).

226. Glaunsinger, B. & Ganem, D. Lytic KSHV Infection Inhibits Host Gene Expression by Accelerating Global mRNA Turnover. *Mol. Cell* **13**, 713–723 (2004).

227. Kamitani, W. *et al.* Severe acute respiratory syndrome coronavirus nsp1 protein suppresses host gene expression by promoting host mRNA degradation. *Proc. Natl. Acad. Sci.* **103**, 12885–12890 (2006).

228. Kwong, A. D. & Frenkel, N. Herpes simplex virus-infected cells contain a function(s) that destabilizes both host and viral mRNAs. *Proc. Natl. Acad. Sci.* **84**, 1926–1930 (1987).

229. Rowe, M. *et al.* Host shutoff during productive Epstein–Barr virus infection is mediated by BGLF5 and may contribute to immune evasion. *Proc. Natl. Acad. Sci.* **104**, 3366–3371 (2007).

230. Weston, S. *et al.* The SKI complex is a broad-spectrum, host-directed antiviral drug target for coronaviruses, influenza, and filoviruses. *Proc National Acad Sci* 202012939 (2020) doi:10.1073/pnas.2012939117.

231. Wilkinson, M., Yllanes, D. & Huber, G. Polysomally protected viruses. *Phys Biol* (2021) doi:10.1088/1478-3975/abf5b5.

232. Fujimura, T. & Esteban, R. Cap Snatching of Yeast L-A Double-stranded RNA Virus Can Operate in Trans and Requires Viral Polymerase Actively Engaging in Transcription. *J Biol Chem* **287**, 12797–12804 (2012).

233. Fujimura, T. & Esteban, R. Cap Snatching in Yeast L-BC Double-stranded RNA Totivirus. *J Biol Chem* **288**, 23716–23724 (2013).

234. Fujimura, T. & Esteban, R. Cap-snatching mechanism in yeast L-A double-stranded RNA virus. *Proc National Acad Sci* **108**, 17667–17671 (2011).

235. Fujimura, T. & Esteban, R. The cap-snatching reaction of yeast L-A double-stranded RNA virus is reversible and the catalytic sites on both Gag and the Gag domain of Gag-Pol are active. *Mol Microbiol* **111**, 395–404 (2019).

236. Masison, D. C. *et al.* Decoying the cap-mRNA degradation system by a double-stranded RNA virus and poly(A)-mRNA surveillance by a yeast antiviral system. *Mol Cell Biol* **15**, 2763–2771 (1995).

237. Blanc, A., Goyer, C. & Sonenberg, N. The coat protein of the yeast double-stranded RNA virus L-A attaches covalently to the cap structure of eukaryotic mRNA. *Mol Cell Biol* **12**, 3390–3398 (1992).

238. Fujimura, T. & Esteban, R. Yeast Double-stranded RNA Virus L-A Deliberately Synthesizes RNA Transcripts with 5′-Diphosphate. *J Biol Chem* **285**, 22911–22918 (2010).

239. Masison, D. C., Reidy, M. & Kumar, J. J Proteins Counteract Amyloid Propagation and Toxicity in Yeast. *Biology* **11**, 1292 (2022).

240. Esteban, R., Vega, L. & Fujimura, T. 20S RNA Narnavirus Defies the Antiviral Activity of *SKI1/XRN1* in *Saccharomyces cerevisiae*. *J Biol Chem* **283**, 25812–25820 (2008).

241. Murphy, K. A., Tabuloc, C. A., Cervantes, K. R. & Chiu, J. C. Ingestion of genetically modified yeast symbiont reduces fitness of an insect pest via RNA interference. *Sci Rep* **6**, 22587 (2016).

242. Ludlow, C. L. *et al.* Independent Origins of Yeast Associated with Coffee and Cacao Fermentation. *Curr Biol* **26**, 965–971 (2016).

243. Haile, M. & Kang, W. H. The Role of Microbes in Coffee Fermentation and Their Impact on Coffee Quality. *J. Food Qual.* **2019**, 1–6 (2019).

244. Espinal, R. B. A. *et al.* Uncovering a Complex Virome Associated with the Cacao Pathogens *Ceratocystis cacaofunesta* and *Ceratocystis fimbriata*. *Pathogens* **12**, 287 (2023).

245. Sherman, F. An Introduction to the Genetics and Molecular Biology of the Yeast *Saccharomyces cerevisiae*. vol. 6 302–325 (1998).

246. Sherman, F. Getting Started with Yeast. (2002).

247. Glingston, R. S., Yadav, J., Rajpoot, J., Joshi, N. & Nagotu, S. Contribution of yeast models to virus research. *Appl Microbiol Biot* 1–24 (2021) doi:10.1007/s00253-021-11331-w.

248. Zhao, R. Y. Yeast for virus research. *Microb Cell* **4**, 311–330 (2017).

249. Mardanov, A. V., Beletsky, A. V., Tanashchuk, T. N., Kishkovskaya, S. A. & Ravin, N. V. A novel narnavirus from a *Saccharomyces cerevisiae* flor strain. *Arch Virol* **165**, 789–791 (2020).

250. Roossinck, M. J. *et al.* Ecogenomics: using massively parallel pyrosequencing to understand virus ecology. *Mol. Ecol.* **19**, 81–88 (2010).

251. Buck, K. W. Semi-conservative replication of double-stranded RNA by a virion-associated RNA polymerase. *Biochem. Biophys. Res. Commun.* **84**, 639–645 (1978).

252. Zhu, J. Z. *et al.* A Novel Partitivirus That Confer Hypovirulence to the Plant Pathogenic Fungus *Colletotrichum liriope*s. *Front. Microbiol.* **12**, 653809 (2021).

253. Crucitti, D. *et al.* Identification and Molecular Characterization of Novel Mycoviruses in *Saccharomyces* and Non-*Saccharomyces* Yeasts of Oenological Interest. *Viruses* (2021).

254. Peter, J. *et al.* Genome evolution across 1,011 *Saccharomyces cerevisiae* isolates. *Nature* **556**, 339–344 (2018).

255. Crabtree, A. M. *et al.* A Rapid Method for Sequencing Double-Stranded RNAs Purified from Yeasts and the Identification of a Potent K1 Killer Toxin Isolated from *Saccharomyces cerevisiae*. *Viruses* **11**, 70 (2019).

256. Fink, G. R. & Styles, C. A. Curing of a Killer Factor in *Saccharomyces cerevisiae*. *Proc National Acad Sci* **69**, 2846–2849 (1972).

257. Crabtree, A. *et al.* Novel Double-Stranded RNA Viruses Discovered within *Saccharomyces cerevisiae*. *Access Microbiol* **1**, (2019).

258. Shi, X. & Kaminskyj, S. G. W. 5’ RACE by Tailing a General Template-Switching Oligonucleotide. *Biotechniques* **29**, 1192–1195 (2000).

259. Scotto–Lavino, E., Du, G. & Frohman, M. A. 5′ end cDNA amplification using classic RACE. *Nat Protoc* **1**, 2555–2562 (2006).

260. Khramtsov, N. V. & Upton, S. J. High-Temperature Inducible Cell-Free Transcription and Replication of Double-Stranded RNAs within the Parasitic Protozoan *Cryptosporidium parvum*. *Virology* **245**, 331–337 (1998).

261. Høie, M. H. *et al.* NetSurfP-3.0: accurate and fast prediction of protein structural features by protein language models and deep learning. *Nucleic Acids Res.* **50**, gkac439- (2022).

262. Jia, H. & Gong, P. A Structure-Function Diversity Survey of the RNA-Dependent RNA Polymerases From the Positive-Strand RNA Viruses. *Front Microbiol* **10**, 1945 (2019).

263. Velthuis, A. J. W. te. Common and unique features of viral RNA-dependent polymerases. *Cell Mol Life Sci* **71**, 4403–4420 (2014).

264. Černý, J., Bolfíková, B. Č., Valdés, J. J., Grubhoffer, L. & Růžek, D. Evolution of Tertiary Structure of Viral RNA Dependent Polymerases. *Plos One* **9**, e96070 (2014).

265. Hansen, J. L., Long, A. M. & Schultz, S. C. Structure of the RNA-dependent RNA polymerase of poliovirus. *Structure* **5**, 1109–1122 (1997).

266. Schwan, R. F. & Wheals, A. E. The Microbiology of Cocoa Fermentation and its Role in Chocolate Quality. *Crit. Rev. Food Sci. Nutr.* **44**, 205–221 (2004).

267. Hays, M., Young, J. M., Levan, P. F. & Malik, H. S. A natural variant of the essential host gene MMS21 restricts the parasitic 2-micron plasmid in *Saccharomyces cerevisiae*. *eLife* **9**, e62337 (2020).

268. Dihanich, M., Tuinen, E. van, Lambris, J. D. & Marshallsay, B. Accumulation of viruslike particles in a yeast mutant lacking a mitochondrial pore protein. *Mol Cell Biol* **9**, 1100–1108 (1989).

269. Dobson, M. J. *et al.* The 2μm Plasmid Causes Cell Death in *Saccharomyces cerevisiae* with a Mutation in Ulp1 Protease. *Mol. Cell. Biol.* **25**, 4299–4310 (2005).

270. Edwards, M. D., Symbor-Nagrabska, A., Dollard, L., Gifford, D. K. & Fink, G. R. Interactions between chromosomal and nonchromosomal elements reveal missing heritability. *Proc National Acad Sci* **111**, 7719–7722 (2014).

271. Nibert, M. L., Woods, K. M., Upton, S. J. & Ghabrial, S. A. *Cryspovirus*: a new genus of protozoan viruses in the family *Partitiviridae*. *Arch Virol* **154**, 1959–1965 (2009).

272. Nader, J. L. *et al.* Evolutionary genomics of anthroponosis in *Cryptosporidium*. *Nat. Microbiol.* **4**, 826–836 (2019).

273. el-Sherbeini, M. & Bostian, K. A. Viruses in fungi: infection of yeast with the K1 and K2 killer viruses. *Proc National Acad Sci* **84**, 4293–4297 (1987).

274. Yu, X. *et al.* Extracellular transmission of a DNA mycovirus and its use as a natural fungicide. *Proc. Natl. Acad. Sci.* **110**, 1452–1457 (2013).

275. Sepp, T., Wang, A. L. & Wang, C. C. Giardiavirus-resistant *Giardia lamblia* lacks a virus receptor on the cell membrane surface. *Journal of Virology* **68**, (1994).

276. Roossinck, M. J. Lifestyles of plant viruses. *Philosophical Transactions Royal Soc B Biological Sci* **365**, 1899–1905 (2010).

277. Xue, B. *et al.* Structural Disorder in Viral Proteins. *Chem. Rev.* **114**, 6880–6911 (2014).

278. Xie, H. *et al.* Functional Anthology of Intrinsic Disorder. 1. Biological Processes and Functions of Proteins with Long Disordered Regions. *J. Proteome Res.* **6**, 1882–1898 (2007).

279. Schulenburg, C. & Hilvert, D. Dynamics in Enzyme Catalysis. *Top. Curr. Chem.* **337**, 41–67 (2013).

280. Mata, C. P. *et al.* Acquisition of functions on the outer capsid surface during evolution of double-stranded RNA fungal viruses. *Plos Pathog* **13**, e1006755 (2017).

281. Luque, D., Mata, C. P., Suzuki, N., Ghabrial, S. A. & Castón, J. R. Capsid Structure of dsRNA Fungal Viruses. *Viruses* **10**, 481 (2018).

282. Wright, P. E. & Dyson, H. J. Intrinsically disordered proteins in cellular signalling and regulation. *Nat. Rev. Mol. Cell Biol.* **16**, 18–29 (2015).

283. Liu, J. *et al.* Intrinsic Disorder in Transcription Factors. *Biochemistry* **45**, 6873–6888 (2006).

284. Mishra, P. M., Verma, N. C., Rao, C., Uversky, V. N. & Nandi, C. K. Intrinsically disordered proteins of viruses: Involvement in the mechanism of cell regulation and pathogenesis. *Prog. Mol. Biol. Transl. Sci.* **174**, 1–78 (2020).

285. Vuuren, H. J. J. van & Wingfield, B. D. Killer Yeasts - Cause of Stuck Fermentations in a Wine Cellar. *S. Afr. J. Enol. Vitic.* **7**, (2017).

286. Orban, T. I. & Izaurralde, E. Decay of mRNAs targeted by RISC requires *XRN1*, the Ski complex, and the exosome. *Rna* **11**, 459–469 (2005).

287. Chau, S. *et al.* Diverse innate immune factors protect yeast from lethal viral pathogenesis. *Biorxiv* 2022.02.14.480455 (2022) doi:10.1101/2022.02.14.480455.

288. Neiman, A. M. Sporulation in the Budding Yeast *Saccharomyces cerevisiae*. *Genetics* **189**, 737–765 (2011).

289. Sherman, F. Getting Started with Yeast. in (eds. Guthrie, C. & Fink, G. R.) vol. 194 3–933 (1991).

290. Day, M. Chapter One Yeast Petites and Small Colony Variants For Everything There Is a Season. *Adv Appl Microbiol* **85**, 1–41 (2013).

291. Conde, J. & Fink, G. R. A mutant of *Saccharomyces cerevisiae* defective for nuclear fusion. *Proc National Acad Sci* **73**, 3651–3655 (1976).

292. Lacroute, F. Regulation of Pyrimidine Biosynthesis in *Saccharomyces cerevisiae*. *J. Bacteriol.* **95**, 824–832 (1968).

293. Jones, M. E. Orotidylate Decarboxylase of Yeast and Man. *Curr. Top. Cell. Regul.* **33**, 331–342 (1992).

294. Suzuki, H., Murakami, A. & Yoshida, K. Counterselection System for *Geobacillus kaustophilus* HTA426 through Disruption of pyrF and pyrR. *Appl. Environ. Microbiol.* **78**, 7376–7383 (2012).

295. Loyse, A., Dromer, F., Day, J., Lortholary, O. & Harrison, T. S. Flucytosine and cryptococcosis: time to urgently address the worldwide accessibility of a 50-year-old antifungal. *J. Antimicrob. Chemother.* **68**, 2435–2444 (2013).

296. DeMaeseneire, S. L. *Myrothecium gramineum* as a novel fungal expression host. (2007).

297. Boeke, J. D., Trueheart, J., Natsoulis, G. & Fink, G. R. 5-Fluoroorotic acid as a selective agent in yeast molecular genetics. *Methods Enzym.* **154**, 164–175 (1987).

298. Boeke, J. D., Croute, F. L. & Fink, G. R. A positive selection for mutants lacking orotidine-5′-phosphate decarboxylase activity in yeast: 5-fluoro-orotic acid resistance. *Mol. Gen. Genet. MGG* **197**, 345–346 (1984).

299. Pardini, B. *et al.* 5-Fluorouracil-based chemotherapy for colorectal cancer and MTHFR/MTRR genotypes. *Br. J. Clin. Pharmacol.* **72**, 162–163 (2011).

300. Goldring, E. S., Grossman, L. I. & Marmur, and J. Isolation of Mutants Containing Mitochondrial Deoxyribonucleic Acid of Reduced Size. *J. Bacteriol.* **107**, 377–381 (1971).

301. Ferguson, L. R. & Borstel, R. C. von. Induction of the cytoplasmic "petite" mutation by chemical and physical agents in *S. cerevisiae*. *Mutation Research* **265**, 103–148 (2018).

302. Redshaw, P. A. Induction of Petite Mutations During Germination and Outgrowth of *Saccharomyces cerevisiae* Ascospores. *J. Bacteriol.* **124**, 1411–1416 (1975).

303. Slonimski, P. P., Perrodin, G. & Croft, J. H. Ethidium bromide induced mutation of yeast mitochondria: Complete transformation of cells into respiratory deficient non-chromosomal "petites." *Biochem Bioph Res Co* **30**, 232–239 (1968).

304. Whittaker, P. A., Hammond, R. C. & Luha, A. A. Mechanism of Mitochondrial Mutation in Yeast. *Nature New Biology* **238**, 266–268 (1972).

305. Madhani, H. *From a to α: Yeast as a Model for Cellular Differentiation*. (Cold Spring Harbor Laboratory Press, 2006).

306. Haber, J. E. Mating-type gene switching in *Saccharomyces cerevisiae*. *Trends Genet.* **8**, 446–452 (1992).

307. Cubillos, F. A., Louis, E. J. & Liti, G. Generation of a large set of genetically tractable haploid and diploid *Saccharomyces* strains. *Fems Yeast Res* **9**, 1217–1225 (2009).

308. Giaever, G. & Nislow, C. The Yeast Deletion Collection: A Decade of Functional Genomics. *Genetics* **197**, 451–465 (2014).

309. Soares, E. V. Flocculation in *Saccharomyces cerevisiae*: a review. *J Appl Microbiol* **110**, 1–18 (2011).

310. Masy, C. L., Henquinet, A. & Mestdagh, M. M. Flocculation of *Saccharomyces cerevisiae*: inhibition by sugars. *Can J Microbiol* **38**, 1298–1306 (1992).

311. Verstrepen, K. J., Derdelinckx, G., Verachtert, H. & Delvaux, F. R. Yeast flocculation: what brewers should know. *Appl Microbiol Biot* **61**, 197–205 (2003).

312. Syller, J. Facilitative and antagonistic interactions between plant viruses in mixed infections. *Mol. Plant Pathol.* **13**, 204–216 (2012).

313. Dobbs, E. *et al.* Viral Interactions and Pathogenesis during Multiple Viral Infections in *Agaricus bisporus*. *mBio* **12**, e03470-20 (2021).

314. Gonzalez, A. J., Ijezie, E. C., Balemba, O. B. & Miura, T. A. Attenuation of Influenza A Virus Disease Severity by Viral Coinfection in a Mouse Model. *J. Virol.* **92**, (2018).

315. Cox, G. *et al.* Priming With Rhinovirus Protects Mice Against a Lethal Pulmonary Coronavirus Infection. *Front. Immunol.* **13**, 886611 (2022).

316. Reinisch, K. M. The dsRNA Viridae and their catalytic capsids. *Nat Struct Biol* **9**, 714–716 (2002).

317. Tang, J. *et al.* The structural basis of recognition and removal of cellular mRNA 7-methyl G 'caps' by a viral capsid protein: a unique viral response to host defense. *J Mol Recognit* **18**, 158–168 (2005).

318. Voth, W. P., Jiang, Y. W. & Stillman, D. J. New 'marker swap' plasmids for converting selectable markers on budding yeast gene disruptions and plasmids. *Yeast* **20**, 985–993 (2003).

319. Glover, J. R. & Lindquist, S. Hsp104, Hsp70, and Hsp40 A Novel Chaperone System that Rescues Previously Aggregated Proteins. *Cell* **94**, 73–82 (1998).

320. Anckar, J. & Sistonen, L. Regulation of HSF1 Function in the Heat Stress Response: Implications in Aging and Disease. *Annu Rev Biochem* **80**, 1089–1115 (2011).

321. Yamamoto, A., Mizukami, Y. & Sakurai, H. Identification of a Novel Class of Target Genes and a Novel Type of Binding Sequence of Heat Shock Transcription Factor in *Saccharomyces cerevisiae* *. *J. Biol. Chem.* **280**, 11911–11919 (2005).

322. Solís, E. J. *et al.* Defining the Essential Function of Yeast Hsf1 Reveals a Compact Transcriptional Program for Maintaining Eukaryotic Proteostasis. *Mol. Cell* **63**, 60–71 (2016).

323. Yesbolatova, A. *et al.* The auxin-inducible degron 2 technology provides sharp degradation control in yeast, mammalian cells, and mice. *Nat Commun* **11**, 5701 (2020).

324. Beelman, C. A. & Parker, R. Differential effects of translational inhibition in cis and in trans on the decay of the unstable yeast MFA2 mRNA. *J Biol Chem* **269**, 9687–9692 (1994).

325. Passos, D. O. & Parker, R. Chapter 20 Analysis of Cytoplasmic mRNA Decay in *Saccharomyces cerevisiae*. *Methods Enzymol* **448**, 409–427 (2008).

326. Okada, R., Kiyota, E., Moriyama, H., Fukuhara, T. & Natsuaki, T. A simple and rapid method to purify viral dsRNA from plant and fungal tissue. *J Gen Plant Pathol* **81**, 103–107 (2015).

327. Baym, M. *et al.* Inexpensive Multiplexed Library Preparation for Megabase-Sized Genomes. *Plos One* **10**, e0128036 (2015).

328. Holm, L. DALI and the persistence of protein shape. *Protein Sci.* **29**, 128–140 (2020).

329. Darriba, D., Taboada, G. L., Doallo, R. & Posada, D. ProtTest 3: fast selection of best-fit models of protein evolution. *Bioinformatics* **27**, 1164–1165 (2011).

330. Guindon, S. *et al.* New Algorithms and Methods to Estimate Maximum-Likelihood Phylogenies: Assessing the Performance of PhyML 3.0. *Syst. Biol.* **59**, 307–321 (2010).

331. Naitow, H., Canady, M. A., Lin, T., Wickner, R. B. & Johnson, J. E. Purification, Crystallization, and Preliminary X-ray Analysis of L-A: A dsRNA Yeast Virus. *J Struct Biol* **135**, 1–7 (2001).

332. Astell, C. R. *et al.* The sequence of the DNAs coding for the mating-type loci of *Saccharomyces cerevisiae*. *Cell* **27**, 15–23 (1981).

333. Sanderson, B. A., Araki, N., Lilley, J. L., Guerrero, G. & Lewis, L. K. Modification of gel architecture and TBE/TAE buffer composition to minimize heating during agarose gel electrophoresis. *Anal Biochem* **454**, 44–52 (2014).

334. Arras, S. D. M. *et al.* Creeping yeast: a simple, cheap and robust protocol for the identification of mating type in *Saccharomyces cerevisiae*. *FEMS Yeast Res.* **22**, foac017 (2022).

335. Gong, P. & Peersen, O. B. Structural basis for active site closure by the poliovirus RNA-dependent RNA polymerase. *Proc National Acad Sci* **107**, 22505–22510 (2010).

APPENDIX A: MATERIALS & METHODS

5’ RACE

To determine the sequence of the termini of PV genomes, the 5’ RACE kit from Invitrogen was used per the manufacturer’s instructions (Fig A.1).

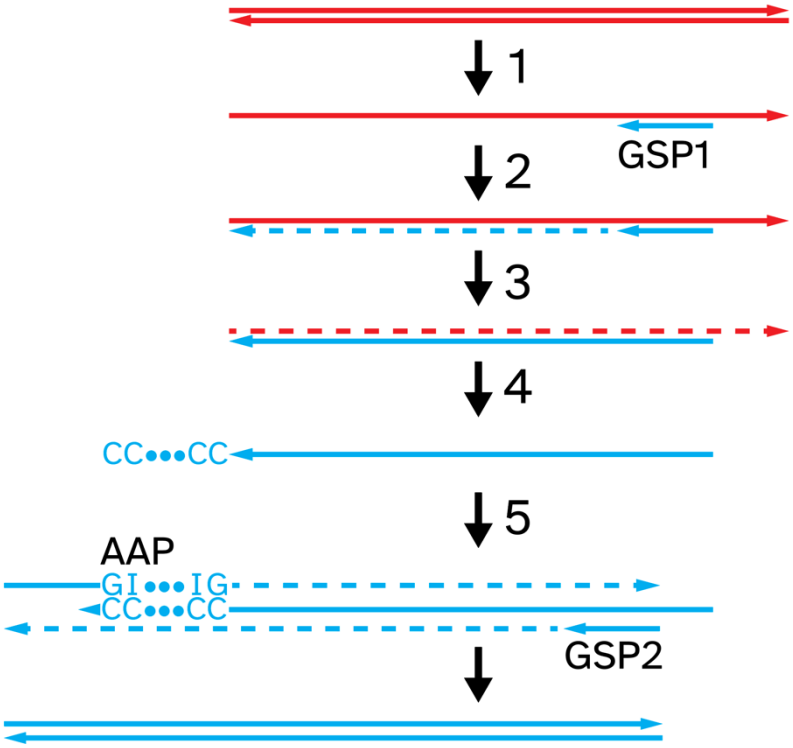

Figure A.1: An overview of the 5' RACE procedure.
(**1**) dsRNAs are denatured and gene-specific primer 1 (GSP1) is annealed. (**2**) First strand cDNA synthesis is primed by GSP1. (**3**) RNAs are digested, and cDNAs are purified by S.N.A.P. column chromatography. (**4**) A poly(C) tail is added by TdT. (**5**) PCR amplification of poly(C) cDNA. AAP, abridged anchor primer.

Obtaining the full sequence of ScPV1-5509 dsRNA1 required optimization and modifications. First, Superscript IV reverse transcriptase (Invitrogen) was used instead of Superscript II; a longer GSP1 was designed to suit the higher temperatures of cDNA synthesis associated with SSIV. To ensure that everything was working, aliquots were saved at each step and used in a PCR scheme similar to that in the troubleshooting chapter of the 5’ RACE manual (Table A.1).

Table A.1: Troubleshooting PCR scheme.

Rxn	Template	Primers	Expected (bp)	Observed (bp)
1	1:500 cDNA	NTT153, NTT155	241	241
2	1:100 SNAP-purified cDNA	NTT153, NTT155	241	241
3	1:100 poly(C) cDNA	NTT153, NTT155	241	-
4	1:100 poly(C) cDNA	NTT153, AAP	≈500	-
5	(-) TdT control tailing reaction	NTT153, NTT155	241	241
6	(-) TdT control tailing reaction	NTT153, AAP	-	-
7	1:20 dsRNAs from Y-5509	NTT153, NTT155	241	-
8	1:20 dsRNAs from BJH001	NTT153, NTT155	-	-

These results indicate an issue is occurring at the TdT tailing step. The manual suggests doing a TdT time course; that is, remove 5 µL aliquots at 2.5, 5, 10, and 20 minutes and amplify with GSP2 & AAP (Table A.2 and Fig A.2).

Table A.2: TdT time course.

Rxn	TdT	Time	Primers	Expected (bp)	Observed (bp)
1	+	2.5	NTT153, NTT155	241	241
2	+	5	"	241	241
3	+	10	"	241	241
4	+	20	"	241	241
5	+	2.5	NTT153, AAP	>241	≈600
6	+	5	"	>241	≈600
7	+	10	"	>241	≈600
8	+	20	"	>241	≈600
9	-	2.5	NTT153, NTT155	241	241
10	-	5	"	241	241
11	-	10	"	241	241
12	-	20	"	241	241
13	-	2.5	NTT153, AAP	0	0
14	-	5	"	0	0
15	-	10	"	0	0
16	-	20	"	0	0

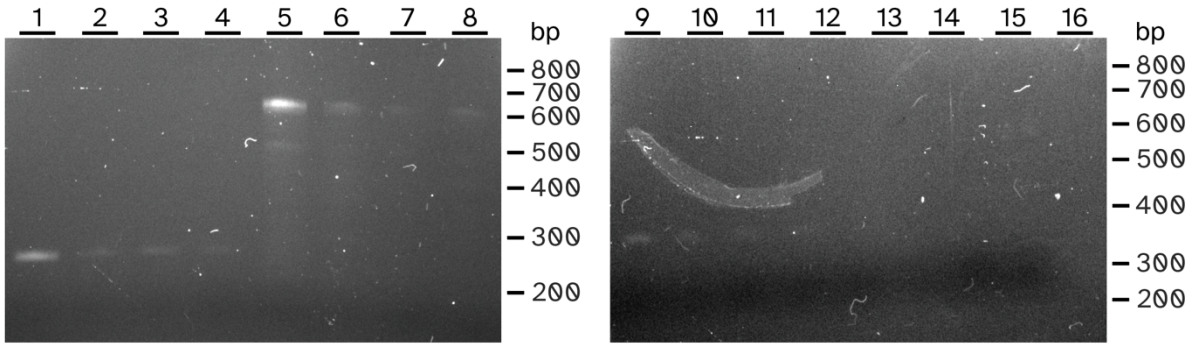

Figure A.2: Electrophoresis of PCR products from Table A.2.

Decreasing band intensity indicates that PCR efficiency decreased with increased dC-tailing time. Therefore, cDNA incubated with TdT for 2.5 min was chosen as the template for PCR amplification. 5' RACE products were cloned into the pCR8 vector using the TOPO-TA cloning kit (Thermo Fisher Scientific).

Curing of viruses and satellite dsRNAs from *S. cerevisiae* by XRN1 overexpression

The strain *S. cerevisiae* YTag085 (an M2 killer yeast) (Appendix L) was transformed with the high copy plasmid pPAR219 to express *XRN1* cloned from *S. cerevisiae*[197]. The loss of the killer phenotype in 183 clones was confirmed by a killer assay using two different K2-susceptible strains of yeast (BY4741 and DBY7730). Cured clones were then assayed for dsRNAs by cellulose chromatography.

Cycloheximide curing of satellite dsRNAs

10 µL of an overnight YPD culture of *S. cerevisiae* strain CYC1172 was transferred to YPD plates containing up to 1.5 mg/L of cycloheximide and incubated at ambient temperature for 3–5 days. Colonies growing on the highest concentration of cycloheximide were streaked to single colonies on standard YPD media and incubated at ambient temperature for 3–5 days. Ten colonies were assayed for the loss of the killer phenotype as described under "killer phenotype assays."

Cytoduction

To induce respiratory deficiency, cells of *S. cerevisiae* strain 1368 (*MAT*α *his4 kar1 ura3Δ0* [L-A-HNB M1]) were grown to log phase. Ethidium bromide was added to a final concentration of 10 µg/mL. The cells continued incubating until they reached stationary phase. Cells were harvested by centrifugation for 5 min at 3000 x g and rinsed with sterile water. Cells were streaked on YPD agar and grown at 30°C for 1-2 days, after which respiratory deficient mutants were isolated by growing on YPG agar (1% yeast extract, 2% peptone, 30% glycerol) at 30°C.

CYC1172 (*MAT***a**/α *HO KAR1 URA3* [L-A-lus, L-BC, M2, ScPV3]) was grown on GNA presporulation agar (3% nutrient broth, 1% yeast extract, 5% dextrose) for 1-2 days and

sporulated in 2 mL liquid sporulation medium (1% potassium acetate, 0.005% zinc acetate). The sporulation rate was monitored by microscopy. Asci were harvested by centrifugation, rinsed, digested in 200-400 µL Zymolyase® solution (1M sorbitol, 2.5 mg/mL Zymolyase®-20T (Amsbio)) for 30 min, and sonicated at ≈70% power for ≈10 s. Efficiency of ascus disruption was monitored by microscopy. Digested asci were gently resuspended in 600-1000 µL sterile water.

Respiratory deficient mutants were patched onto a YPD agar plate, to which ≈10 µL of the digested ascus suspension was added. Cells were incubated at 30°C overnight. Patches were replicated on YPG agar (1% yeast extract, 2% peptone, 30% glycerol) and incubated at 30°C. Colonies that grew on YPG agar were streaked onto CM 5-FOA agar (10 mg/L uracil, 0.2% 5-FOA, pH 4.5) incubated at 30°C for 1-2 days.

Double-stranded RNA extraction

YPD cultures were grown overnight at 30°C and washed once with sterile water. The cultures were then centrifuged for 5 min at 3000 × g and the supernatant aspirated. The following protocol was modified from the dsRNA extraction method previously published by Okada et. al[326]. Cellulose columns were prepared by puncturing the bottom of a 0.6 mL tube with a hot 20-gauge needle and nesting it in a 2.0 mL tube. Approximately 0.06 g of cellulose powder D (Advantec, Japan) was added to the 0.6 mL tube. The columns were rinsed with 500 µL of wash buffer (1X STE (100 mM NaCl; 10 mM Tris–HCl, pH 8.0; 1 mM EDTA, pH 8.0) containing 16% (v/v) ethanol) just before use. Wash buffer was removed by a 10 s centrifugation. To extract dsRNAs, 450 µL of 2X STE was added to the harvested yeast cells. The cell mixture was vortexed for 3 min at 3000 rpm (Disruptor Genie, Scientific Industries, Bohemia, NY, USA) to disrupt cells. 50 µL of 10% (w/v) SDS solution and 250-500 µL of phenol–chloroform–isoamyl alcohol [25:24:1] pH 8.0 were added to the crude cell extracts and vortexed until homogenous. Samples were centrifuged at 20,000 x g for 5 min and the supernatant was transferred to a clean tube, whereupon a one-fifth volume of ethanol was added to precipitate the nucleic acids from solution. This mixture was transferred to the pre-prepared cellulose spin column centrifuged on ‘Short’ for 10 s, and the flow-through

was discarded. 400 µL of wash buffer was added to the columns, centrifuged on 'Short' for 10 s and the flow-through was discarded. This step was repeated up to twice more. The columns were dried by centrifugation on 'Short' for 10 s. The 0.6 mL tubes were transferred to clean 2.0 mL tubes, 400 µL of 1X STE was added, and centrifuged on 'Short' for 10 s to collect the eluate. 40 µL of aqueous 3 M sodium acetate, pH 5.2, and 1 mL of absolute ethanol were added to the eluate, which was inverted to mix, and then centrifuged at 20,000 × g for 5 min to precipitate the dsRNAs. The supernatant was aspirated, and dsRNA pellets were allowed to air-dry, before being suspended in 15-20 µL of nuclease-free water. All strain information and their dsRNA content are compiled in Appendix C. The yield may be increased by recovering the supernatant from multiple phenol-chloroform extractions and loading it onto a single cellulose column (Fig A.3).

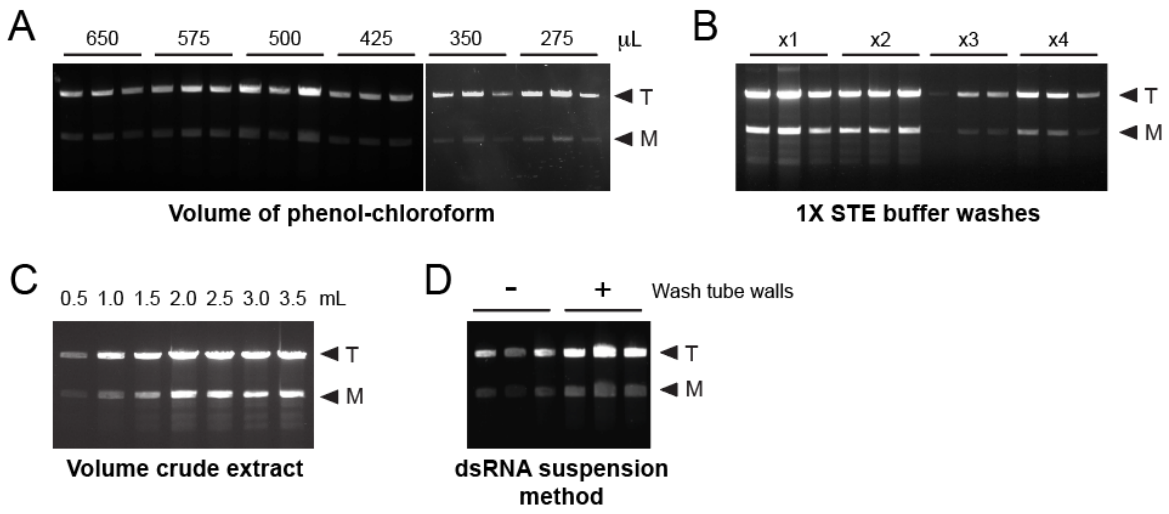

Figure A.3: Optimizing dsRNA extraction from *S. cerevisiae*.
The effect on dsRNA yield by varying (**A**) the volume of phenol-chloroform (**B**) the number of 1X STE buffer washes of the cellulose chromatography column (**C**) the volume of crude cell extract, and (**D**) dsRNA suspension method (the walls of the tube were washed after dsRNA precipitation). The largest improvements in yield were observed by increasing the volume of cell extract (after phenol-chloroform extraction) loaded onto the cellulose column, reducing the number of 1X STE washes after the crude extract, and washing the walls of the tubes after dsRNA precipitation. dsRNAs extracted were derived from totiviruses (T) and satellite dsRNAs (M).

Illumina library preparation using a modified Nextera protocol

All cDNA samples were normalized to 2.5 ng/μL for the desired final average library insert size of 550 bp. Fluorometric quantification was performed with SpectraMax Gemini XPS plate reader (Molecular Devices, San Jose, CA, USA) and PicoGreen (Invitrogen). For the fluorometric quantification, 2 μL of cDNA was diluted in 98 μL 1X TE buffer (10 mM Tris-HCl, 1 mM EDTA, pH 7.5), and mixed with 100 μL of PicoGreen (diluted 1:200 in TE). Standards were prepared as per the manufacturer's protocol and by scaling the volumes to one-tenth of that stated. Samples and standards were incubated at ambient temperature, in the dark, for 5 min, before analysis. Tagmentation, PCR (Applied Biosystems thermal cycler, Hercules, CA, USA), PCR-mediated adapter addition and library amplification were performed according to Baym et. al[327], with the post-tagmentation PCR using the following thermal cycling parameters: (1) 72°C for 3 min, (2) 98°C for 5 min, (3) 98°C for 10 s, (4) 63°C for 1 min, (5) 72°C for 30 s, (6) go to step 3 for 13 cycles, (7) 72°C 5 min. For magnetic bead purification, 0.8X sample volume of HighPrep™ PCR reagent was used while following the manufacturer's protocol. Samples were suspended in 50 μL of nuclease-free water and a two-sided size selection was performed to further narrow the insert size distribution.

Then, 0.4X sample volume of HighPrep reagent was added to the sample with magnetic beads, and after an incubation at ambient temperature, for 5 min, the beads were discarded; 0.6X sample volume of HighPrep reagent was then added to the sample with magnetic beads and after incubation at ambient temperature for 5 min, the supernatant was removed. DNAs were then eluted from the magnetic beads and suspended in 50 μL of nuclease-free water. Samples were then quantified with a fluorometer and pooled by mass proportionally to the desired read distribution in the downstream sequencing run. Library-distribution, size-weighted fragment length, and nucleic acid concentration were determined by fragment analysis (Fragment Analyzer, Agilent Technologies Inc, La Jolla, CA, USA).

Killer phenotype assays

Putative killer yeasts were spotted at high cell density onto YPD dextrose 'killer assay' agar plates (0.003% (w/v) methylene blue, pH 4.6), seeded with a killer toxin-susceptible yeast strain. Plates were incubated at ambient temperature for 4-7 days, whereafter plates were visually inspected for evidence of killer toxin production. Toxin production by a strain of yeast was identified by either a zone of growth inhibition or methylene blue-staining of the yeasts that were spread as a lawn.

Molecular modeling

ColabFold version 1.4 was used to generate models using the open reading frame of the CP and RdRP of viruses CSpV1, ScPV1-5509, ScPV2-858, ScPV3-1172 with the following parameters (msa_mode: MMseqs2 (uniref+environment); model_type: auto; pair_mode: unpaired+paired; num_recyles: 3). Five unrelaxed structures of each CP and RdRP were generated. RdRP models were generated with similar local distance difference test (pLDDT) values per residue (Fig B.3). The highest average pLDDT score for each model was chosen for energy minimization and analysis. Energy minimization was carried out for each model using standard energy minimization protocol described in our previous study[93]. A dodecahedron box was generated around each model and solvated using a 10 Å layer of TIP3P. Ions were added to maintain charge neutrality at a concentration of 0.15 mol/L using Na^+ and Cl^- ions. The force field parameter used for protein and ions was AMBER99SB*-ILDNP. Each system underwent energy minimization using the steepest descent algorithm for 10,000 steps via the GROMACS package. Stereochemical analysis was carried out with the SWISS-MODEL structure assessment tool for each model after the energy minimization (https://swiss-model.expasy.org/) to verify that model sterics were physically reasonable after energy minimization. All PDB formatted files for each relaxed model can be found in S1 File. The final energy minimized RdRP and CP model structures were submitted to the DALI server to identify structural homologs. The cealign command in the PyMOL visualization software package was used to identify regions of homology between CPs and homologous CP structures identified by DALI[328].

Phylogenetic analysis

RdRP protein sequences from ScPVs and other PVs from previously described genera (Appendix H) were aligned using MUSCLE and were inspected manually for accuracy. PROTTEST3 v3.4.2 was used to determine each dataset's appropriate amino acid substitution matrix[329]. The search space used consisted of all possible matrices and decorations with eight categories for the +I and +I+G models. The best-fit model was determined to be VT+I+G+F, with the next best model having a delta AIC of 28.52. PhyML v3.3.20220408 was used to create phylogenetic models[330]. PhyML parameters were chosen based on the results of PROTTEST3. The analysis consisted of 1000 bootstrap replicates, the VT amino acid substitution model was used, the proportion of invariable sites was determined by maximum likelihood, amino acid frequencies were estimated empirically by the frequency of occurrence in the dataset, the BEST tree search method was used for tree estimation, and the analysis was started with five random trees.

Preparing dsRNAs for next generation sequencing

Poly(A) polymerase (New England Biolabs) was used to synthesize a poly(A) tails at the 3′ termini of denatured dsRNAs. To 12.5 µL of purified dsRNAs, the following was added: 1.5 µL 10X poly(A)polymerase reaction buffer, 1.5 µL ATP [10 mM], 0.5 µL of poly(A) polymerase (diluted 1:32 in nuclease-free water), and 0.5 µL murine RNase inhibitor. Samples were incubated at 37°C for 30 min, 65°C for 20 min, 98°C for 5 min, and then immediately placed in a wet ice slurry. Superscript IV (Invitrogen, Carlsbad, CA, USA) with an "anchored" NV(dT)20 primer (Invitrogen) was used to reverse transcribe the poly(A)-tailed single-stranded RNAs (ssRNAs) into cDNAs according to the manufacturer's protocol. Murine RNase Inhibitor (New England Biolabs) was used in place of the RNaseOUT™ RNase Inhibitor. Each sample was digested with 1 µL of RNase H (New England Biolabs) and incubated at 37°C for 20 min to remove ssRNAs. cDNAs were annealed at 65°C, for 2 h. To fully extend cDNA overhangs, 1 µL of E. coli DNA Polymerase I enzyme (New England Biolabs) was added to 3.5 µL of NEB Buffer 2.0 and 0.5 µL of 10 mM dNTPs and was incubated at 37°C, for 30 min. DMSO was

then added to a final concentration of 15% (v/v) and the reaction was incubated at 75°C, for 20 min to deactivate the polymerase. 5 µL of cDNAs were used as a template for PCR amplification, using 25 µL of Phusion Master Mix with HF Buffer (New England Biolabs), 1.0 µL of anchored oligo(dT) primer (0.7 ug/µL), and 1.5 µL of DMSO, to a final reaction volume of50 µL. Reactions were subjected to the following parameters on a thermal cycler: (1) 72°C for 10 min, (2) 98°C for 30 s, (3) 98°C for 5 s, (4) 50°C for 10 s, and 72°C for 45 s, (5) go to step 3 for 30 cycles, (6) 72°C for 5 min. Six 50 µL PCR reactions were pooled and concentrated using HighPrep™ PCR reagent with magnetic beads, following the manufacturer's protocol, using 0.5X sample volume of the reagent and five times the specified volume of ethanol wash (MagBio, Gaithersburg, MD, USA). Samples were eluted from the beads using 30 µL of nuclease-free water and subjected to fragment analysis (Fragment Analyzer, Advanced Analytical), prior to Illumina library preparation and NGS.

ScPV stability

Yeast strains were streaked onto two YPD agar plates each and incubated at either 25°C or 4°C for 6 weeks. Cells were cultured in 12 mL YPD broth and incubated at 25°C for 2 days, and their dsRNAs were extracted and analyzed by agarose gel electrophoresis.

Sequencing analysis of dsRNA metagenomic data from *S. cerevisiae*

109 contigs (>300 nt in length) were identified as matching "Viruses (taxid: 10239)" using BLASTx (Max targets 10, Threshold 1 x 10^{-6}). Each hit was classified by virus family, and the coverage scores were totaled.

Sequencing dsRNAs

The prepared DNA libraries were sequenced by the IBEST Genomics Resources Core at the University of Idaho, using an Illumina MiSeq sequencing platform and Micro v2 300 cycle reagent kit. Base calling and demultiplexing was performed using the Illumina bcl2fastq v2.17.1.14 software tool (Illumina, San Diego, CA, USA).

Total nucleic acid extraction from *S. cerevisiae*

200 µL of a 2 mL overnight culture of yeast was centrifuged at 8000 x g for 1 min and the supernatant aspirated. Cells were suspended in 100 µL of 200 mM LiOAc, 1% (w/v) SDS and incubated for 5 min at 70°C. 300 µL of 100% ethanol was added and vortexed. This was centrifuged at 15,000 x g for 3 min and the supernatant aspirated. 200 µL of 70% ethanol was added and the tubes were flicked. This was centrifuged at 30,000 x g for 1-3 min. The supernatant was completely aspirated, and the pellet was suspended in 100 µL ddH_2O.

Transformation of *S. cerevisiae*

1 mL of an overnight yeast culture was diluted in 9 mL YPD broth and incubated at 30°C for 4-6 hr. The cells were harvested, suspended in 10 mL sterile 100 mM LiOAc and incubated at 30°C for 10 min. After the cells were pelleted, the following components were added in the following order and mixed gently: 240 µL PEG4000 (50% w/v), 18 µL 2M LiOAc, 50 µL denatured salmon sperm DNA (2 mg/mL), and ≈1 µg mutagenic DNA. The cell suspension was incubated at 30°C for 30 min and at 42°C for 20 min. The cells were pelleted by centrifugation and gently resuspended in 200 µL sterile ddH_2O, after which serial dilutions were spread of the appropriate selective medium. If the selective marker was G418 resistance, the cells were first recovered for 4-16 hrs. before being spread on 1X G418 (200 µg/mL). The selection plates would be replicated onto 2X G418 (400 µg/mg) the following day.

Transmission electron microscopy

For the negative staining of VLPs, 5 µL of purified particles from strain YO1126 were applied to a 400-mesh copper grid coated with carbon-Formvar (Ted Pella) for 20 seconds, wicking with a filter paper, and washed three times on 50 µL water droplets. A staining solution of 2% uranyl acetate (pH ≈ 3) was added to the sample-side of the grid, wicking, and reapplied for 20 seconds before removal by wicking and lateral aspiration. Images were obtained on an FEI Tecnai F20 transmission electron microscope, captured with a BM UltraScan camera, and stored in digital micrograph 3 format.

Virus particle purification

This protocol was adapted from that of Naitow et al.[331]. Cells were inoculated in 1000 mL yeast peptone dextrose (YPD) liquid media and incubated at 30°C for 24 hours. Cells were harvested by centrifugation for 5 min at 3800 × g and washed with double-deionized water. Washed cells were suspended in spheroplasting buffer (100 mM Tris-HCl, 1M D-sorbitol, 20 mM β-mercaptoethanol, 0.5 mg/mL Zymolyase®-20T, pH 7.6) and incubated for 90 min at ambient temperature, stirring gently. Digested cells were harvested by centrifugation for 5 min at 3,800 × g and suspended in buffer A (50 mM Tris-HCl, 150 mM NaCl, 5 mM EDTA, 1 mM dithiothreitol, pH 7.6), after which they were lysed by passing the cell suspension twice through a French pressure cell press (Thermo Scientific) at 20,000 psi. Cell debris was removed by centrifugation for 20 min at 9,600 × g, and the supernatant was adjusted to 3% PEG-8000 and 0.5 M NaCl before rocking gently for 1 hour at 4°C. The precipitate was harvested by centrifugation for 20 min at 9600 × g, gently suspended in 15 mL of 50 mM sodium phosphate buffer (pH 7.0) and incubated on ice overnight with rocking. Insoluble precipitates were removed by centrifugation at 7000 × g for 10 min. The supernatant was layered onto 5 mL 20% sucrose cushion in an ultracentrifuge tube (Thermo Scientific, Nalgene High-Speed Round-Bottom PPCO Centrifuge Tubes) and centrifuged at 80,000 × g for 2 hours at 4°C. The pellet was recovered and suspended in 500 µL sodium phosphate buffer and layered onto a discontinuous sucrose gradient (10–50% in 5% increments of 1 mL each). This was centrifuged at 70,000 × g for 2 hours at 4°C.

Yeast chromosomal DNA extraction

A 2-10 mL culture of yeast was harvested and resuspended in 500 µL TE buffer. The cell suspension was briefly centrifuged, and the supernatant was aspirated. 200 µL breaking buffer and ≈300 µL glass beads were added. In a fume hood, 200 µL phenol-chloroform-isoamyl alcohol were added, and the tube was vortexed for 3 min at 3000 rpm in a Disruptor Genie. The tube was briefly centrifuged and 200 µL TE buffer was added, vortexed briefly, and centrifuged at 21,000 x g for 5 min. The aqueous layer was transferred to a new microcentrifuge tube. 1 mL 100% ethanol was added and

mixed by inversion. The tube was centrifuged at 21,000 x g for 3 min. The supernatant was removed, and the pellet was resuspended in 400 µL TE buffer. 30 µL 1 mg/mL DNase-free RNase A was added and incubated at 37°C for 5 min. 10 µL 4M ammonium acetate and 1 mL 100% ethanol were added, mixed by inversion, and centrifuged at 20,000 x g for 3 min. The supernatant was carefully aspirated, and the pellet was allowed to dry (≈20 min) and resuspended 100 µL TE buffer or ddH_2O.

Yeast strain construction

S. cerevisiae can exist as three cell types: the *MAT***a** haploid, the *MAT*α haploid, and the *MAT***a**/α diploid[305,332] (Fig. A.4). All three cell types can reproduce by undergoing mitosis to form daughter cells of the same cell type, but only diploid cells can reproduce by meiosis. This is followed by sporulation, which results in the formation of four

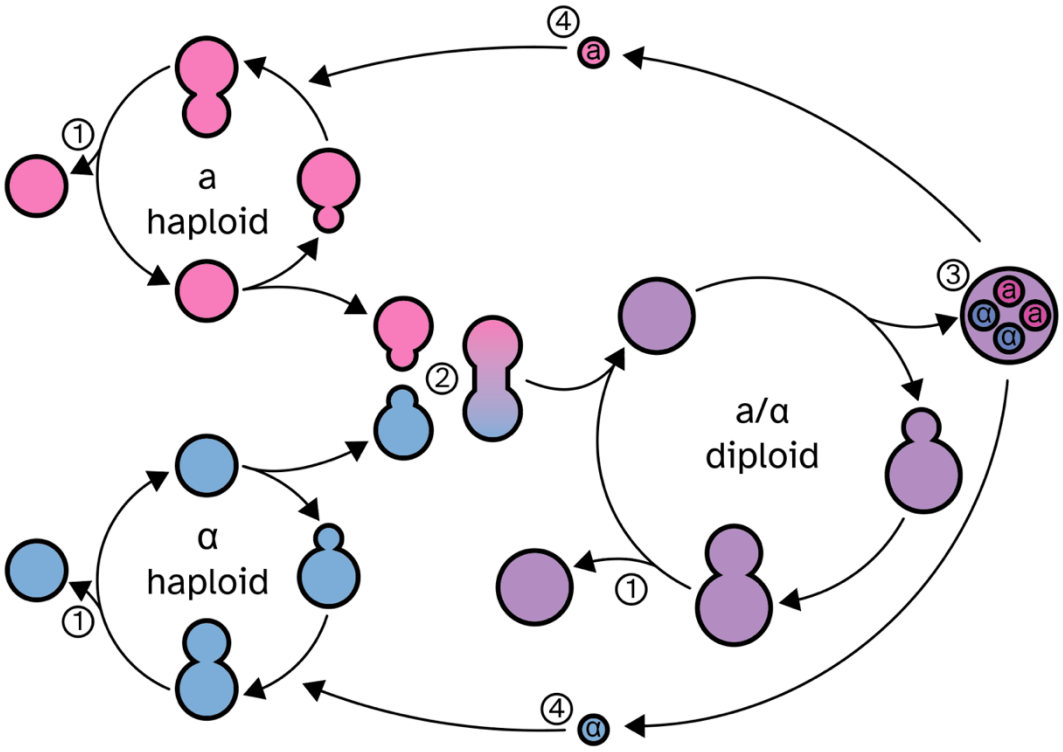

Figure A.4: A schematic of S. *cerevisiae* reproduction.
(**1**) Both haploid and diploid cells reproduce by mitosis, in a process called budding, and produce daughter cells of the same cell type. (**2**) When a haploid cell detects the mating pheromone of the opposite mating type, they form a mating projection in the direction of the pheromone and form a diploid cell. (**3**) Diploid cells can undergo meiosis and sporulation. (**4**) Ascospores germinate into haploid cells. Recreated from Yeast Lifecycle.svg from Wikipedia.

ascospores that are contained in the ascus, which is the remnant of the mother cell. *MAT***a** cells secrete a mating pheromone called **a**-factor, and *MAT*α cells secrete α-factor. Each cell type also expresses receptors for the mating pheromone from the opposite mating type. Diploid cells do not produce mating pheromone. When a haploid cell detects the mating pheromone of the opposite cell type, it will stop dividing and prepare to mate. Because yeast cells are non-motile, they must form a structure called a mating projection in the direction of their partner. Upon contact, the cell wall at the tip of the mating projection is degraded, allowing the cell membranes to fuse. Then, the nuclei migrate towards each other and fuse.

Some *S. cerevisiae* strains can switch mating types, a property called homothallism[305,306]. This may be advantageous because diploid cells divide more quickly and thus have a competitive advantage over haploid cells. This is possible because chromosome III encodes an extra, silent copy of *MAT***a** and *MAT*α. The *MAT***a** allele is encoded at a locus called *HMR***a** (homthallic right), located on the far-right side of the chromosome, and the *MAT*α allele is encoded at *HML*α (homthallic left), which is on the far-left side (Fig A.5). The process is initiated by an enzyme called HO (homothallic endonuclease), which makes a double-stranded break in *MAT*. Information from the appropriate *HM* locus is copied and replaces the allele present at *MAT*; the exact details of recombination are unknown. To ensure that the proper allele is copied, the left arm of chromosome III contains a recombination enhancer (*RE*) element; without it,

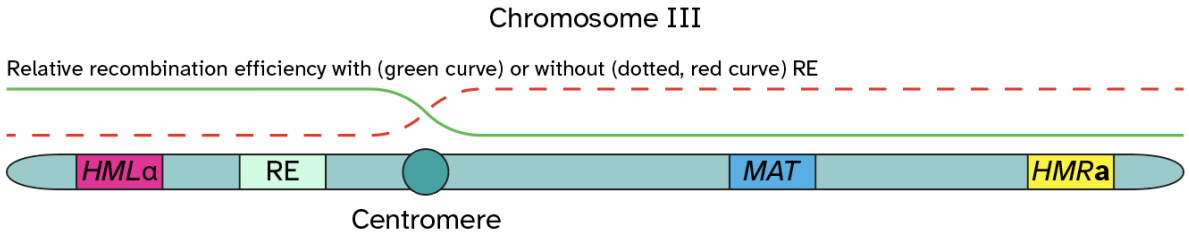

Figure A.5: The silent mating type cassettes *HML*α and *HMR*a are present on opposite sides of chromosome III.
Homothallic endonuclease (HO) makes a double-stranded break at *MAT*, and information from the appropriate silent locus is copied and replaces the allele in the *MAT* locus. Proper selection of the silent locus is ensured by a recombination enhancer (RE), which increases efficiency of recombination in the left arm of chromosome III in *MAT***a** cells but is repressed in *MAT*α cells.

recombination activity in the left arm is much lower compared to the right arm. Thus, in *MAT***a** cells, *HML*α is favored over *HMR***a** as a donor. However, in *MAT*α cells, *RE* is repressed, in part, by α2, a protein encoded by *MAT*α. Thus, in *MAT*α cells, *HMR***a** is favored over *HML*α as a donor. Some commonly used laboratory strains of *S. cerevisiae* contain inactive *HO* genes and are unable to undergo mating type switching. On the other hand, wild yeasts typically have intact *HO* genes and will readily switch mating types.

Therefore, the *HO* gene must be disrupted before wild yeasts can be used in genetic experiments. This process was typically referred to as domestication. The first step was to determine whether wild yeast could be transformed in the first place. Therefore, a purple chromogenic plasmid was purified from *S. cerevisiae* strain YMD3450. Briefly, cells were harvested and incubated in 1M sorbitol, 100 mM EDTA, 0.96 mg/mL Zymolyase®-100T, pH 7.5 at 37°C for 1 hr. Cells were pelleted, and plasmids were extracted using the QIAprep® Spin Miniprep Kit (Qiagen). 10-beta competent *E. coli* (NEB®) cells were transformed with purified plasmid according to the manufacturer's directions and selected on ampicillin. Plasmids were extracted using the QIAprep® Spin Miniprep Kit again. *S. cerevisiae* strains BY4741, CYC1172, YO1126, and YO858 were transformed with the chromogenic plasmid and selected on 200-400 µg/mL G418 (Fig A.6).

Chromosomal DNA was purified from *S. cerevisiae* strain YJM975 *MAT*α *ho::HygMX* from the collection generated by Cubillos et al[307]. The *ho::HygMX* cassette was amplified using primers NTT033 and NTT034. *S. cerevisiae* strains CYC1172, YO1126, and YO815 were transformed with *ho::HygMX* and selected on YPD agar containing 300 µg/mL hygromycin B (AG Scientific). Cells were grown for 1-2 days on GNA presporulation agar (3% nutrient broth, 1% yeast extract, 5% dextrose) for 1-2 days and sporulated in 2 mL SPO medium (0.25% yeast extract, 0.25% dextrose, 1.5% potassium acetate, 0.002% (histidine, leucine, lysine, tryptophan, methionine, arginine), 0.004% (adenine, uracil, tyrosine), 0.01% phenylalanine, 0.035% threonine, filter-sterilized). The sporulation rate was monitored by microscopy. When the sporulation rate was at

least 25%, 50 µL of cell suspension was centrifuged, and the supernatant was removed. Cells were suspended in 50 µL 1 mg/mL yeast lytic enzyme (AG Scientific) and digested for precisely 12 min, after which the reaction was quenched by slowly adding 0.5–1 mL sterile water. Asci were dissected with a 25 µm fiber optic cable glued to a micromanipulator mounted onto a Nikon Eclipse 50i microscope. Ascospores were incubated at 30°C for 2-3 days until they germinated and formed colonies. The dissection plate was replicated onto a YPD agar plate containing 300 µg/mL hygromycin B to select for *ho::HygMX* spore clones. Alternatively, disruption of *HO* could be verified by PCR using primers NTT031-032 or NTT033-034.

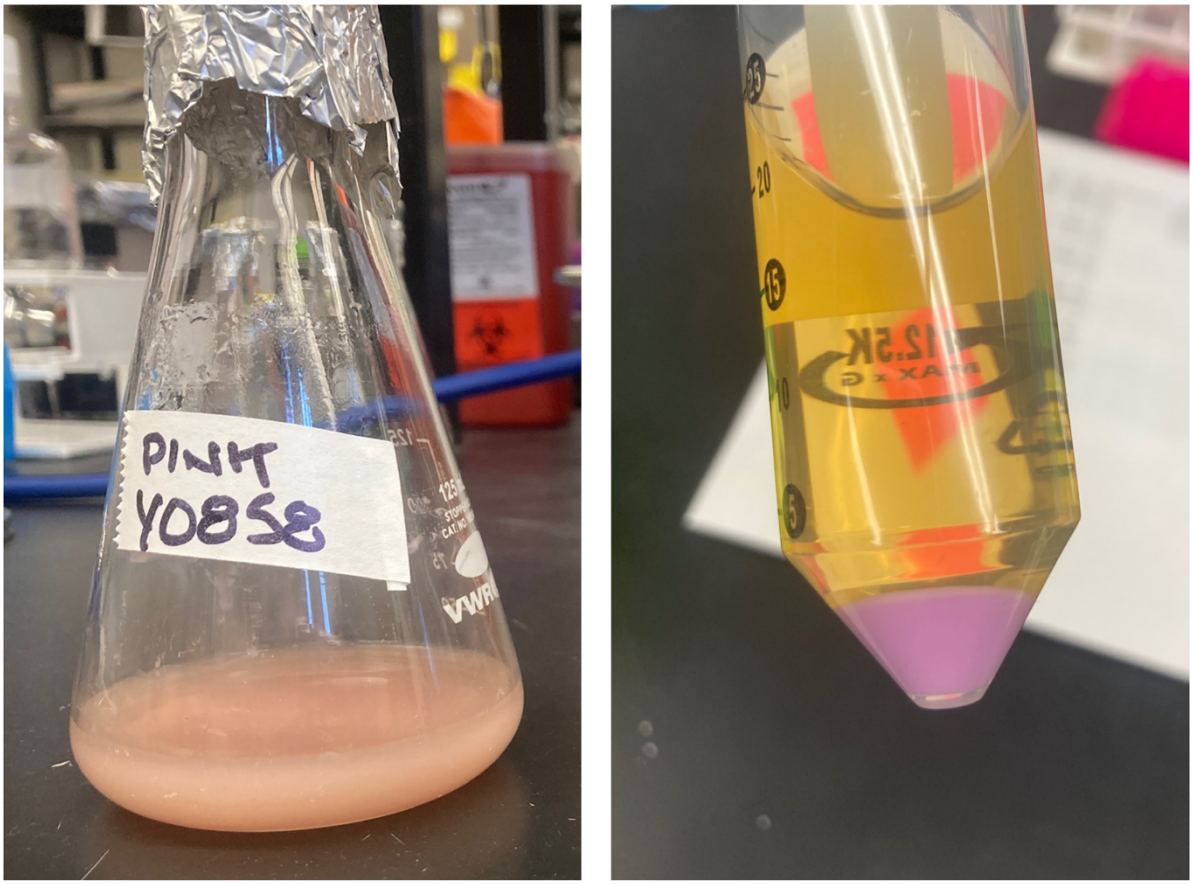

Figure A.6: S. *cerevisiae* strain YO858 expressing a pink chromogenic plasmid.

Mating type was determined in a mating type halo assay. Strains DBY7730 (*MAT***a**) and DBY7442 (*MAT*α) were cultured in 2 mL YPD broth overnight at 30°C, with shaking. The DBY7742 culture was diluted 1:10, and the DBY7730 culture was diluted 1:20. Triton

X-100 was added to a final concentration of 0.05%. 400-500 µL of each cell suspension was spread onto a 100 mm YPD agar plate. Strains of interest were pinned onto the lawn using sterile toothpicks or a metal pinner, and the plates were incubated 2 days at 30°C. DBY7730 and DBY7442 carry mutations that make them supersensitive to mating pheromone, so a colony of the opposite mating type can inhibit the growth of the lawn strain, forming a halo (Fig A.7A). Thus, a colony with a halo on the DBY7730 lawn is *MAT*α, and a colony with a halo on the DBY7742 lawn is *MAT***a**. Diploid cells do not produce mating pheromone and will not produce a halo on either lawn. Halos cannot be attributed to killer toxin production, since the agar is ≈ pH 7 and is incubated at 30°C, two conditions that inactivate killer toxins[133].

Alternatively, mating type could be determined by PCR using primers NTT041-043 (Fig A.7B). NTT41 is a reverse primer that hybridizes within the *MAT* locus, and NTT42 and NTT43 are the *MAT*α-specific and *MAT***a**-specific forward primers, respectively. A cell with the *MAT*α locus will produce a 404 bp amplicon, and a cell with the *MAT***a** locus will produce a 544 bp amplicon, and a diploid cell will produce both. NTT43 does not hybridize within either *HML*α or *HMR***a** and thus cannot yield a false result.

A spore clone of the appropriate mating type (usually *MAT*α) is mated with a lab strain containing the desired mutations, such as gene deletions or auxotrophies. Roughly equal size colonies of *MAT***a** cells and *MAT*α cells were suspended in 1 mL ddH_2O (separately). 10 µL of the *MAT***a** cell suspension was added to the *MAT*α cell suspension (1 to 100 ratio). 5 µL of this mixture was dotted onto a YPD plate and incubated overnight at 30°C. Cells were streaked onto a YPD plate, onto which had been spread 125 µL of 1 mg/mL alpha factor (may be diluted further for ease of spreading evenly over a large area) and incubated 2 days at 30°C. Diploids were verified by a mating type halo assay and/or PCR. The rationale of this technique is that all *MAT***a** cells will mate with *MAT*α cells and form diploids, and the alpha factor will inhibit the growth of the *MAT*α cells. Diploids were verified in a mating type halo assay or by PCR, and presence of virus was verified by electrophoresing dsRNAs or probing total nucleic acids with RT-PCR.

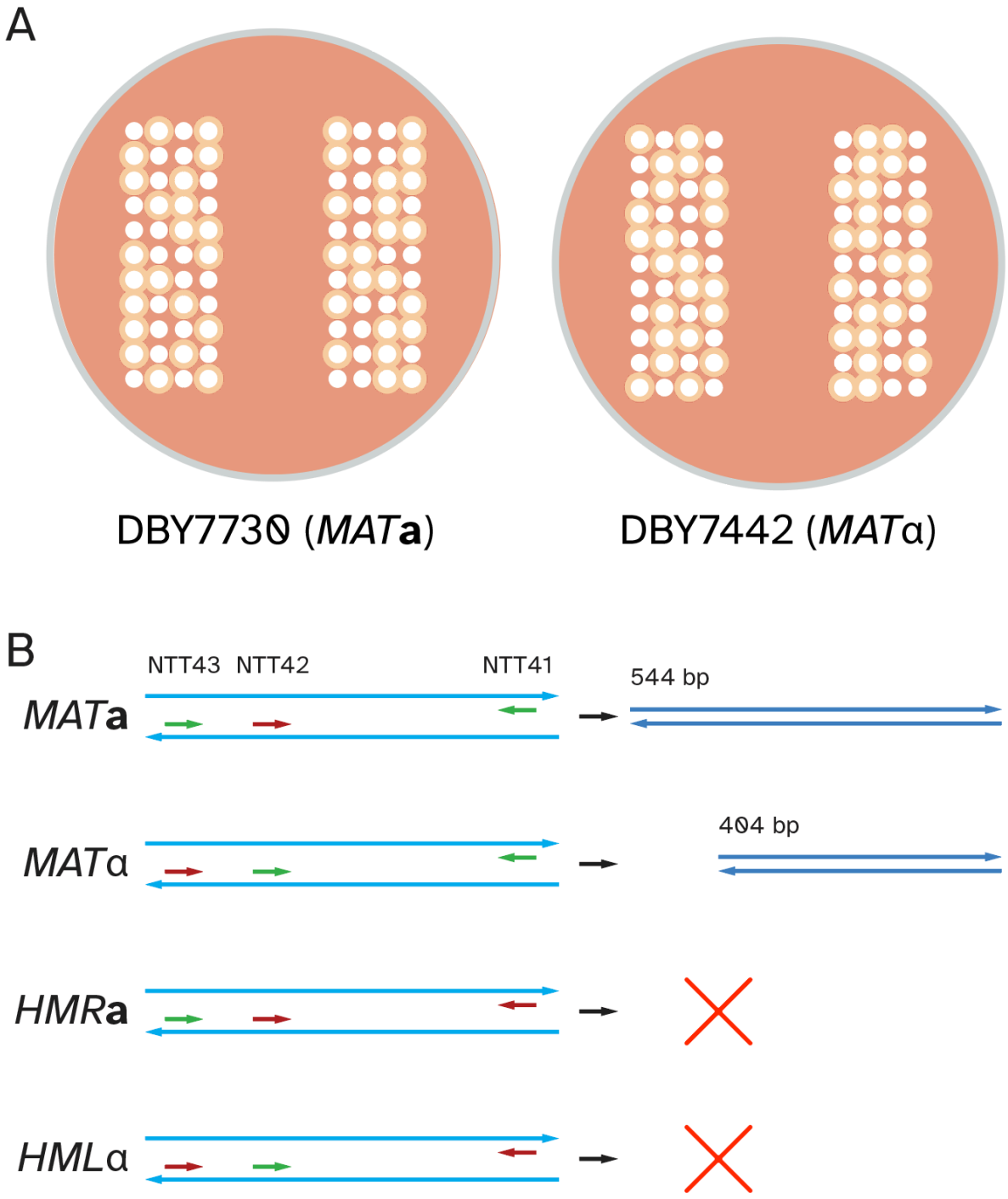

Figure A.7: Determining yeast mating type.
(**A**) Spore colonies (white circles) are pinned onto YPD agar plates seeded with DBY7730 (*MAT***a**) or DBY7442 (*MAT*α) (red color). Zones of growth inhibition (orange halos surrounding white circles) indicate production of mating pheromone that arrested the cell cycle of the lawn strain. (**B**) Green, hybridization of primer to genomic DNA. Red, no hybridization of primer to genomic DNA.

APPENDIX B: SUPPLEMENTARY FIGURES FOR CHAPTER 2

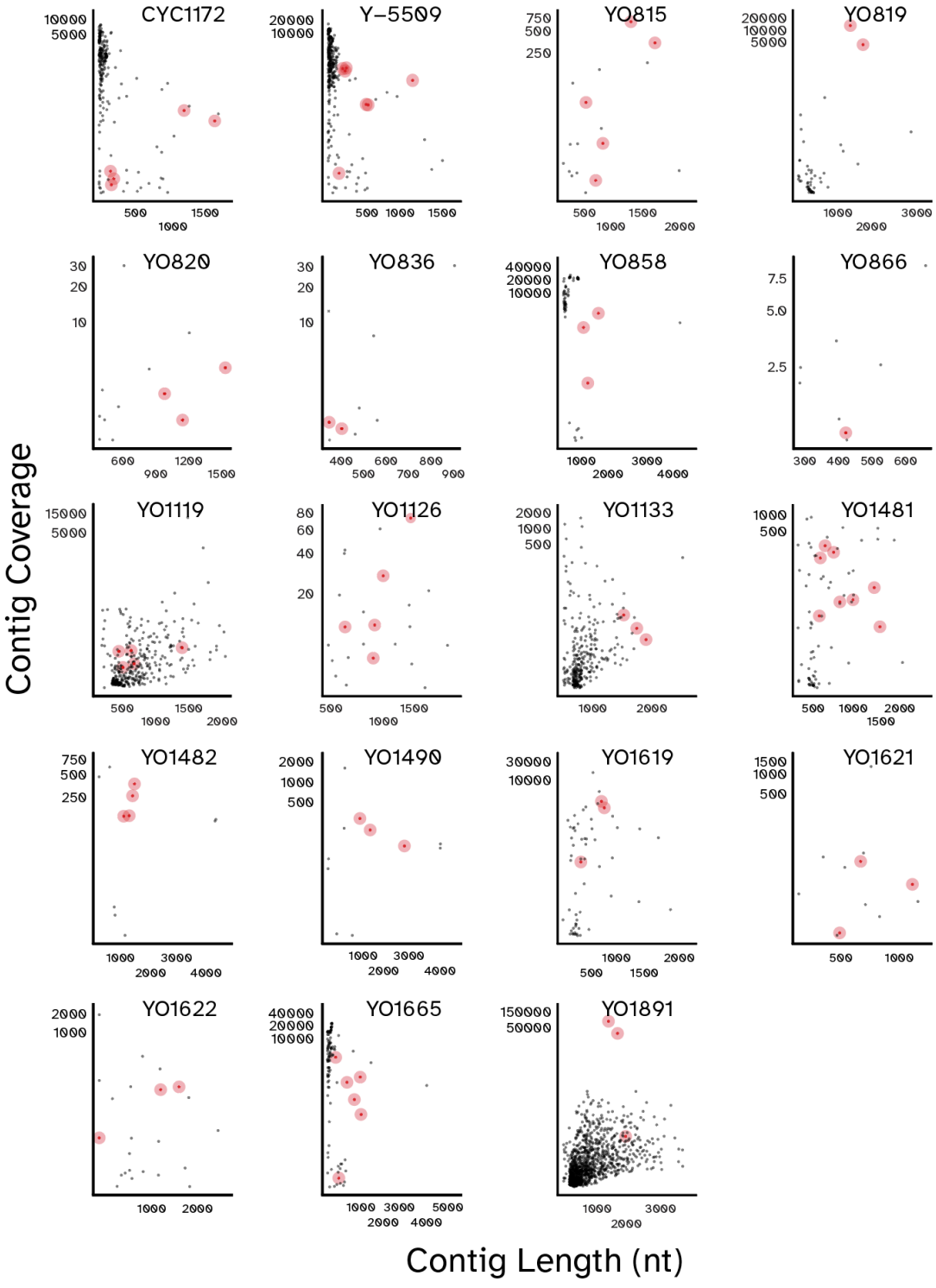

Figure A.8: Contig size and coverage plots from the sequencing of dsRNAs from 11 strains of S. *cerevisiae* with PVs.

Each point represents a single contig generated by RNA sequencing. Red points are contigs that had sequence homology to known PVs by BLASTx.

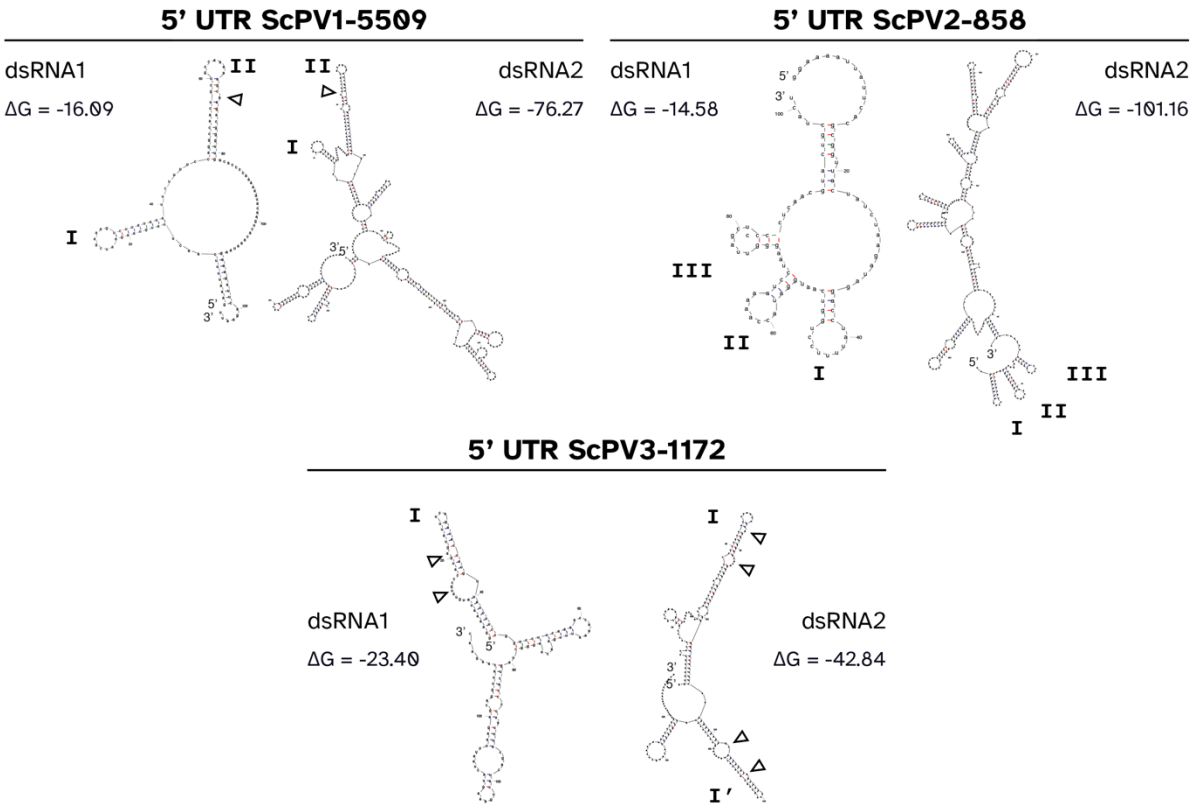

Figure A.9: RNA secondary structure predictions of the 5' UTRs of ScPVs using mFold.
Numerals are used to denote similar stem-loop structures in the RNA, and arrows are used to mark bulges.

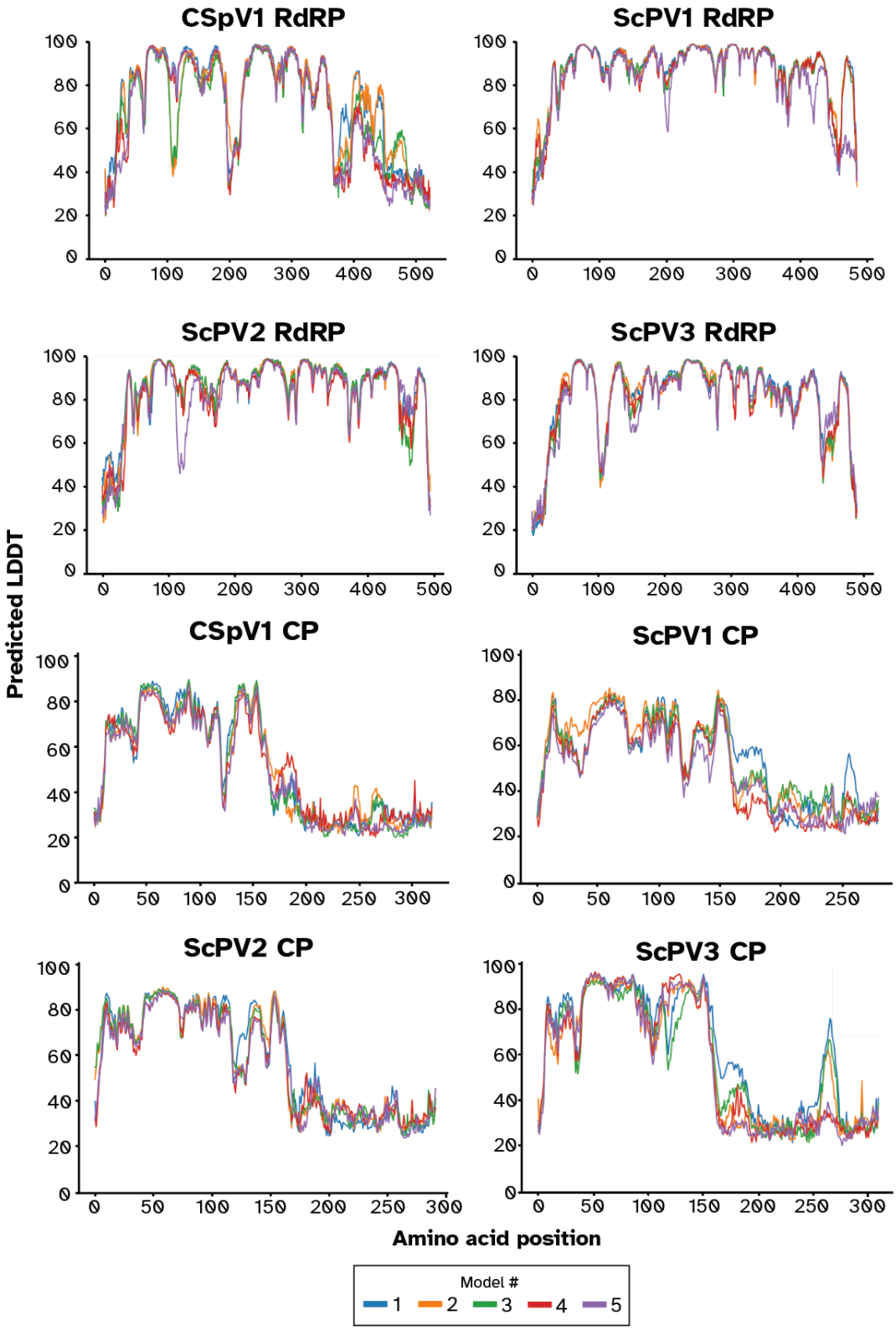

Figure A.10: Local difference distance test per residue (pLDDT) output from AlphaFold2 runs of each RdRP and CP model.

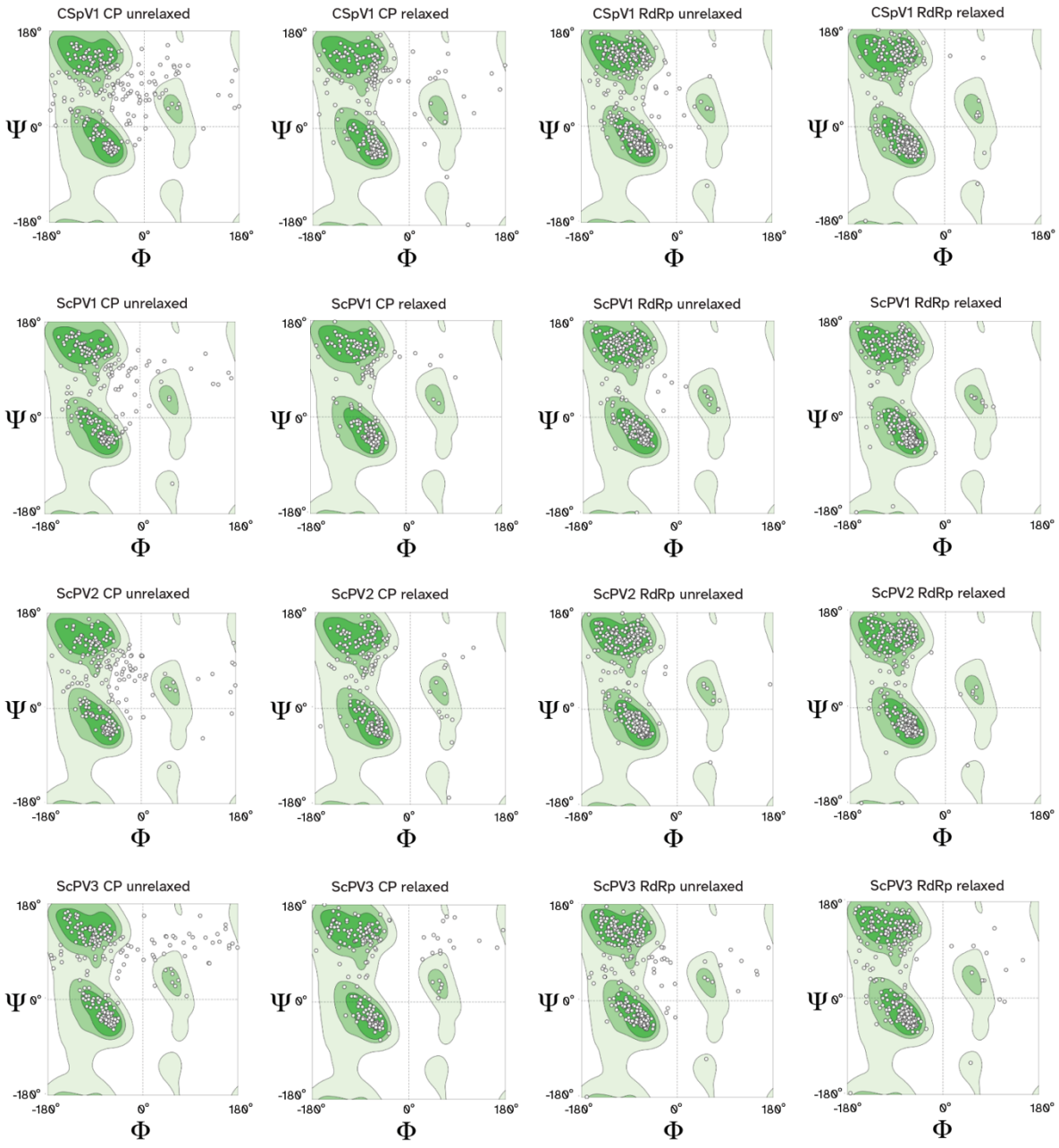

Figure A.11: Ramachandran plots of relaxed and unrelaxed AlphaFold2 models of the CP and RdRP of ScPVs and CSpV1.

Ramachandran plots of AlphaFold2 models for CP and RdRP proteins. Each point represents an amino acid residue and its ϕ and Ψ bond angles. The shaded area of the plots represents standard angles for α-helices, β-sheets, and left-handed helices from a database of 12,521 non-redundant experimental structures.

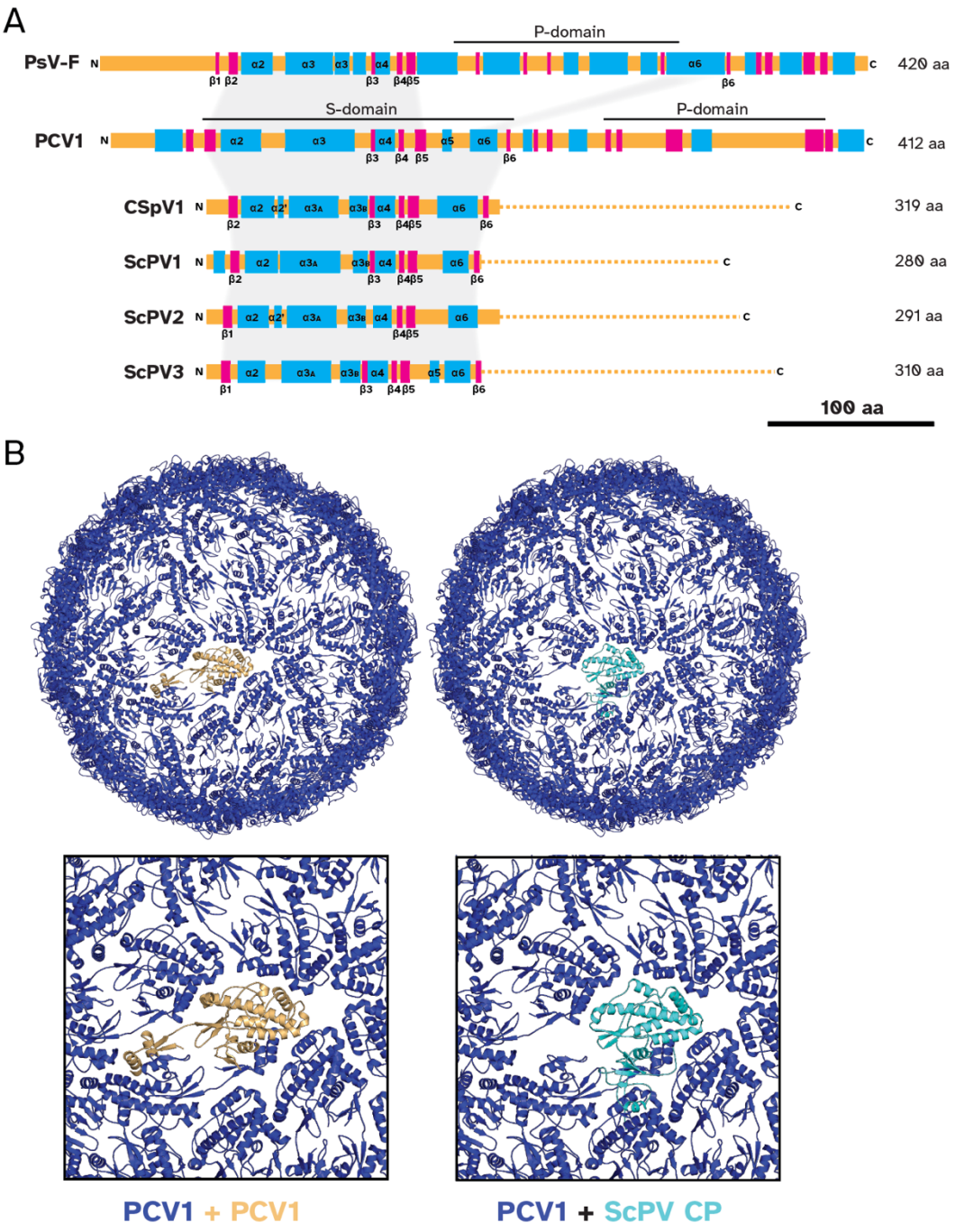

Figure A.12: Secondary structure comparison of CP proteins from different PVs.
(**A**) Secondary structures were derived from crystal structures of the CP of PCV1 (PDB:7ncr) and PsV-F (PDB:3es5) and molecular models of ScPVs and CsPV1. The α-helices and β-sheets are represented as blue and magenta boxes, respectively. The P-domain α-helices and β-sheets are numbered relative to PCV1, with the commonalities between structures highlighted in gray. Unstructured polypeptide chains are represented in orange. The C-terminal domains of ScPVs and CsPV1 that were not modeled with high confidence are represented by dashed lines. (**B**) A comparison between the native PCV1 particle structure and replacing a CP monomer from PCV1 (left panel, beige) with a single CP monomer from ScPV1 (right panel, light blue).

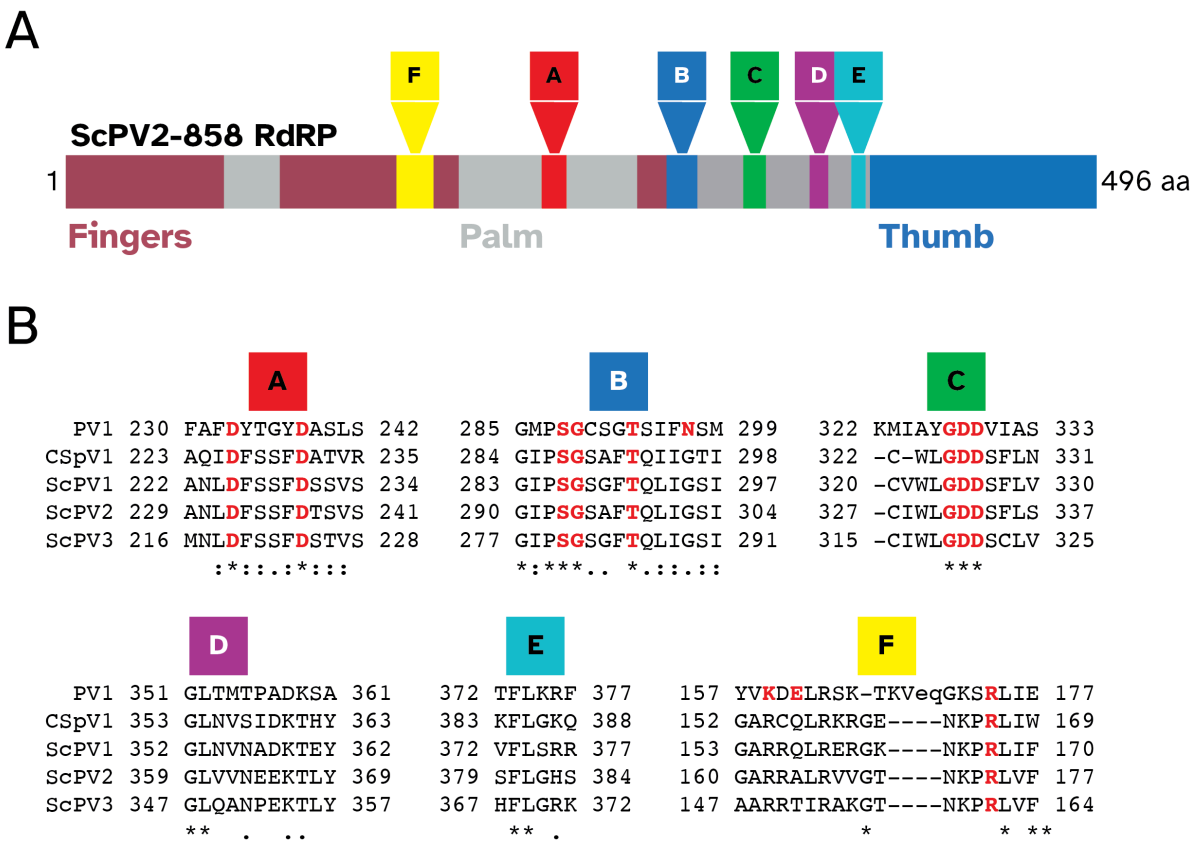

Figure A.13: The RdRPs of ScPVs have motifs conserved with RdRPs from CSpV1 and poliovirus. (**A**) Domain diagram of the RdRP of ScPV2-858 showing the position of motifs A-F. (**B**) A multiple sequence alignment of the residues of the RdRP conserved catalytic motifs. Red text indicates residues 100% conserved between the positive sense RNA viruses[335], CSpV1, ScPV1, ScPV2, and ScPV3.

APPENDIX C: DESCRIPTION OF STRAINS SURVEYED FOR THE PRESENCE OF ScPVs BY dsRNA EXTRACTION.

1. Ludlow, C. L. *et al*. Independent Origins of Yeast Associated with Coffee and Cacao Fermentation. *Curr Biol* **26**, 965–971 (2016).
2. Peter, J. *et al*. Genome evolution across 1,011 *Saccharomyces cerevisiae* isolates. *Nature* **556**, 339–344 (2018).
3. Complutense Yeast Collection
4. Crucitti, D. *et al*. Identification and Molecular Characterization of Novel Mycoviruses in *Saccharomyces* and Non-*Saccharomyces* Yeasts of Oenological Interest. *Viruses* (2021).
5. ARS Culture Collection (NRRL)

Strain	Ref	Source	Geographical origin	Protocol	TV	Sat	PV
CYC1172	3	Grape must	Spain	Gen	1	1	1
D254	4	Grape must	France	Opt	1	0	1
Y-5509	5	Coconut pod drippings	Arguelles, Manila, Philippines	Gen	1	0	1
AAM	2	Bakery	France	Gen	0	0	0
AAQ	2	Beer	USA	Gen	0	0	0
ABE	2	Human, clinical	NA	Gen	1	1	0
ABG	2	Human, clinical	NA	Gen	1	0	0
ABP	2	Prickly pear	Spain	Gen	0	0	0
ABS	2	Cocoa beans	NA	Opt	0	0	0
ACA	2	Rotting fig	California, USA	Gen	0	0	0
ACD	2	Exudate from *Quercus* sp.	USA	Gen	0	0	0
ACF	2	Distillery	France	Gen	1	1	0
ACP	2	Wine	Russia	Gen	1	1	0
ACR	2	Grapes	Netherlands	Gen	0	0	0
ACV	2	Wine	South Africa	Gen	1	0	0
AEI	2	Bakery	NA	Gen	1	1	0
AFB	2	Brewery	UK	Gen	1	1	0
AHI	2	White wine	Spain	Gen	1	1	0

Strain	Ref	Source	Geographical origin	Protocol	TV	Sat	PV
AHN	2	Grape must	South Africa	Gen	1	1	0
AIK	2	Palm nuts	Cameroon	Gen	0	0	0
AIQ	2	Spontaneous alcoholic fermentation	Italy	Gen	1	1	0
AKG	2	Palm wine	Nigeria	Gen	1	1	0
AKP	2	Heart of palm processing equipment	Ecuador	Gen	1	1	0
AKV	2	Grass	Ecuador	Gen	1	1	0
ALE	2	Hemipteran insect	Ecuador	Gen	1	1	0
ALG	2	Cocoa fruit	Ecuador	Opt	1	1	0
AMN	2	Leaf of *Wendlandia formosana*	Taiwan	Gen	0	0	0
ANN	2	Cocoa bean fermentation	Ghana	Opt	0	0	0
AQT	2	Beer	Belgium	Gen	0	0	0
ARA	2	Distillery	NA	Gen	0	0	0
ARB	2	Bakery	NA	Gen	0	0	0
ARE	2	Leaf of *Eucalyptus* sp.	NA	Gen	0	0	0
ARH	2	Fermenting Cacao	Indonesia	Gen	0	0	0
ARL	2	Lychee flower	China	Gen	0	0	0
ASL	2	Bakery levain	Turkey	Gen	0	0	0
ASP	2	Unknown	France	Gen	0	0	0
ASR	2	Vineyard	Italy	Gen	1	1	0
AST	2	Vineyard	Italy	Gen	1	0	0
ASV	2	Vineyard	Italy	Gen	1	0	0
ATA	2	Vineyard	France	Gen	0	0	0
ATB	2	Mushroom	NA	Gen	0	0	0
ATD	2	Clinical	NA	Gen	0	0	0
ATE	2	Seg. Y55	France	Gen	0	0	0
ATM	2	Wine	California, USA	Gen	1	0	0
ATS	2	Flower	Spain	Gen	0	0	0
AVB	2	Tanning liquor	Spain	Gen	1	1	0
AVK	2	Wine	Peru	Gen	1	1	0
BAF	2	Palm wine	Djibouti	Gen	1	1	0
BAH	2	Bark from *Carya* sp.	China	Gen	0	0	0
BAL	2	Rotten wood	China	Gen	1	1	0
BAV	2	Bark of grape vine	Italy	Gen	1	1	0
BBA	2	Litter by trunk of *Quercus* sp.	Italy	Gen	1	1	0

Strain	Ref	Source	Geographical origin	Protocol	TV	Sat	PV
BBB	2	Soil by trunk of *Quercus* sp.	Italy	Gen	1	1	0
BBI	2	Blossoms of *Prunus domestica L.*, 'Stanley'	Slovakia	Gen	1	1	0
BBL	2	Beetle *Mimela aurata*	Bulgaria	Gen	0	0	0
BBQ	2	Forest soil, 30C	Hungary	Gen	0	0	0
BBS	2	Forest soil, 30C	Hungary	Gen	0	0	0
BDM	2	Plant material	Madagascar	Gen	1	1	0
BEE	2	Human feces	French Guiana	Gen	1	0	0
BEG	2	High sugar foodstuff	Japan	Gen	1	1	0
BEK	2	Brewery	Chad	Gen	0	0	0
BEP	2	Homemade apple vingar	Slovenia	Gen	1	1	0
BEQ	2	Dry wine-berry selection	Slovenia	Gen	0	0	0
BFC	2	Kefyr	Slovenia	Gen	0	0	0
BFD	2	Mashed pears	Slovenia	Gen	1	1	0
BLG	2	Grape must	Spain	Gen	1	1	0
BLI	2	Grape must	Spain	Gen	1	1	0
BLK	2	Grape must treated with SO_2	Spain	Gen	1	1	0
BPI	2	Tecc	Ethiopia	Gen	1	1	0
BPP	2	Grape must	Italy	Gen	1	1	0
BPQ	2	Grape must	Malta	Gen	1	1	0
BQE	2	Sagrantino wine	Italy	Gen	1	1	0
BQP	2	Prosecco wine	Italy	Gen	1	1	0
BRA	2	Surface of *Tuber magnatum*	Italy	Gen	1	1	0
BRB	2	Winery	Italy	Gen	1	1	0
BRC	2	Winery	Italy	Gen	1	1	0
BRD	2	Dried sausages under oil	Italy	Gen	1	1	0
BRF	2	Wine fermenter	Italy	Gen	1	1	0
BSK	2	Spoiled ice tea	France	Gen	1	0	0
CBF	2	Sourdough levan	Italy	Gen	0	0	0
CBK	2	Chalcidoidea	Germany	Gen	0	0	0
CCM	2	Fir tree needles	Ukraine	Gen	0	0	0
CCP	2	*Quercus* sp.	Japan	Gen	0	0	0
CCQ	2	Tree exudate	Japan	Gen	0	0	0
CDF	2	Fruit of *Grataegus dachurica*	Russia	Gen	1	1	0

Strain	Ref	Source	Geographical origin	Protocol	TV	Sat	PV
CDG	2	Grape berries of wild *Vitus amurensis*	Russia	Gen	1	0	0
CDH	2	Exudate of *Quercus mongolica*	Russia	Gen	0	0	0
CDI	2	Exudate of *Quercus mongolica*	Russia	Gen	1	1	0
CDM	2	Cushvara river	Brazil	Gen	1	0	0
CDS	2	Tomato	Spain	Gen	0	0	0
CEA	2	Soil	Spain	Gen	0	0	0
CEB	2	Soil	Spain	Gen	1	1	0
CEC	2	Soil	Spain	Gen	0	0	0
CED	2	Soil	Spain	Gen	0	0	0
CEV	2	Moromi of Chinese wine kaoliangchiu	China	Gen	0	0	0
CFA	2	Palm wine	Djibouti	Gen	1	1	0
CFE	2	Carlsberg beer	United Kingdom	Gen	1	1	0
CFI	2	Carlsberg beer	UK	Gen	0	0	0
CFN	2	Carlsberg beer	NA	Gen	0	0	0
CFP	2	Carlsberg beer	NA	Gen	0	0	0
CFT	2	Spoiled Adriatic orchard figs	California, USA	Gen	0	0	0
CFV	2	Citrus fermentation	NA	Gen	0	0	0
CGB	2	Beetle from infested *Prunus bokhariensis*	California, USA	Gen	1	1	0
CGS	2	Fermenting grape must (sweet wine)	Lebanon	Gen	1	0	0
CHB	2	Fermenting grape must (white wine)	Lebanon	Gen	1	1	0
CHC	2	Fermenting grape must (red wine)	Lebanon	Gen	1	1	0
CHD	2	Fermenting grape must (white wine)	Lebanon	Gen	1	1	0
CHF	2	Fermenting grape must (red wine)	Lebanon	Gen	0	0	0
CHR	2	Vagina	France	Gen	0	0	0
CIC	2	Mouth	Spain	Gen	0	0	0
CIE	2	Mouth	Spain	Gen	0	0	0
CIF	2	Feces	Spain	Gen	0	0	0
CII	2	Sputum	Netherlands	Gen	0	0	0

Strain	Ref	Source	Geograph-ical origin	Proto-col	TV	Sat	PV
CKD	2	Feces (therapy isolate)	France	Gen	0	0	0
CKE	2	Feces (therapy isolate)	France	Gen	0	0	0
CKF	2	Feces (therapy isolate)	France	Gen	0	0	0
CKG	2	*S. boulardii*¬¨,Ä†isolates lychee (reference strain Biocodex)	Vietnam	Gen	0	0	0
CKH	2	*S. boulardii*¬¨,Ä†isolates (from UltraLevure packet)	France	Gen	0	0	0
CKI	2	*S. boulardii*¬¨,Ä†isolates (from Perenterol capsule)	Belgium	Gen	0	0	0
CKK	2	Feces, clinical	France	Gen	0	0	0
CKL	2	Feces, therapy	France	Gen	0	0	0
CKM	2	Feces, therapy	France	Gen	0	0	0
CKQ	2	Feces (therapy isolate)	France	Gen	0	0	0
CKS	2	Unknown	France	Gen	0	0	0
CKT	2	Unknown	France	Gen	0	0	0
CLA	2	Unknown	France	Gen	0	0	0
CLB	2	Tree leaves	France	Gen	0	0	0
CLC	2	Dead tree	France	Gen	0	0	0
CPD	2	Spoiled beer	NA	Gen	0	0	0
CPE	2	Unknown	Spain	Gen	1	1	0
CPN	2	*Agave* spp. fermentation	Mexico	Gen	1	0	0
CQC	2	Cocoa bean fermentation	West Africa	Opt	0	0	0
CQD	2	Cocoa bean fermentation	West Africa	Opt	0	0	0
CQE	2	Cocoa bean fermentation	West Africa	Gen	0	0	0
CQF	2	Cocoa bean fermentation	West Africa	Opt	0	0	0
CQG	2	Cocoa bean fermentation	West Africa	Opt	0	0	0
CQH	2	Cocoa bean fermentation	West Africa	Opt	0	0	0
CQI	2	Cocoa bean fermentation	West Africa	Opt	0	0	0
CQK	2	Cocoa bean fermentation	West Africa	Opt	0	0	0
CQL	2	Cocoa bean fermentation	West Africa	Opt	0	0	0
CQM	2	Cocoa bean fermentation	West Africa	Opt	0	0	0
CQN	2	Cocoa bean fermentation	West Africa	Opt	0	0	0
CQP	2	Cocoa bean fermentation	West Africa	Opt	0	0	0
CQR	2	Sake	Japan	Gen	0	0	0
YAA	2	Unknown	NA	Gen	0	0	0
YAB	2	Unknown	NA	Gen	1	0	0
YAD	2	Human	Romania	Gen	0	0	0

Strain	Ref	Source	Geographical origin	Protocol	TV	Sat	PV
YAE	2	Feces	NA	Gen	0	0	0
YAM	2	Unknown	NA	Gen	1	1	0
YAP	2	Unknown	California, USA	Gen	1	0	0
YAQ	2	Unknown	California, USA	Gen	1	0	0
YAR	2	Unknown	California, USA	Gen	1	0	0
YAW	2	Unknown	Texas, USA	Gen	1	0	0
YAX	2	Unknown	Texas, USA	Gen	0	0	0
YAY	2	Unknown	Italy	Gen	0	0	0
YBH	2	Unknown	Italy	Gen	1	0	0
YBU	2	Unknown	Washington DC, USA	Gen	1	1	0
YBV	2	Unknown	Michigan, USA	Gen	0	0	0
YBW	2	Unknown	Minnesota, USA	Gen	1	0	0
YBX	2	Unknown	Italy	Gen	0	0	0
YBY	2	Unknown	Italy	Gen	0	0	0
YCA	2	Unknown	South Africa	Gen	1	1	0
YCB	2	Unknown	South Africa	Gen	0	0	0
YDO	2	Segregant of NRRL Y-53	Ohio, USA	Gen	1	0	0
YO0433	1	Rhodendron	Washington, USA	Opt	0	0	0
YO0458	1	Soil	California, USA	Gen	0	0	0
YO0653	1	Olives	Washington, USA	Gen	0	0	0
YO0655	1	Olives	Washington, USA	Gen	0	0	0
YO0658	1	Olives	Washington, USA	Gen	0	0	0
YO0750	1	Pineapple skin	Washington, USA	Kinda Opt	0	0	0
YO0814	1	Cacao	Nigeria	Gen	0	0	1
YO0815	1	Cacao	Nigeria	Gen	0	0	1
YO0818	1	Cacao	Nigeria	Gen	0	0	1
YO0819	1	Cacao	Nigeria	Gen	0	0	1
YO0820	1	Cacao	Nigeria	Gen	0	0	1

Strain	Ref	Source	Geograph-ical origin	Proto-col	TV	Sat	PV
YO0822	1	Cacao	Nigeria	Gen	0	0	0
YO0823	1	Cacao	Nigeria	Gen	0	0	0
YO0835	1	Cacao	Ecuador	Gen	1	0	0
YO0836	1	Cacao	Ecuador	Gen	1	0	1
YO0838	1	Cacao	Ecuador	Gen	0	0	0
YO0839	1	Cacao	Ecuador	Gen	0	0	0
YO0840	1	Cacao	Costa Rica	Gen	0	0	0
YO0841	1	Cacao	Costa Rica	Gen	0	0	0
YO0842	1	Cacao	Costa Rica	Gen	0	0	0
YO0843	1	Cacao	Costa Rica	Gen	0	0	0
YO0844	1	Cacao	Costa Rica	Gen	0	0	0
YO0846	1	Cacao	Peru	Gen	0	0	0
YO0847	1	Cacao	Peru	Gen	0	0	0
YO0849	1	Cacao	Peru	Gen	0	0	0
YO0850	1	Cacao	Peru	Gen	0	0	0
YO0851	1	Cacao	Peru	Opt	0	0	0
YO0852	1	Cacao	Dominican Republic	Gen	1	0	0
YO0853	1	Cacao	Dominican Republic	Gen	1	0	1
YO0854	1	Cacao	Dominican Republic	Gen	0	0	0
YO0855	1	Cacao	Dominican Republic	Gen	1	0	0
YO0856	1	Cacao	Dominican Republic	Gen	0	0	0
YO0857	1	Cacao	Dominican Republic	Gen	0	0	0
YO0858	1	Cacao	Dominican Republic	Kinda Opt	1	0	1
YO0859	1	Cacao	Peru	Gen	0	0	0
YO0861	1	Cacao	Peru	Gen	0	0	0
YO0866	1	Cacao	Haiti	Gen	1	0	1
YO0868	1	Cacao	Haiti	Gen	1	0	1
YO0870	1	Cacao	Haiti	Gen	0	0	0
YO0871	1	Cacao	Haiti	Gen	0	0	0
YO0872	1	Cacao	Haiti	Gen	0	0	0
YO0874	1	Cacao	Haiti	Gen	1	0	0
YO0875	1	Cacao	Haiti	Gen	1	0	0

Strain	Ref	Source	Geograph-ical origin	Proto-col	TV	Sat	PV
YO0876	1	Cacao	Madagascar	Gen	0	0	0
YO1055	1	Cacao	Costa Rica	Gen	0	0	0
YO1056	1	Cacao	Costa Rica	Gen	0	0	0
YO1060	1	Cacao	Costa Rica	Opt	0	0	0
YO1061	1	Cacao	Costa Rica	Gen	0	0	0
YO1112	1	Coffee	Honduras	Gen	0	0	0
YO1113	1	Coffee	Honduras	Gen	0	0	0
YO1114	1	Coffee	Mexico	Gen	0	0	0
YO1115	1	Coffee	Mexico	Gen	0	0	0
YO1116	1	Coffee	Nicaragua	Gen	1	1	0
YO1117	1	Cacao	Costa Rica	Gen	0	0	0
YO1119	1	Cacao	Costa Rica	Gen	1	0	1
YO1124	1	Coffee	Honduras	Gen	0	0	1
YO1125	1	Coffee	Honduras	Gen	1	0	0
YO1126	1	Coffee	Honduras	Gen	0	0	1
YO1128	1	Coffee	Yemen	Gen	0	0	0
YO1129	1	Coffee	Yemen	Gen	0	0	0
YO1130	1	Coffee	Yemen	Gen	0	0	0
YO1132	1	Coffee	Ethiopia	Opt	0	0	0
YO1133	1	Coffee	Ethiopia	Gen	0	0	1
YO1134	1	Coffee	Yemen	Gen	0	0	0
YO1135	1	Coffee	Yemen	Gen	0	0	0
YO1137	1	Coffee	Colombia	Gen	0	0	0
YO1138	1	Coffee	Colombia	Gen	1	0	0
YO1140	1	Coffee	Honduras	Gen	0	0	0
YO1200	1	Coffee	Indonesia	Gen	0	0	0
YO1201	1	Coffee	Indonesia	Gen	0	0	0
YO1224	1	Coffee	Guatemala	Gen	0	0	0
YO1225	1	Coffee	Nicaragua	Gen	0	0	0
YO1226	1	Coffee	Kenya	Gen	0	0	0
YO1228	1	Coffee	Nicaragua	Gen	1	0	0
YO1348	1	Coffee	Guatemala	Gen	1	1	1
YO1349	1	Coffee	Colombia	Gen	1	0	1
YO1357	1	Coffee	Indonesia	Gen	0	0	0
YO1477	1	Coffee	Rwanda	Opt	1	1	1
YO1478	1	Coffee	Rwanda	Gen	0	0	0
YO1479	1	Coffee	Rwanda	Gen	0	0	0
YO1480	1	Coffee	Rwanda	Gen	0	0	0

Strain	Ref	Source	Geographical origin	Protocol	TV	Sat	PV
YO1481	1	Coffee	Indonesia	Gen	1	0	1
YO1482	1	Coffee	Indonesia	Gen	1	1	1
YO1485	1	Coffee	Ethiopia	Gen	1	1	0
YO1487	1	Coffee	Kenya	Gen	1	0	0
YO1489	1	Coffee	Indonesia	Gen	1	1	1
YO1490	1	Coffee	Indonesia	Gen	1	1	1
YO1594	1	Coffee	Colombia	Gen	1	0	1
YO1595	1	Coffee	Colombia	Gen	0	0	0
YO1599	1	Coffee	Colombia	Gen	1	0	1
YO1600	1	Coffee	Peru	Gen	1	0	1
YO1601	1	Coffee	Peru	Opt	1	0	0
YO1604	1	Coffee	Costa Rica	Gen	1	0	1
YO1605	1	Coffee	Costa Rica	Gen	0	0	1
YO1608	1	Coffee	Costa Rica	Gen	0	0	1
YO1609	1	Coffee	Indonesia	Gen	0	0	0
YO1610	1	Coffee	Indonesia	Gen	0	0	1
YO1611	1	Coffee	Indonesia	Gen	0	0	0
YO1612	1	Coffee	Indonesia	Gen	0	0	1
YO1613	1	Coffee	Indonesia	Gen	0	0	0
YO1615	1	Coffee	United States	Gen	1	0	1
YO1619	1	Coffee	Uganda	Opt	1	0	1
YO1620	1	Coffee	Uganda	Gen	1	1	1
YO1621	1	Coffee	Uganda	Gen	1	1	1
YO1622	1	Coffee	Uganda	Gen	1	1	1
YO1658	1	Cacao	Ivory Coast	Opt	0	0	0
YO1659	1	Cacao	Ivory Coast	Gen	1	0	0
YO1660	1	Cacao	Ivory Coast	Opt	0	0	1
YO1661	1	Cacao	Ivory Coast	Gen	0	0	0
YO1662	1	Cacao	Ivory Coast	Gen	1	0	0
YO1663	1	Cacao	Ivory Coast	Gen	1	0	0
YO1665	1	Cacao	Ecuador	Gen	1	0	1
YO1666	1	Cacao	Ecuador	Gen	0	0	0
YO1667	1	Cacao	Ecuador	Gen	0	0	0
YO1669	1	Cacao	Papua New Guinea	Opt	0	0	0
YO1671	1	Cacao	Papua New Guinea	Gen	1	0	0

Strain	Ref	Source	Geographical origin	Protocol	TV	Sat	PV
YO1675	1	Cacao	Ecuador	Gen	1	0	0
YO1676	1	Cacao	Ecuador	Opt	0	0	0
YO1680	1	Cacao	Ecuador	Gen	0	0	0
YO1681	1	Cacao	Ecuador	Opt	0	0	0
YO1682	1	Cacao	Ecuador	Gen	0	0	0
YO1696	1	Cacao	Venezuela	Opt	1	0	0
YO1697	1	Cacao	Venezuela	Gen	1	0	0
YO1701	1	Cacao	Venezuela	Gen	1	0	0
YO1705	1	Cacao	Peru	Opt	1	0	1
YO1706	1	Cacao	Peru	Gen	0	0	0
YO1707	1	Cacao	Colombia	Gen	0	0	0
YO1713	1	Cacao	Venezuela	Gen	1	0	0
YO1715	1	Cacao	Venezuela	Opt	1	0	0
YO1717	1	Cacao	Venezuela	Gen	1	0	1
YO1719	1	Cacao	Venezuela	Opt	0	0	0
YO1722	1	Cacao	Nicaragua	Gen	1	0	0
YO1723	1	Cacao	Nicaragua	Opt	1	0	1
YO1724	1	Cacao	Venezuela	Gen	0	0	0
YO1880	1	Coffee	Honduras	Gen	1	0	0
YO1882	1	Coffee	Peru	Opt	1	0	0
YO1885	1	Coffee	Peru	Opt	1	0	0
YO1888	1	Coffee	Honduras	Gen	1	0	0
YO1889	1	Coffee	Honduras	Opt	0	0	0
YO1890	1	Coffee	Honduras	Opt	0	0	1
YO1891	1	Coffee	Honduras	Opt	0	0	1
YO1892	1	Coffee	Honduras	Opt	1	0	0
YO1893	1	Coffee	Honduras	Gen	1	0	0
YO1919	1	Coffee	Peru	Gen	1	0	0
YO1924	1	Coffee	Rwanda	Gen	0	0	0
YO1925	1	Coffee	Honduras	Opt	0	0	0

APPENDIX D: MSA OF ScCV1 SEQUENCES, ScPV3, & PRIMERS FROM CRUCITTI ET AL., 2021

Mismatches between ScCV1-D254 or ScCV-U43 and ScPV3-1172 are denoted by '-'. For ease of reading, matches are not denoted. Mismatches between either ScCV1-D254 or ScCV-U43 and a primer are denoted by '-'. Matches between ScCV1-D254, ScCV-U43, and a primer are denoted by '*'. Mismatches between a primer and both ScCV1-D254 and ScCV-U43 are denoted by '!' and are bolded. Lowercase letters in the virus sequence indicate an untranslated region, and uppercase letters indicate an open reading frame.

```
Primer               ScCV1-RdRp-I-f                ScCV1-RdRp-REV
Virus-primer id      !!!!!!!!!!!!!!!!!!!!          ***-**-**************
Primer sequence      CAGATACCATGTTATTTTCCGG         GCCTGTCACACCTGCTATTG
ScCV1-D254-dsRNA1    ----------------------        GCCTGTCACACCTGCTATTG
ScCV1- U43-dsRNA1    ----------------------        GCCCGTTACACCTGCTATTG
ScPV3-1172-dsRNA1    cagataccatgttattttccgg         GCCCGTTACACCTGCTATTG
Virus id                                              -  -
Position             28                            552
```

```
Primer                      ScCV1-RdRp-II-f
Virus-primer id             -**************!*!!!!!!
Primer sequence             GTTAATGGATCTTTGTTCGTCG
ScCV1-D254-dsRNA1           GTTAATGGATCTTTCTGATCTT
ScCV1- U43-dsRNA1           ATTAATGGATCTTTCTGATCTT
ScPV3-1172-dsRNA1           ATTAATGGATCTTTCCGATCTT
Virus id                    -               -
Position                    858
```

```
Primer                   ScCV1-RdRp-II-r
Virus-primer id          *********-!!!!!!!!!!!!
Primer sequence          cagtgcgtaatccttaaagacg
ScCV1-D254-dsRNA1        cagtgcgtatc-----------
ScCV1- U43-dsRNA1        ----------------------
ScPV3-1172-dsRNA1        cagtgcgtaatccttaaagacg
Virus id
Position                 1645
```

```
Primer
Virus-primer id
Primer sequence
Primer                   ScCV1-CP-I-f
Virus-primer id          !!!!!!!!!!!!*********
Primer sequence          ATTTGCAGTTATTCAGTAGCG
ScCV1-D254-dsRNA2        -------------cagtagcg
ScCV1- U43-dsRNA2        ------------tcagtagcg
ScPV3-1172-dsRNA2        atttgcagttattcagtagcg
Virus id
Position                 127
```

```
Primer                  ScCV1-CP-FW
Virus-primer id         ***!****************
Primer sequence         CCTGCCTCAAATCCTCCTGG
ScCV1-D254-dsRNA2       CCTACCTCAAATCCTCCTGG
ScCV1- U43-dsRNA2       CCTACCTCAAACCCTCCTGG
ScPV3-1172-dsRNA2       CCTGCCTCAAATCCTCCTGG
Virus id                   -       -
Position                814
```

```
Primer              ScCV1-CP-II-r
Virus-primer id     **************!!!!!!!!!!
Primer sequence     CGTACAACGAAGTAACGAAGAGTG
ScCV1-D254-dsRNA2   cgtacaacgaa-------------
ScCV1- U43-dsRNA2   cgtacaacgaagta----------
ScPV3-1172-dsRNA2   cgtacaacgaagtaacgaagagtg
Virus id                     -------------
Position            1176
```

APPENDIX E: NAMES, ORIGIN, AND ORF LENGTH OF REPRESENTATIVE STRAINS OF ScPV

Virus name	Host strain	Origin	Source	CP (aa)	RdRP (aa)
ScPV1-5509	Y-5509	Philippines	Coconut pod	280	486
ScPV2-858	YO858	Dominican Republic	Cacao	292	496
ScPV3-1172	CYC 1172	Spain	Grape must	310	491
ScPV1-1481	YO1481	Indonesia	Coffee	280	486
ScPV1-1482	YO1482	Indonesia	Coffee	280	486
ScPV1-1490	YO1490	Indonesia	Coffee	280	486
ScPV1-1619	YO1619	Uganda	Coffee	280	486
ScPV1-1621	YO1621	Uganda	Coffee	280	486
ScPV1-1622	YO1622	Uganda	Coffee	280	486
ScPV2-1481	YO1481	Indonesia	Coffee	292	496
ScPV2-1482	YO1482	Indonesia	Coffee	292	496
ScPV2-1490	YO1490	Indonesia	Coffee	292	496
ScPV2-1619	YO1619	Uganda	Coffee	292	496
ScPV2-1665	YO1665	Ecuador	Cacao	292	496

APPENDIX F: THE PERCENTAGE IDENTITY BETWEEN THE CP AND RdRP PROTEINS OF ScPVs AND CSpV1.

ScPV1-1622, ScPV1-1490, and ScPV2-1490 are identical to ScPV1-1621, ScPV1-1481, and ScPV2-1481, respectively, and are omitted to save space.

CP percent amino acid sequence identity

RdRP percent amino acid sequence identity

	CsPV1	ScPV3-1172	ScPV1-5509	ScPV1-1619	ScPV1-1621	ScPV1-1481	ScPV1-1482	ScPV2-858	ScPV2-1481	ScPV2-1482	ScPV2-1619	ScPV2-1665
CsPV1	•	18.6	17.1	17.1	17.1	16.8	17.1	22.2	20.1	22.5	22.2	21.6
ScPV3-1172	32.7	•	20.3	19.9	20.3	19.3	19.0	30.2	28.8	29.9	30.5	28.6
ScPV1-5509	37.7	45.6	•	97.5	100.0	95.4	95.7	25.7	23.3	25.7	25.3	25.3
ScPV1-1619	37.7	45.4	98.8	•	97.5	97.9	93.2	25.3	23.0	25.3	25.0	25.0
ScPV1-1621	37.5	45.4	98.6	98.6	•	97.5	95.7	25.7	23.3	25.7	25.3	25.3
ScPV1-1481	37.7	45.4	97.5	97.9	97.5	•	95.4	25.0	22.6	25.0	24.7	24.7
ScPV1-1482	37.7	45.8	97.1	97.1	98.4	97.5	•	24.7	22.6	24.7	24.7	24.3
ScPV2-858	35.3	49.3	48.2	48.4	48.4	48.6	48.6	•	73.1	98.6	96.9	79.1
ScPV2-1481	35.1	49.3	48.4	48.6	48.6	48.8	11.2	97.8	•	73.4	75.8	73.7
ScPV2-1482	35.3	49.5	48.2	48.4	48.4	48.6	48.8	99.4	98.4	•	96.2	80.1
ScPV2-1619	35.3	49.3	48.2	48.4	48.4	48.6	48.8	100.0	97.8	99.4	•	79.5
ScPV2-1665	34.6	48.7	48.2	48.2	48.4	48.6	48.8	92.3	91.5	92.1	92.3	•

APPENDIX G: THE DETECTION OF ScPVs IN STRAINS OF YEASTS KNOWN TO HARBOR dsRNAs USING RT-PCR OR SHORT-READ SEQUENCING.

f, full; n, not detected; p, partial

	Multiplex RT-PCR							NGS (de novo or mapping algorithms) and RACE						Overall		
Strain	ScPV1- 5509	ScPV1- 1126	ScPV2- 858	ScPV2- 1126	ScPV2- 815	ScPV3- 1172	None	ScPV5509 RdRP ORF	ScPV1-5509 CA ORF	ScPV2-858 RdRP ORF	ScPV2-858 CA ORF	ScPV3-1172 RdRP ORF	ScPV3-1172 CA ORF	ScPV1	ScPV2	ScPV3
CYC1172	-	-	-	-	-	1	-	n	n	n	n	f	f	-	-	1
D254	-	-	-	-	-	1	-	-	-	-	-	-	-	-	-	1
Y-5509	1	-	-	-	-	-	-	f	f	n	n	n	n	1	-	-
YO0814	1	-	-	-	-	-	-	-	-	-	-	-	-	1	-	-
YO0815	-	-	-	-	1	-	-	n	n	p	f	n	n	-	1	-
YO0818	1	-	-	-	-	-	-	-	-	-	-	-	-	1	-	-
YO0819	-	-	-	-	-	-	1	n	n	p	f	n	n	-	1	-
YO0820	-	-	-	-	-	-	1	p	n	p	p	n	n	1	1	-
YO0836	-	-	-	-	-	-	1	n	n	n	n	n	n	-	-	-
YO0853	-	1	1	-	-	-	-	-	-	-	-	-	-	1	1	-
YO0858	-	-	1	-	-	-	-	n	n	f	f	n	n	-	1	-
YO0866	-	-	-	-	-	-	1	n	n	n	n	n	n	-	-	-
YO0868	-	-	1	-	-	-	-	-	-	-	-	-	-	-	1	-
YO1119	-	-	-	-	-	-	1	p	n	n	n	n	n	1	-	-
YO1124	-	1	1	-	-	-	-	-	-	-	-	-	-	1	1	-
YO1126	-	1	-	1	-	-	-	p	p	p	f	n	n	1	1	-
YO1133	-	-	-	-	-	-	1	p	f	p	n	n	n	1	1	-
YO1348	-	1	1	-	-	-	-	-	-	-	-	-	-	1	1	-
YO1349	-	-	1	-	-	-	-	-	-	-	-	-	-	-	1	-
YO1477	1	-	1	-	-	-	-	-	-	-	-	-	-	1	1	-
YO1481	1	-	1	-	-	-	-	f	f	f	f	n	n	1	1	-
YO1482	1	-	1	-	-	-	-	f	f	f	f	n	n	1	1	-
YO1489	1	-	1	-	-	-	-	-	-	-	-	-	-	1	1	-

	Multiplex RT-PCR							NGS (de novo or mapping algorithms) and RACE						Overall		
Strain	ScPV1- 5509	ScPV1- 1126	ScPV2- 858	ScPV2- 1126	ScPV2- 815	ScPV3- 1172	None	ScPV5509 RdRP ORF	ScPV1-5509 CA ORF	ScPV2-858 RdRP ORF	ScPV2-858 CA ORF	ScPV3-1172 RdRP ORF	ScPV3-1172 CA ORF	ScPV1	ScPV2	ScPV3
YO1490	1	-	1	-	-	-	-	f	f	f	f	n	n	1	1	-
YO1594	-	-	1	-	-	-	-	-	-	-	-	-	-	-	1	-
YO1599	-	1	1	-	-	-	-	-	-	-	-	-	-	1	1	-
YO1600	-	-	1	-	-	-	-	-	-	-	-	-	-	-	1	-
YO1604	-	-	1	-	-	-	-	-	-	-	-	-	-	-	1	-
YO1605	-	-	1	-	-	-	-	-	-	-	-	-	-	-	1	-
YO1608	-	-	1	-	-	-	-	-	-	-	-	-	-	-	1	-
YO1610	1	-	-	-	-	-	-	-	-	-	-	-	-	1	-	-
YO1612	1	-	-	-	-	-	-	-	-	-	-	-	-	1	-	-
YO1615	1	-	1	-	1	-	-	-	-	-	-	-	-	1	1	-
YO1619	1	-	-	-	1	-	-	f	f	f	f	n	n	1	1	-
YO1620	-	-	1	-	1	-	-	-	-	-	-	-	-	-	1	-
YO1621	-	-	-	-	1	-	-	f	f	n	n	n	n	1	1	-
YO1622	-	-	-	-	1	-	-	f	f	n	n	n	n	1	1	-
YO1660	-	-	-	-	1	-	-	-	-	-	-	-	-	-	1	-
YO1665	-	-	-	1	-	-	-	n	n	f	f	n	n	-	1	-
YO1705	1	-	1	-	-	-	-	-	-	-	-	-	-	1	1	-
YO1717	-	-	1	-	-	-	-	-	-	-	-	-	-	-	1	-
YO1723	-	-	1	-	-	-	-	-	-	-	-	-	-	-	1	-
YO1890	1	-	-	-	-	-	-	-	-	-	-	-	-	1	-	-
YO1891	-	-	-	-	-	-	1	p	f	n	n	n	n	1	-	-

APPENDIX H: NAMES, ABBREVIATIONS, AND ACCESSION NUMBERS OF PVs USED IN THE PHYLOGENETIC ANALYSIS OF ScPVs.

Virus name	Abbreviation	Protein	Accession number
Beet cryptic virus 1	BCV1	RdRP	EU489061
Carrot cryptic virus	CarCV	RdRP	FJ550604
Cherry chlorotic rusty spot associated partitivirus	CCRSaPV	RdRP	AJ781168
Flammulina velutipes browning virus	FvBV	RdRP	AB465308
Vicia cryptic virus	VCV	RdRP	AY751737
White clover cryptic virus 1	WCCV1	RdRP	AY705784
Chondrostereum purpureum cryptic virus 1	CpCV1	RdRP	AM999771
Heterobasidion partitivirus 1	HetPV1	RdRP	HQ541323
Heterobasidion partitivirus 3	HetPV3	RdRP	FJ816271
Rosellinia necatrix partitivirus 2	RnPV2	RdRP	AB569997
Heterobasidion partitivirus 12	HetPV12	RdRP	KF963175
Heterobasidion partitivirus 13	HetPV13	RdRP	KF963177
Heterobasidion partitivirus 15	HetPV15	RdRP	KF963186
Cannabis cryptic virus	CanCV	RdRP	JN196536
Crimson clover cryptic virus 2	CCCV2	RdRP	JX971982
Dill cryptic virus 2	DCV2	RdRP	JX971984
Hop trefoil cryptic virus 2	HTCV2	RdRP	JX971980
Primula malacoides virus 1	PmV1	RdRP	EU195326
Red clover cryptic virus 2	RCCV2	RdRP	JX971978
White clover cryptic virus 2	WCCV2	RdRP	JX971976
Atkinsonella hypoxylon virus	AhV	RdRP	L39125
Ceratocystis resinifera virus 1	CrV1	RdRP	AY603052
Fusarium poae virus 1	FpV1	RdRP	AF047013
Heterobasidion partitivirus 2	HetPV2	RdRP	HM565953
Heterobasidion partitivirus 8	HetPV8	RdRP	JX625227
Pleurotus ostreatus virus 1	PoV1	RdRP	AY533038
Rhizoctonia solani virus 717	RHsV717	RdRP	AF133290
Rosellinia necatrix partitivirus 1	RnPV1	RdRP	AB113347
Heterobasidion partitivirus 7	HetPV7	RdRP	JN606091
Cryptosporidium parvum partitivirus 1	CSpV1	RdRP	KY884720

Virus name	Abbreviation	Protein	Accession number
Beet cryptic virus 2	BCV2	RdRP	HM560703
Fig cryptic virus	FCV	RdRP	FR687854
Pepper cryptic virus 1	PepCV1	RdRP	JN117276
Pepper cryptic virus 2	PepCV2	RdRP	JN117278
Aspergillus ochraceous virus	AoV	RdRP	EU118277
Discula destructiva virus 1	DdV1	RdRP	AF316992
Discula destructiva virus 2	DdV2	RdRP	AY033436
Fusarium solani virus 1	FsV1	RdRP	D55668
Gremmeniella abietina RNA virus MS1	GaRV-MS1	RdRP	AY089993
Ophiostoma partitivirus 1	OPV1	RdRP	AM087202
Penicillium stoloniferum virus F	PsV-F	RdRP	AY738336
Penicillium stoloniferum virus S	PsV-S	RdRP	AY156521
Hubei tetragnatha maxillosa virus 8	HtmV8	RdRP	NC_033313
Penicillium brasilianum partitivirus 1	PbPV1	RdRP	MK279470
Saccharomyces cerevisiae partitivirus 2-858	ScPV2-858	RdRP	OP555747
Saccharomyces cerevisiae partitivirus 1-5509	ScPV1-5509	RdRP	OP555748
Saccharomyces cerevisiae partitivirus 3-1172	ScPV3-1172	RdRP	OP555750
Saccharomyces cerevisiae partitivirus 2-1665	ScPV2-1665	RdRP	P562006
Saccharomyces cerevisiae partitivirus 1-1482	ScPV1-1482	RdRP	P561998
Saccharomyces cerevisiae partitivirus 1-1621	ScPV1-1621	RdRP	P561995
Saccharomyces cerevisiae partitivirus 2-1481	ScPV2-1481	RdRP	P562010
Saccharomyces cerevisiae partitivirus 2-1490	ScPV2-1490	RdRP	P562008
Saccharomyces cerevisiae partitivirus 2-1619	ScPV2-1619	RdRP	P562007
Saccharomyces cerevisiae partitivirus 1-1619	ScPV1-1619	RdRP	P561996
Saccharomyces cerevisiae partitivirus 1-1490	ScPV1-1490	RdRP	P561997
Saccharomyces cerevisiae partitivirus 1-1481	ScPV1-1481	RdRP	P561999
Saccharomyces cerevisiae partitivirus 2-1482	ScPV2-1482	RdRP	P562009
Saccharomyces cerevisiae partitivirus 1-1622	ScPV1-1622	RdRP	P561994
Saccharomyces cerevisiae cryspovirus 1	ScCV	RdRP	UGZ04790
Otarine picobirnavirus	OtPV1	RdRP	YP_009351841

APPENDIX I: MOLECULAR MODELING STRUCTURE ASSESSMENT SCORES

Model	Molprobity Score	Clash Score	Ramachandran favored	Ramachandran outliers	Rotamer outliers	Bad bonds	Bad angles	Twisted non-proline	QMEAN DisCo Global
CSpV1 RdRp, Unrelaxed	2.4	30.5	0.935	0.016	0.007	116/4127	45/5581	44947	0.60±.05
CSpV1 RdRp, Relaxed	1.2	1.14	0.946	0.005	0.005	0/4101	18/5505	3/426	0.53±.05
ScPV1-5509 RdRp, Unrelaxed	2.8	38.4	0.893	0.046	0.015	129/4482	111/6052	8/500	0.54±.05
ScPV1-5509 RdRp, Relaxed	1.1	0.7	0.949	0.013	0.007	0/4444	27/5940	2/427	0.44±.05
ScPV2-858 RdRp, Unrelaxed	2.3	29.9	0.946	0.019	0.005	107/4051	42/5468	1/462	0.58±.05
ScPV2-858 RdRp, Relaxed	1.3	1.16	0.938	0.009	0.012	0/4027	23/5398	1/416	0.52±.05
ScPV3-1172 RdRp, Unrelaxed	2.7	39.1	0.906	0.059	0.014	93/4122	68/5589	11/467	0.57±.05
ScPV3-1172 RdRp, Relaxed	1.2	0.51	0.906	0.025	0.007	0/4094	20/5507	10/415	0.49±.05
CSpV1 CA, Unrelaxed	3.4	47.4	0.683	0.217	0.037	91/2477	188/3359	17/270	.35±.05
CSpV1 CA, Relaxed	1.6	1.28	0.841	0.039	0.012	0/2451	30/3296	9/236	0.37±.05
ScPV1-5509 CA, Unrelaxed	3.8	54.9	0.64	0.237	0.08	102/2676	257/3636	45/300	0.40±.05
ScPV1-5509 CA, Relaxed	3.1	14.2	0.752	0.124	0.079	18/2653	58/3569	24/256	0.29±.05
ScPV2-858 CA, Unrelaxed	3.5	54.8	0.766	0.158	0.043	75/2385	129/3231	14/256	0.45±.05
ScPV2-858 CA, Relaxed	2.2	2.86	0.845	0.046	0.038	0/3170	26/3170	4/227	0.38±.05
ScPV3-1172 CA, Unrelaxed	3.5	54.2	0.731	0.172	0.04	87/2556	148/3468	41/291	0.48±.05
ScPV3-1172 CA, Relaxed	2	1.24	0.83	0.072	0.036	0/2533	32/3401	19/248	0.35±.05

APPENDIX J: PRIMERS USED IN THIS STUDY.

Primer3 was used to design primers, generally with the following parameters:

- Primer size – Min: 20, Opt: 25, Max: 30
- Primer Tm – Min: 64, Opt: 65, Max: 66
- CG clamp: 2

Basic thermocycler parameters for PCR: (1) 00:30, 98°C; (2) 00:10, 98°C; (3) 00:30, 58°C; (4) 00:15-00:30 per kb, 72°C; (5) Repeat steps 2-4 29X; (6) 10:00, 72°C.

Basic thermocycler parameters for single-step RT-PCR: (1) 10:00, 60°C; (2) 02:00, 98°C; (3) 00:10, 98°C; (4) 00:10, 64°C; (5) 00:15, 72°C; (6) Repeat steps 3-5 29X; (7) 5:00, 72°C.

Name	Sequence	Target	Length (bp)
PRUI109	TCCCTATCCAAGTGGAGAGAGTTCG	ScPV3-1172 CA	181
PRUI110	GGTTTTCTATAACCAGGAGGATTTGAGG	"	"
PRUI111	GATCTTTCCGATCTTGAGAAATCTATGC	ScPV3-1172 RdRp	225
PRUI112	AAGCCAAATACAACTCGACAAAACG	"	"
PRUI116	ATGCTCGGAATGAGATATCAAGTGC	ScPV1-5509 CA	181
PRUI117	CAACAAGACGATACAAGGCATTCG	"	"
PRUI118	TGGCATGTAAAGGAGGTTCTGTAGC	ScPV1-5509 RdRp	197
PRUI119	AACTCGCACTGTGTTATACATCAAGAGG	"	"
PRUI164	CGAATAAACCGCGTTTAGTTTTTGC	ScPV2-858 RdRp	239
PRUI165	AAAGGCCCTTCTGATCAACTTTGG	"	"
PRUI166	CCAATGGAAGACGATCTTGACG	ScPV2-858 CA	186
PRUI167	GATAGGAGCTGGTTTTGTCTGTTCG	"	"
PRUI199	ACAGACGTTTTCACGACCTTTTAGG	ScPV1-1126 CA	226
PRUI200	TACAACGCGTTCAATTCAACATAGG	"	"
PRUI201	ATTAGAGTAAAGCATCGTGGCATCC	ScPV1-1126 RdRp	167
PRUI202	TCAAACACCAAGAAGCTATCATCTCC	"	"
PRUI203	ACGTGCCTTTTTCTGAATATCACG	ScPV2-1126 CA	194
PRUI204	CCTCCACTCTGGTAAGAAAGTTTTGG	"	"
PRUI205	ATACGAAGAGCGTTTTCAATCATGC	ScPV2-1126 RdRp	173
PRUI206	CCAATCAACTGAGTAAATGCAGAGC	"	"

Name	Sequence	Target	Length (bp)
NTT001	ATTCTTAGGATGGTCCGTGAATTGG	ScPV2-1126 RdRp	149
NTT002	AAAACGCTCTTCGTATCAACTGAGG	"	"
NTT003	AATTAGAGTAAAGCATCGTGGCATCC	ScPV1-1126 RdRp	73
NTT004	CGCATTAACGATAGATCCAATCAGC	"	"
NTT005	AATACCACATCTCCGACGATTAGGC	ScPV3-1172 RdRp	277
NTT006	GAAGTCATAAGCCTCGTTCAACACC	"	"
NTT009	CAGCTATGGAAGAGAAGTGGAATGC	ScPV2-815 RdRp	353
NTT010	ACACTAAACGGGGTTTGTTCTGTCC	"	"
NTT031	TCGTATGGTTCATACCCTGACTTGG	HO	3426
NTT032	GACTTGAAGAACATCCCAATGATGC	"	“
NTT033	GGCGTCTTTTGGGGTGTAACG	HO	3628
NTT034	AACCAAACCACCGTTCAATTCC	"	"
NTT041	AGTCACATCAAGATCGTTTATGG	MAT	-
NTT042	GCACGGAATATGGGACTACTTCG	"	404
NTT043	ACTCCACTTCAAGTAAGAGTTTG	"	544
NTT106	TTCTTTGAAATATCCTTAGAAGCTGTCTCC	ScPV2-858 CA	829
NTT108	AATTTTCTCGACCAATGGAAGACG	"	728
NTT110	TGCTTAGCACTGCCCTAATTATTTTCC	"	160
NTT112	CCACAAAATGTAATTCTCTCGAAAACC	"	124
NTT114	CCTGGTCAATGGATACCAAAAATCC	ScPV2-858 RdRp	846
NTT116	CATCTGCTACCTTCAGACACTTCAGC	"	126
NTT118	TCCCTAAATCAATGTATTTGGCTTGG	"	192
NTT132	AGATAGGAGCTGGTTTTGTCTGTTCG	ScPV2-858 CA	829
NTT133	GGACGTATCCCCACTCACTTAACG	"	728
NTT134	TATGCGCAGAATCACACAGATCG	"	160
NTT135	CAGACACAATGTTTTTCGGTTCAGC	"	124
NTT136	TCCCCACTCACTTAACGGACTAGC	ScPV2-858 RdRp	1077
NTT137	CTTACCATCACGTTTAACGGTACGC	"	126
NTT138	CTTGAAACTATGACCAAGAAAGGAAACC	"	192
NTT152	CATAATGCAAGACCATTGTGTTTGG	ScPV1-5509 RdRp 3' ORF	378+
NTT153	TCCAAATTTTCCAACTTAGGATTAAACG	"	284+
NTT154	CTTTCAAGGCGGATGACCTATGG	"	200+
NTT155	CTTGCTCATTGAAGCCAAATGC	"	241
NTT156	GATGATAGCTTCTTGG	"	347+

Name	Sequence	Target	Length (bp)
NTT157	TCCGAAGGAAGAAGCTGAATTGC	ScPV3-1172 RdRp 5' ORF	337+
NTT158	CGGAATAGTGACTTTGAAATAAATCAAGC	"	285+
NTT159	GCAATGTCCATTTTCGATTCATCC	"	244+
NTT160	TTGTTAAAGAAGAATATTGGCGAGACG	"	156

APPENDIX K: ACCESSION NUMBERS FOR ALL ScPV SEQUENCES DETERMINED IN THIS WORK

Name	dsRNA	Accession #
ScPV2-858	1; RdRp	OP555747
ScPV2-858	2; CP	OP555746
ScPV1-5509	1; RdRp	OP555748
ScPV1-5509	2; CP	OP555749
ScPV3-1172	1; RdRp	OP555750
ScPV3-1172	2; CP	OP555751
ScPV1-1622	1; RdRp	P561994
ScPV1-1622	2; CP	P562000
ScPV1-1619	1; RdRp	P561996
ScPV1-1619	2; CP	P562002
ScPV1-1482	1; RdRp	P561998
ScPV1-1482	2; CP	P562004
ScPV1-1621	1; RdRp	P561995
ScPV1-1621	2; CP	P562001
ScPV1-1490	1; RdRp	P561997
ScPV1-1490	2; CP	P562003
ScPV1-1481	1; RdRp	P561999
ScPV1-1481	2; CP	P562005
ScPV2-1619	1; RdRp	P562007
ScPV2-1619	2; CP	P562012
ScPV2-1490	1; RdRp	P562008
ScPV2-1490	2; CP	P562013
ScPV2-1482	1; RdRp	P562009
ScPV2-1482	2; CP	P562014
ScPV2-1481	1; RdRp	P562010
ScPV2-1481	2; CP	P562015
ScPV2-1665	1; RdRp	P562006
ScPV2-1665	2; CP	P562011

APPENDIX L: YEAST STRAINS USED IN THIS WORK.

Strain	MAT	HO	Genotype
BJH001	*MATa*	*ho*	*his3Δ200 leu2Δ0 met17Δ0 ura3Δ0 XRN1*
BY4741	*MATa*	*ho*	*his3Δ1 leu2Δ0 met17Δ0 ura3Δ0 XRN1*
BY4741	*MATa*	*ho*	*his3Δ1 leu2Δ0 met17Δ0 ura3Δ0 xrn1Δ::KanMX*
CYC1172	*MATa/α*	*HO/HO*	*HIS3/HIS3 LEU2/LEU2 MET17/MET17 URA3/URA3*
Y-5509	*MATa/α*	*HO/HO*	*HIS3/HIS3 LEU2/LEU2 MET17/MET17 URA3/URA3*
YO815	*MATa/α*	*HO/HO*	*HIS3/HIS3 LEU2/LEU2 MET17/MET17 URA3/URA3*
YO819	*MATa/α*		*HIS3 LEU2 MET17 URA3*
YO820	*MATa/α*	*HO/HO*	*HIS3/HIS3 LEU2/LEU2 MET17/MET17 URA3/URA3*
YO836			*HIS3 LEU2 MET17 URA3*
YO858	*MATa/α*	*HO/HO*	*HIS3/HIS3 LEU2/LEU2 MET17/MET17 URA3/URA3*
YO866			*HIS3 LEU2 MET17 URA3*
YO1119	*MATa/α*		*HIS3 LEU2 MET17 URA3*
YO1126	*MATa/α*		*HIS3 LEU2 MET17 URA3*
YO1133	*MATa/α*		*HIS3 LEU2 MET17 URA3*
YO1477	*MATa/α*		*HIS3 LEU2 MET17 URA3*
YO1481	*MATa/α*		*HIS3 LEU2 MET17 URA3*
YO1482	*MATa/α*		*HIS3 LEU2 MET17 URA3*
YO1489			*HIS3 LEU2 MET17 URA3*
YO1490	*MATa/α*		*HIS3 LEU2 MET17 URA3*
YO1599	*MATa/α*		*HIS3 LEU2 MET17 URA3*
YO1604			*HIS3 LEU2 MET17 URA3*
YO1605	*MATa/α*		*HIS3 LEU2 MET17 URA3*
YO1608	*MATa/α*		*HIS3 LEU2 MET17 URA3*
YO1610			*HIS3 LEU2 MET17 URA3*
YO1612	*MATa/α*		*HIS3 LEU2 MET17 URA3*
YO1615	*MATa/α*		*HIS3 LEU2 MET17 URA3*
YO1619	*MATa/α*		*HIS3 LEU2 MET17 URA3*
YO1620			*HIS3 LEU2 MET17 URA3*
YO1621	*MATa/α*		*HIS3 LEU2 MET17 URA3*
YO1622	*MATa/α*		*HIS3 LEU2 MET17 URA3*
YO1665	*MATa/α*		*HIS3 LEU2 MET17 URA3*
YO1891	*MATa/α*		*HIS3 LEU2 MET17 URA3*
YTag006	*MATa/α*	*HO/ho::HygMX*	*HIS3/HIS3 LEU2/LEU2 MET17/MET17 URA3/URA3*

Strain	MAT	HO	Genotype
YTag009	*MATα*	*ho::HygMX*	*HIS3 LEU2 MET17 URA3*
YTag015	*MATa/α*	*HO/ho::HygMX*	*HIS3/HIS3 LEU2/LEU2 MET17/MET17 URA3/URA3*
YTag058	*MATα*	*ho::HygMX*	*HIS3 LEU2 MET17 URA3*
YTag063	*MATa/α*	*ho/ho::HygMX*	*HIS3/his3Δ1 LEU2/leu2Δ0 MET17/met17Δ0 URA3/ura3Δ0 XRN1/?*
YTag085	*MATa*	*?*	*his3Δ1 leu2Δ0 MET17 ura3Δ0*
YTag121	*MATa/α*	*ho/ho::HygMX*	*HIS3/his3Δ1 LEU2/leu2Δ0 MET17/met17Δ0 URA3/ura3Δ0 xrn1Δ::KanMX/?*
DBY7730	*MATa*	*ho*	*his6 rme met1 ura1 can1 cyh1 sst1-3 ade2*
DBY7442	*MATα*	*ho*	*leu ade sst2 ura*

APPENDIX M: TIPS AND TRICKS

Tried and liked

- When casting SDS-polyacrylamide gels,
    - Expired TEMED can be used if the amount is increased ≈4 times.
    - Place Parafilm between the glass panes and the foam gaskets to ensure a secure seal. Check for leaks with water.
    - Make the separating gel with 25% glycerol and immediately pour the stacking gel.
- To remove bubbles in reaction mixtures, remove the straw from a squeeze bottle and fill ≈1/3 with ethanol. Gently blow the ethanol vapor into each tube. From u/what_are_you_saying.
- Store 0.2 mL tubes containing aliquots of reagent in a 50 mL conical vial instead of a rack. This saves room and PCR tube racks. From u/what_are_you_saying.
- To conserve tips during gel electrophoresis, place the dye in the cap of each tube and briefly centrifuge to mix. From u/Sonoris.
- To aspirate a large supernatant from a small, fragile pellet, insert a 1250 µL pipet tip into a 250 µL pipet tip and that into a 25 µL tip. From u/DocViking.

Tried and disliked

- Sanderson et al.[333] claim that omitting EDTA and reducing the Tris and boric acid components to 0.5X allows electrophoresis to be performed at high voltages (20-25 V/cm), reducing the run time 3-fold. In my opinion, these results are exaggerated and are not significantly better than running a 1X TBE gel at 140V for 30 min.
- The results from the creeping yeast mating type assay described by Arras et al[334]. are not replicable.
- U/so-and-so prepares a large bottle of 1% TAE agarose solution and stores it in a 60°C water bath so it is ready to dilute and pour when needed. It can take hours to dissolve all the agarose needed for much more than 100 mL of TAE agarose solution, so this approach does not save time.